inquiro

Volume 8 • 2014

UAB's UNDERGRADUATE RESEARCH JOURNAL

THE UNIVERSITY OF ALABAMA AT BIRMINGHAM

This is an internal document of

THE UNIVERSITY OF ALABAMA AT BIRMINGHAM

Front cover art:
"Tree of Life"
Catherine Ritchey, Senior,
Biomedical Engineering major

Inside cover art:
"Cell Study"
Sarah Adkins, Senior,
Biology and Studio Art Major

INQUIRO STAFF 2014

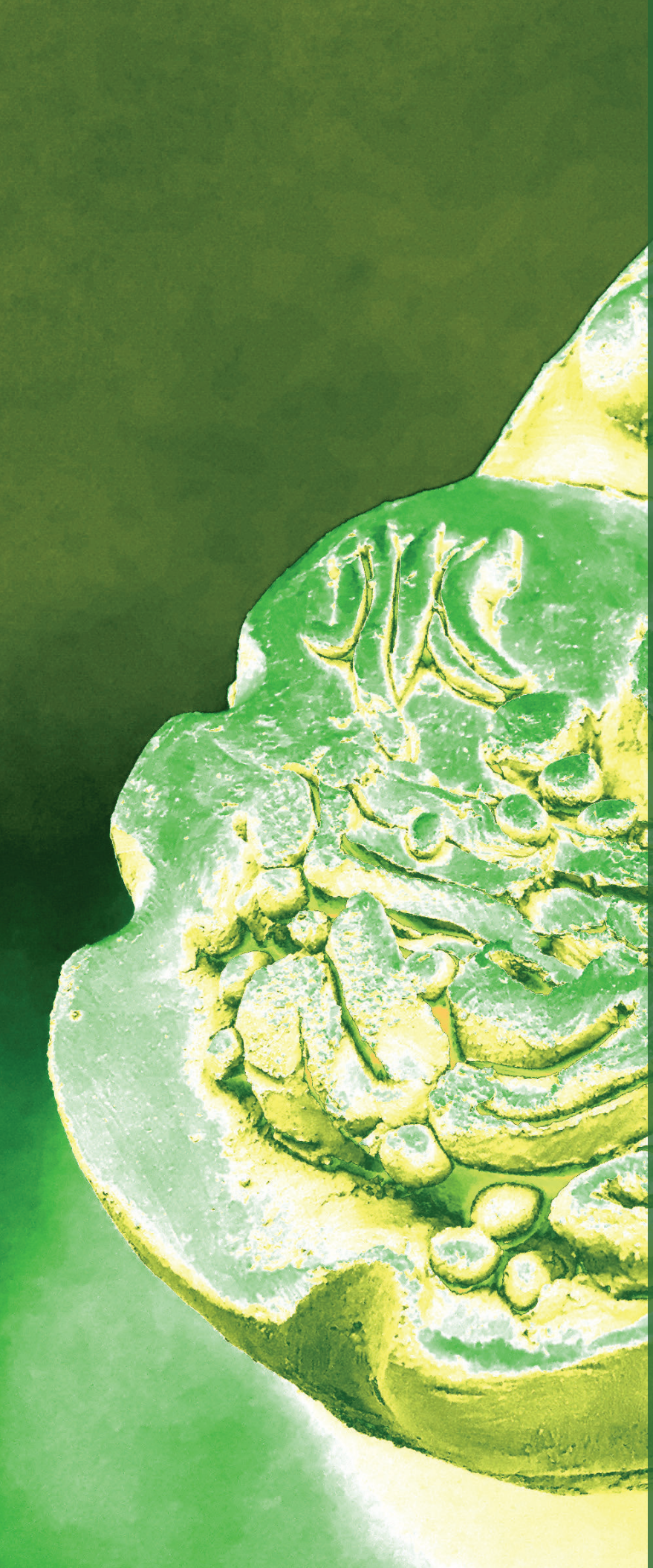

inquiro

Volume 8 • 2014

Founded and staffed by undergraduates at the University of Alabama at Birmingham, *Inquiro* is an annual journal produced with the mission of highlighting the contributions of undergraduates to UAB's many outstanding research programs and supporting the development of these student researchers by providing an outlet for them to publish their work. Any students who have conducted research at UAB, including those visiting from another institution, are invited to submit research manuscripts, short reports derived from scientific posters, or personal narratives regarding their research experiences. Authors retain full rights to their work, and are free to submit to other journals after publishing in *Inquiro*.

inquiro staff

letter from the editor

Science unifies the human race. People from every corner of the globe foster an innate thirst for knowledge and a curiosity about the strange and wonderful world around them. This shared desire to unravel the mysteries of the universe has led to collaborations between nations on an unprecedented scale. Projects like the International Space Station and the Large Hadron Collider at the European Organization for Nuclear Research (CERN) have seen contributions in materials, design, and manufacturing from fifteen and twenty-six nations, respectively, making them the most cooperative endeavors in human history.

While collaboration in science is inspired by something we all share—a curiosity about our world—our differences are what make this cooperation so fruitful. Science thrives best in an environment in which people with different academic and personal backgrounds are free to exchange ideas and share resources that can lead to innovative solutions to research questions. One reason that undergraduate research at UAB is so successful is that UAB encourages the collaborations and interdisciplinary conversations that are so important for creating such an environment.

I had the opportunity to become involved in research early in my career at UAB, working on a genetics project in the Department of Epidemiology. As my scientific interests broadened and matured, I was able to develop and complete a joint project between the Department of Physics and the Department of Neurobiology. These projects would not have been possible without the environment of constructive cooperation at UAB. As I prepare to pursue a graduate degree in biophysics, I have reflected on the opportunities that UAB has given me as an undergraduate student to refine my intellectual interests and develop my skills as a young scientist, including peer mentoring, technical writing, presenting at national and international conferences, and publishing. Working as an editor for Inquiro has allowed me to take an active role in the latter and to help broaden the opportunities for other undergraduates to disseminate their own scientific work.

John was drawn to UAB in large part because of the wealth and depth of research opportunities it offers to its undergraduates. Since his Freshman year, his experiences designing, conducting, presenting, and publishing on research projects have allowed him to explore and refine his interests and have confirmed his desire for a life and career in which science will play a large role. His work with Inquiro has been motivated by his love of language and writing, his wish to share the joy of scientific investigation and discovery, and his hope of making important opportunities in writing and publication more available to UAB's young scientists.

During the past year, John and I have endeavored to make this edition of Inquiro more accessible to everyone. We have increased the number of student staff members on our Editorial Board and looked to better represent the diversity of people and interests within the community of students, faculty, and researchers at UAB. We have also significantly expanded our Science News section in hopes of giving our student writers more opportunities to speak about the areas of science that excite them both inside and outside of UAB. As part of this effort, you will notice two new kinds of articles in the Science News section. In addition to the traditional news articles and faculty interviews, this edition of Inquiro introduces book reviews and film reviews. In these pieces, you will find accounts of media both new and old that focus on interesting scientific discoveries and those who made them, as well as comments from our staff about their relevance to the scientific community and to aspiring scientists today. We hope that you will find these reviews entertaining and insightful.

As always, however, the heart of this edition lies in a strong collection of research articles from young scientists in the UAB community. We have worked with our authors and reviewers this year to ensure that these manuscripts are easy to read and understand for non-experts yet uncompromised in their scientific integrity and rigor. The research articles in this edition represent such academic fields as physics and materials engineering, chemistry, microbiology, neuroscience, psychology, and bioinformatics. Additionally, we have included two narrative pieces detailing students' personal experiences with the process of scientific research. We hope that these articles give you a glimpse into the kinds of exciting research projects that undergraduate students can undertake at UAB and inspire you to learn about and become involved with undergraduate research.

In addition to our incredible student staff, Inquiro owes its continued success to a host of university faculty and staff. Our faculty reviewers volunteer their own time to help our student authors improve the strength of their manuscripts and to ensure that our research articles adhere to a rigorous standard of quality. Mike Sloane continues to offer his advice on the journal's operation. Peter O'Neil has provided guidance on how the journal can better reach its target audience. In the Office of Undergraduate Research, Nick Bieser has assisted us with creating and improving the online submission and review forms, and Tomader Ali has offered ideas about new directions for the journal. Ryan McAnulty of UAB Printing Services has helped us to set our content within a professional-quality design and worked with us to ensure that every aspect of the issue meets Inquiro's high standards. Finally, Robert Palazzo and Suzanne Austin have provided the financial and administrative support without which the publication of this issue would have been impossible. To our student staff, authors, and artists; faculty reviewers and mentors; and supporters in the UAB staff and administration, we offer our sincere gratitude.

Whether you are interested in reading a fascinating research article, a student perspective on undergraduate research at UAB, or a discussion of new discoveries in the scientific community at large, we think that you will find something in these pages that will engage your passions and your curiosity. We hope that this edition of Inquiro motivates students to seek out the many opportunities available at UAB to bolster their careers as research scientists and encourages faculty to continue to mentor the bright young minds that make up the community of undergraduate researchers.

Chapin Cavender, Senior Chief Editor 2014-2015

inquiro
Volume 8 • 2014

table of contents

Acknowledging the Ethical Dilemmas of 3D Bioprinting

Maggie Collier

The scientist on the stage, who says that he has a method that could eradicate transplant lists and save innumerable lives, is at once nonchalant and spellbinding. It is as though the vision he articulates—a better world where it is routine to grow bladders in a lab and to print skin grafts directly onto wounds—is already a reality for him even as his audience sits captivated by it, some chuckling in wonder at the novelty of the ideas. Their heart rates rise along with their curiosities as he finally introduces the sophisticated piece of equipment that he believes will usher in a new age in medical advancement. The 3D bioprinter—engulfed in light on the projector screen as it is unveiled—moves with fluidity, its metallic surfaces and bright pink bioink cartridge emphasizing its allure. According to the scientist, the video shows the device in the midst of printing a completely organic kidney. As proof, and as uneasiness settles over the crowd, he asks a colleague to bring him a kidney that they had printed earlier. Intrigue outweighs discomfort: the audience sits with eyes fixed on the bioprinting pioneer as he dons gloves and carefully cups his hands around the printer's product. Before their eyes, his promise of a better tomorrow has been transfigured into real, printed flesh.

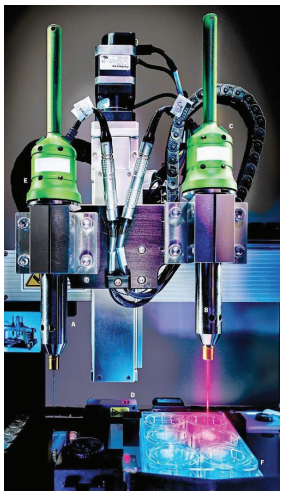

The NovoGen MMX Bioprinter

The pursuit of providing organs through scientific advancements is not an uncommon theme in science fiction. For example, consider Milla Jovovich's character being bioprinted in *The Fifth Element*, or the secret behind *The Island*. Such stories can be valuable as well as exciting: they show how seemingly impossible scientific advancements could affect society, and beneath their plots usually lie questions that expose science to an ethical review that is occasionally uncomfortable but always necessary. However, since the fictional advancements often seem infeasible, an audience can ignore these ethical dilemmas easily enough. But what happens when science fiction is no longer fiction? Does the real version seem any different ethically? Such questions are now important because, in the case of organ printing, fiction has become reality. The scientist previously mentioned is Dr. Anthony Atala, a pioneer of the 3D bioprinting industry. The event that was described is a presentation Dr. Atala gave in 2011 for the popular Technology, Entertainment, Design (TED) conference series (Atala 2011).

To approach ethical questions about bioprinting, we should start by considering its history. The technology emerged on the heels of great strides in tissue engineering that occurred in the early 2000s: at the turn of the century, Atala, among others, helped catalyze its development when he successfully transplanted lab-grown bladders into several patients (Atala 2000). After this breakthrough, questions began to emerge about how tissue engineering could be improved to make more complex organs. Then, in 2003, another team of bioprinting pioneers developed one of the earliest known bioprinters by modifying an inkjet printer to print cells and gels into scaffolds (Mironov, Boland, Trusk, Forgacs, & Markwald 2003). This innovation was based on a technology developed in the 1980s called 3D printing: an additive manufacturing form of engineering that prints layers of heated plastic or other material. As a layer is finished, the print platform moves downward in preparation for the printing of the next layer, and 3D modeling software controls where the printhead will lay the material. In the case of bioprinting, the printed material consists of bioinks, which contain cells, hydrogel, and other biological factors. The incredible capabilities of 3D printing can enhance tissue engineering, making bioprinting a worthwhile alternative to conventional tissue engineering approaches.

As of now, the dominant tissue engineering method involves biodegradable scaffolds used to support the three-dimensional shape of a tissue and promote cell adhesion to the scaffold's surface. These scaffolds are usually designed out of polymers and are porous to provide space for vascularization and the seeding of cells inside the scaffold (Mironov et al. 2009). While this method has proved effective, it also has its limitations. Major issues with this method include difficulties in getting thicker tissues to vascularize thoroughly, as well as precisely seeding different cells inside the scaffold (Mironov et al. 2009). However, advancements in bioprinting have produced vascularized tissues without scaffolding (Norotte, Marga, Niklason, & Forgacs 2009). Furthermore, bioprinting obviates the time-intensive work involved in carefully seeding cells onto a scaffold. Although conventional tissue engineering can produce the same tissue constructs as

bioprinters, the speed and precision with which bioprinting occurs make it more efficient for research purposes.

Realizing that bioprinters could revolutionize large-scale tissue manufacturing, many researchers have moved quickly to take advantage of these devices. Some of the early developers of bioprinting founded a company called Organovo to commercialize their bioprinters and 3D printed tissue models. Recently, Organovo achieved one of its major goals: to develop printed liver tissue products, which it is now selling to drug companies to make toxicology testing more accurate (Organovo Holdings, Inc. 2014). Other bioprinting experts, for their part, have been researching ways to mass-produce organs and tissues, and have published papers outlining elaborate systems of automated tissue engineering assembly lines (Mironov, Kasyanov, & Markwald 2011).

While the long-term goal of bioprinting is to print transplantable organs, Organovo and other research groups also focus on short-term goals that, when accomplished, have so far had a remarkable impact on the field of regenerative medicine. In the area of stem cell research, bioprinting has become a good option for engineering microenvironments that encourage a particular pathway of stem cell differentiation (Tasoglu & Demirci 2013). Also, stem cell printing is now sophisticated enough to print various kinds of stem cells that function normally and have a high rate of survival (Tasoglu & Demirci 2013). However, bioprinting seems to be most useful for engineering basic tissues. Already, bioprinted bones and cartilage can be used in various clinical applications, and extensive work on other bioprinted tissues, such as aortic valves, is underway to provide more kinds of transplants (Seol, Kang, Lee, Atala, & Yoo 2014). Unfortunately, even as the technology of bioprinting advances, the field of organ manufacturing turns complicated once the tissues leave the printers.

While the transplantation of a lab-grown bladder is a great feat in regenerative medicine, the ability to print a variety of transplantable organs seems far off. First, a bladder is a very simple organ composed of only two cell types; a kidney, by comparison, consists of many cell types and requires a complex vasculature. In fact, the kidney that Atala presented during his talk is a model with limited survival time (Atala 2011). The difficulty lies in the development of the tissue after printing. Seeking clues from nature to bypass the current developmental barriers of printed organs, some bioprinting researchers are exploring aspects of tissue formation in embryonic development (Mironov et al. 2009). Another barrier, however, is difficulty in printing tissues with complex vasculature systems. Organovo was successful in generating viable liver tissue models, but a full-sized liver is thicker than their models, and thus requires more vasculature. Although bioprinting has significantly improved tissue engineering, transplantable organ regeneration is still bound, for now, to the realm of science fiction. However, this does not mean that the ethical debate surrounding the idea of bioprinted transplantable organs should pause to wait for the technology.

Recently, a group of information technology experts at the research firm Gartner predicted that advancements in 3D bioprinting will catalyze a major ethical debate within a few years (Gartner, Inc. 2014). Currently, many tissue engineers are starting to talk extensively about bioprinting as they become interested in integrating the technology into their work. But to most of the public, bioprinting still sounds like science fiction. One can imagine how the public would react to news that clinical trials for 3D printed organs had begun: having heard almost nothing about the science, they would be faced with innumerable ethical questions to answer and little information to go on. Some of the questions that come to mind deal with availability of use and regulatory precautions. If 3D printers are now inexpensive enough for the common man, is it not plausible that bioprinters could eventually become inexpensive enough as well? Regulations would be required to delineate who is responsible enough to utilize the technology. Also, in the case that printed organs make it to clinical use, who would receive the benefits of this technology? Would the benefits of expanding access to lifesaving tools outweigh the dangers of providing the technology to regions with poor baseline healthcare and weak regulatory abilities? And would abuse of the technology lead to an increase in patients receiving unnecessary body modifications? For transplantable printed organs to cross the boundary between science fiction and reality, society must first consider the ramifications of releasing this technology to the public.

Dr. Atala brings his presentation to a close by showing a video of a previous patient (Atala 2011). Luke, an early test subject who received a lab-grown bladder, explains how Atala's work changed Luke's childhood. Once the video ends, the talk's host invites Luke on stage. The audience tries to maintain composure as Dr. Atala humbly receives accolades from the host and a healthy dose of gratitude from his now twenty-something former patient. Although most people are more comfortable with science fiction stories remaining fiction, there are aspects of ethically challenging advancements that make compromises seem justified. Bioprinting pioneers like Atala are probably aware of the ethical issues that will arise as they get closer to achieving their long-term goals. However, successes like Luke's transplantation are probably what drive researchers deeper into an ever-evolving field that promises to be full of both complexities and triumphs.

References

1. Atala, A. (2000). Tissue engineering of artificial organs. J. Endourol., 14(1), 49-57.

2. Atala, A. (Speaker). (2011 March). Printing a human kidney [TED Talk Video].

3. Gartner, Inc. (2014 January 29). Gartner says uses of 3D printing will ignite major debate on ethics and regulation. Gartner. [Press Release].

4. Hogan, T. (Photographer). (n. d.). The novogen mmx bioprinter [Web Photo].

5. Mironov, V., Boland, T., Trusk, T., Forgacs, G., & Markwald, R. R. (2003). Organ printing: computer-aided jet-based 3D tissue engineering. Trends Biotechnol., 21(4), 157-161. doi: 10.1016/S0167-7799(03)00033-7

6. Mironov, V., Visconti, R. P., Kasyanov, V., Forgacs, G., Drake, C. J., & Markwald, R. R. (2009). Organ printing: tissue spheroids as building blocks. Biomaterials, 30(12), 2164-2174. doi: 10.1016/j.biomaterials.2008.12.084

7. Mironov, V., Kasyanov, V., & Markwald, R. R. (2011). Organ printing: from bioprinter to organ biofabrication line. Curr. Opin. Biotechnol., 22(5), 667-673. doi: 10.1016/j.copbio.2011.02.006

8. Norotte, C., Marga, F. S., Niklason, L. E., & Forgacs, G. (2009). Scaffold-free vascular tissue engineering using bioprinting. Biomaterials, 30(30), 5910-5917. doi: 10.1016/j.biomaterials.2009.06.034

9. Organovo Holdings, Inc. (2014 August 12). Organovo highlights liver toxicology achievement, reports q1 fiscal 2015 results. RP Newswire. [Press Release].

10. Seol, Y. J., Kang, H. W., Lee, S. J., Atala, A., & Yoo, J. J. (2014). Bioprinting technology and its applications. Eur. J. Cardiothorac. Surg., 46(3), 342-348. doi: 10.1093/ejcts/ezu148

11. Tasoglu, S. & Demirci, U. (2013). Bioprinting for stem cell research. Trends Biotechnol., 31(1), 10-19. doi: 10.1016/j.tibtech.2012.10.005

science news

Birmingham Pollution: No Longer the "Toxic City"?

Alex Chang

Birmingham, Alabama, nicknamed the Steel City, has been the industrial center for steel and iron production in the South since the late 1800s. Immediately following the Civil War, Southern investors and Northern bankers pulled together to create large blast furnace complexes, taking advantage of the iron ore, coal, and limestone deposits in Jefferson County (Trent 2007). At one point, Birmingham provided 40 % of the United States' total output of foundry pig iron. The advent of the steel industry spurred the rapid post-Civil War growth that gave Birmingham its other nickname, the Magic City. But Birmingham's early economic successes came at a cost indicated by yet another, less flattering, appellation it has sometimes received: the Toxic City.

For over a century, steel and iron production facilities have been polluting the air of Jefferson County with toxic metals. The soil and water of the region have been damaged along with the air, and Jefferson County's coal-fired power plants are at issue in addition to its foundries. Annually, Alabama's coal-fired power plants release 15 million pounds of toxic metals in on-site ash ponds, and the Alabama Power Company's Miller Steam Plant in western Jefferson County alone releases more toxic metals than any other power plant in the country (Spencer 2012).

After being pushed to the side for many years, the issue of pollution became more of a reality after incidents in neighboring states, such as the 2008 rupture at the Tennessee Valley Authority's Kingston fossil plant, were exposed by the media. As a result of the increasing publicity that pollution began to receive, North Birmingham and Jefferson County residents became concerned regarding local conditions, and community leaders requested that the Jefferson County Department of Health (JCDH) conduct a study of toxic air pollutants in the Jefferson County area.

The Birmingham Air Toxics Study (BATS), held between July 2005 and June 2006 and run by the JCDH, monitored toxic air pollutants in East Thomas, North Birmingham, Providence, and Shuttlesworth. The study aimed to "assess the potential health effects resulting from the local population's exposure to chemicals in ambient air" (JCDH 2009a). A total of 102 air pollutants were collected and tested from all four of the areas to see what potential risks and hazards existed. Fourteen of the 102 air pollutants exceeded the Upper Confidence Level (UCL) set by the Office of Air Quality, Planning and Standards (OAQPS) (JCDH 2009a). The results from this study point to the reasonable assumption that the number of cancer patients should have been increasing due to exposure to toxic metals present in the air; however, several studies analyzing a long period of time have proved that this has not been the case.

Upon examining the death logs of African Americans in Jefferson County from 2000 to 2009, the JCDH noted that "the overall death rate for all causes of death combined, deaths from all cancers combined, and for the following cancers individually: breast, leukemia, liver and lung, were statistically the same…"(JCDH 2009b) . Furthermore, "the death rates from asthma and chronic obstructive pulmonary disease (COPD) were statistically the same…" (JCDH 2009b). Although the potential risk for cancer may indeed

The iconic Sloss Furnaces symbolize both Birmingham's early economic might and the environmental costs that its industries eventually imposed on the region.

be significantly greater in these areas due to the marked increase of pollutants in the air, the number of Jefferson County citizens dying from cancer does not appear to have changed at all in the recent past.

Another examination of logs in the Alabama Cancer Registry from 2002 to 2011 noted that cancer rates among African Americans in North Birmingham showed little difference from those among African Americans in the rest of Alabama. The incidence rates of cancers that were typically related to air, water, or soil pollution were consistent throughout the African American population of Alabama regardless of location. Furthermore, the rates of cancers of the lung, stomach, colon and rectum, liver, pancreas, urinary bladder, lymphoma, and leukemia, "checked out to be within the bounds of the rest of the country's rates" (JCDH 2014). Thus, there is no statistically significant increase in the frequency of cancer as a result of pollution in North Birmingham or Jefferson County.

African Americans were observed in these studies because the area that was studied, ZIP code 35207, is predominately African American (93.0 % African American, 5.6 % white, and 1.4 % other). However, because Jefferson County in general is 42.7 % African American, 55.2 % white, and 2.2 % other, and Alabama overall is 26.9 % African American, 70.9 % White, and 2.1 % other (JCDH 2014), the applicability of the JCDH study to Jefferson County and Alabama as a whole is not circumspect. One possible confound is the fact that some groups of cancers have markedly different rates of incidence among different races in the national population. For example, whites exhibit more oral cavity and pharynx cancer, while African Americans exhibit more esophagus and stomach cancer (JCDH 2014). If some of these cancers are also more or less influenced than others by exposure to pollutants, it becomes less clear how the results of the JCDH study should be interpreted beyond the study region.

A more recent study by the United States Environmental Protection Agency (EPA) had the Agency for Toxic Substances and Disease Registry (ATSDR) look through environmental data for areas around the Walter Coke Inc. facility in North Birmingham to determine if exposure to air contaminants is a public hazard for people who live or work in the area. Unlike past readings of air contaminant levels, as in the BATS study, the more recent ATSDR sampling revealed a decrease in the total air contamination. Instead of exceeding the UCL value, the amount of contaminants in the air matched the minimum EPA target for minimizing cancer risk and even dropped below this value in some areas. Past readings averaged with more recent data result in the estimate that two out of 10,000 people in the Birmingham area will develop cancer if exposed to these contaminants (Department of Health and Human Services 2014).

In the final analysis, recent studies point to the conclusion that pollution does not result in increased risk of cancer in the Birmingham area, but do not conclude that there are no health problems related to pollution. Compared to the rest of the country, Birmingham is no longer a toxic city, but rather is on the low end of the pollution spectrum for major urban centers. Furthermore, in a study recently released by researchers at John Hopkins University, results suggested that cancer risk is often dominated by genetic factors over environmental ones. This does not mean that Birmingham and the rest of the country has no reason to curb pollution, or that environmental factors do not influence cancer risk substantially; but it, along with the most recent environmental data, may mean that Jefferson County residents can breathe a little easier knowing that the health risks they face from pollution are not as great as some once thought (Tomasetti, C. & Vogelstein, B. 2015).

References

1. Department of Health and Human Services, Agency for Toxic Substances and Disease Registry. 2014. Evaluation of Air Exposures in Communities Adjacent to the 35th Avenue Site, Birmingham, Alabama. Retrieved October 9, 2014, from http://www.atsdr.cdc.gov/HAC/pha/

NorthBirminghamAirSite/35th %20Avenue %20Site_PHA_PC_06-26-2014_508.pdf

2. Jefferson County Department of Health, Environmental Services Air and Radiation Protection Division. 2009a. Birmingham Air Toxics Study. Retrieved October 9, 2014, from http://www.jcdh.org/misc/ViewBLOB.aspx?BLOBId=182
3. Jefferson County Department of Health. 2009b. Summary from the Comparison of Death Rates and Birth Outcomes of African-Americans Living in Collegeville, Fairmont and Harriman Park to African-Americans Living in the Rest of Jefferson County, Alabama. Retrieved October 9, 2014, from http://s3.documentcloud.org/documents/1263058/death-rates-and-birth-outcomes-of-blacks-in-n.pdf
4. Jefferson County Department of Health. 2014. Notes on Interpreting the "Comparison of Cancer Incidence Rates for Zip Code 35207 to Jefferson County" (and Alabama). Retrieved October 9, 2014, from http://www.scribd.com/doc/237631623/JCDH-Health-Data
5. Sloss Furnaces. [Web Photo]. Retrieved October 9, 2014, from http://slossfurnaces.com/history/becoming-sloss-furnaces-national-historic-landmark/
6. Spencer, T. (2012, January 6). Jefferson County Plant Disposes Most Toxic Ash in US. Retrieved October 9, 2014, from http://blog.al.com/spotnews/2012/01/jefferson_county_plant_dispose.html
7. Tomasetti, C., & Vogelstein, B. (2015). Variation in cancer risk among tissues can be explained by the number of stem cell divisions. Science, 347(6217), 78-81. Retrieved February 7, 2015, from http://www.sciencemag.org/content/347/6217/78.abstract
8. Trent, C. (2007, August 8). A Look into Alabama's Iron and Steel Industry. Retrieved October 9, 2014, from http://cber.cba.ua.edu/rbriefs/ab2007q3_steel.pdf

science news

Discovery of Supermassive Black Hole in Dwarf Galaxy Shocks Scientists

Amy Stewart

Lurking at the center of our very own Milky Way galaxy is a supermassive black hole. In fact, supermassive black holes are thought to exist at the center of most, if not all, large galaxies. Recently, however, scientists have discovered an example of this kind of astronomical arrangement in the place they least expected: at the heart of one of the smallest dwarf galaxies ever encountered. Using the Hubble Telescope and the Gemini North 8-meter optical and infrared telescope, researcher Anil Seth and his team of astronomers from the University of Utah observed dwarf galaxy M60-UCD1 and collected data that allowed them to calculate the mass of the black hole at its center. M60-UCD1 itself is estimated to contain 140 million stars inside a 300 light-year diameter (Chou, F., Weaver, D., & Villard, R. 2014). In contrast, the Milky Way is approximately 100,000 light years in diameter and is home to between 100 and 300 billion stars (Djorkovski, G. 2004). Even though the Milky Way is 500 times larger and 1,000 times more massive than M60-UCD1, the ultra-compact dwarf galaxy's supermassive black hole has a mass of 21 million suns, while the Milky Way's black hole only measures up to a (relatively) puny 4 million suns. The Milky Way's black hole constitutes less than 0.01 % of its galaxy's total mass, while M60-UCD1's black hole accounts for 15 % (Chou, F., Weaver, D., & Villard, R. 2014).

This discovery implies that supermassive black holes may exist in even more galaxies than previously thought, and has also forced astronomers to reevaluate their predictions regarding the formation of dwarf galaxies. Dwarf galaxies were previously thought to arise independently from other galaxies through the birth of isolated stars, but this new

The Gemini Observatory on Mauna Kea, Hawai'i, at sunset. The 8-meter optical telescope Gemini North, housed here, was used along with the Hubble Space Telescope in the detection of M60-UCD1's black hole.

information suggests that dwarf galaxies are instead the remnants of larger galaxies that were torn apart during spectacular collisions with other large galaxies. According to Seth, "We simply don't know of any other way you could make a black hole so big in an object this small" (Chou, F., Weaver, D., & Villard, R. 2014).

Of these two implications, it will be easier to collect evidence for the existence of more dwarf-galaxy black holes than it will be to prove that dwarf galaxies were created by the collisions of larger galaxies. However, this relative comparison belies the true difficulty in detecting black holes: they remain purely

theoretical objects that are, as far as we know, impossible to observe directly. Their existence is predicted by Einstein's theory of relativity, and their presence in a given location can be inferred by observing the behavior of nearby matter. Current methods use a black hole's gravitational influence to "visualize" it: stars are observed orbiting around a circular region of space that appears empty to traditional techniques, and so the center of the orbit presumably contains a black hole (NASA 2014b). Another method involves the measurement of the high-energy radiation, mostly in the form of X-rays, emitted by a black hole as nearby matter falls inexorably into it in a process known as accretion (NASA 2014a).

New efforts are being made to detect "rogue" black holes, which are found scattered all across a galaxy rather than only at its center. It is possible that the Milky Way contains hundreds of these rogue black holes that were originally native to the dwarf galaxies that are predicted to have collided in the formation of our galaxy. Since these black holes are not located centrally, it is difficult to pinpoint a region within the vast expanse of the Milky Way in which to search for them. Astrophysicist Avi Loeb of Harvard University, however, has proposed a new way to identify these most elusive of black holes. When black holes pass through the disks of gas that fill the space between the stars in the Milky Way, they produce a bow shock, similar to a sonic boom, that accelerates electrons to high energies, causing emission of radio waves that can be detected by current radio observatories. Once a rogue black hole is initially located based on these emissions, the other methods previously described can be used to confirm its presence and mass. The discovery of such rogue black holes in our own galaxy would provide evidence for the collision-based mechanisms now thought to underlie the formation of dwarf galaxies as well as the Milky Way.

While many would probably agree that the information yielded from research on black holes is fascinating, one might reasonably wonder why resources are being devoted to the study of subjects that are theoretical, unobservable, distant, and perhaps irrelevant for our lives on Earth. There are at least two practical reasons why this type of basic research should continue. While basic research is not directed at solving particular practical problems, but rather is often a product of curiosity alone and seeks only to advance fundamental knowledge, the technology developed to enable it nonetheless often finds many practical applications. For example, wireless networking, modern medical imaging techniques, radar technology, and cloud computing all exist because of basic astronomical research. Furthermore, any fundamental discoveries about black hole physics could themselves reveal new possibilities for technologies that could not even have been imagined before. Black holes are incredibly efficient at harnessing energy, converting about 7 % of the mass they consume into energy (in comparison, nuclear fusion only converts about 0.3 % of mass into energy) (Lawrence Livermore National Laboratory 2007) (McClintock, J. & Remillard, R. 2004). Researchers Louise Crane and Shawn Westmoreland from Kansas State University argue that it is "clearly extremely ambitious, but [not] impossible" to harness this efficiency someday by creating an artificial black hole generator to provide energy for power plants or even spacecraft (Crane, L. & Westmoreland, S. 2009). Whether this fantastical technology will ever come to fruition remains to be seen, but it is clear that the natural phenomena must be understood through basic research before there is even a chance.

An equally compelling, albeit less pragmatic, motive for black hole research again ties back to the fact that such research is basic research. At its heart, science seeks to understand how the universe works. Black holes provide clues about how galaxies are formed and have even spawned new predictions about the origins of the universe at large. Humans are innately curious about the world around them; we have always looked to the stars and had a certain fascination with the unknown. Basic research—including on black holes—is thus not only a practical matter, but an activity that lies at the core of what it means to be human.

References

1. Campbell, L. & Thacker R. (2011, September 1). Top Ten Unexpected Benefits of Astronomy.
2. Chou, F., Weaver, D. & Villard, R. (2014, September 17). Hubble Helps Find Smallest Known Galaxy Containing a Supermassive Black Hole. NASA.
3. Crane, L. & Westmoreland, S. (2009, August 12). Are Black Hole Starships Possible? Kansas State University. arXiv:0908.1803v1.
4. Djorkovski, G. (2004). Our Galaxy, the Milky Way. California Institute of Technology.
5. Gemini Images. (n.d.). [Web Photo] Retrieved October 5, 2014, from http://www.gemini.edu/images/stories/news/about/InsidePV_btn.jpg
6. Lawrence Livermore National Laboratory. The Nuclear Physics of Fusion. (2007)
7. McClintock, J. & Remillard, R. (2004, June 23). Black Hole Binaries. Cornell University

Books to Inspire Young Scientists: A Review of *Letters to a Young Scientist* and *Advice for a Young Investigator*

Daniel Gilliam

For an aspiring scientist, the achievements of modern science can be both inspiring and intimidating. Advice and mentorship from an accomplished investigator is valuable for many reasons, not the least of which is that it renders the idea of establishing oneself as a scientist more tangible. This important effect of mentorship has also been captured in several books written by prominent scientists for students considering careers in science. Two of these books have been particularly well received: *Letters to a Young Scientist* by Edward O. Wilson and *Advice for a Young Investigator* by Santiago Ramón y Cajal. Wilson is a highly accomplished author and professor emeritus of biology at Harvard, and is widely regarded as one of the most influential scientists of our time. Ramón y Cajal is something of a legend in science, and his prolific body of work is often seen as the foundation of modern neuroscience. Although the two scientists wrote with a common goal, their books differ in a number of ways that affect the nuances and efficacy of their messages.

The most noticeable difference between the two books is the lapse of over 100 years between the first 1897 publication of *Advice* and the 2013 release of *Letters*. Although *Advice for a Young Investigator* is necessarily somewhat anachronistic, one of the book's most remarkable features is the degree of modern-day relevance it manages to retain. Although the practice of science and the institutional structure underlying it have changed drastically since the time when Ramón y Cajal was conducting his groundbreaking investigations on the structure of the nervous system, the insights offered in his book often reach to the more constant, foundational principles of science. Wilson's and Ramón y Cajal's discussions on the philosophical underpinnings of science are complementary and reinforcing: both highlight the necessity of rational, empirical inquiry for understanding the world, and both disavow unaided intuition as a method for seeking answers to deep mysteries.

The two authors also concur on the useful personal qualities of a good investigator, although their differing presentations of this material highlight the second major difference between the two books. Ramón y Cajal goes through a much more explicit deliberation on the qualities of a person who will make a good investigator, emphasizing the necessity of independent judgment, personal curiosity, and perseverance. He offers a list of archetypal ways of thinking and traits to be avoided, and readers may even identify some of these traits in themselves. Wilson presents similar information in a very different way. He invokes common mythological themes (the journey to an unexplored land, the search for the grail, etc.) as metaphors for the archetypal motivations of scientific minds. This difference in describing the same material is illustrative of both the stylistic differences and substantive similarities between the books.

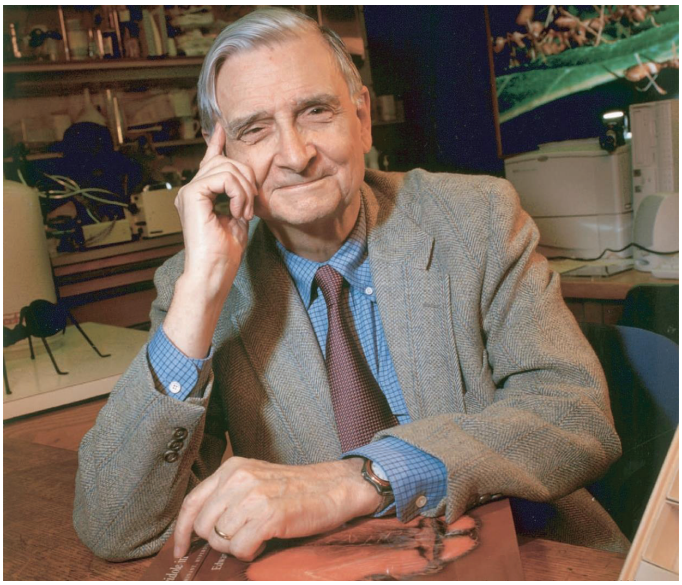

Edward O. Wilson, a native of Alabama, in repose at his Harvard University office.

Santiago Ramón y Cajal, the "Father of Neuroscience," at the microscope.

Because of these stylistic differences, each author is most effective at conveying a different set of messages, which is

one reason why the books complement each other so well. The epistolary form of *Letters to a Young Scientist*, being written as a series of letters, does not always lend itself well to including generalizable, practical advice. This is not to say that Wilson does not effectively offer his unique insight on the progression of a scientific career. However, the more formal, expository format of *Advice for a Young Investigator* enables Ramón y Cajal to cover a broader range of topics in more overt terms. For example, he includes a section devoted to "beginner's traps". One particularly salient counsel from Ramón y Cajal for students in science is to resist the tendency for superficial, encyclopedic learning, which poses even more of a concern today due to the ever-expanding body of scientific knowledge.

A central theme for both books is the notion that success in science does not require innate genius, nor automatically follow from it. Ramón y Cajal includes an anecdote on Marie Curie and the discovery of radium that is particularly effective at demonstrating the interplay of dedication, serendipity, passion, and calculated perseverance in scientific discovery. Ramón y Cajal's intended effect of this message was to humanize great scientists, as shown when he writes that "the discoverer, along with being an illustrious person of great talent and resolve, was in the final analysis a human being like everyone else." As an undergraduate hoping to contribute to scientific progress, it is very encouraging to read these humanizing accounts of great scientific achievements. This is also a central theme in *Letters to a Young Scientist*, and Wilson conveys a similar message by arguing that "ambition and entrepreneurial drive, in combination, beat brilliance." The effect of this message is magnified by the stature of the authors, which is one reason why Wilson's and Ramón y Cajal's writings on the subject are so effective.

In addition to making the possibility of personal scientific achievements more tangible for young scientists, the authors go on to describe the fulfillment gained from a research career and the worthiness of science as a lifelong devotion. To emphasize this point, Wilson opens his book with a prologue titled "You Made the Right Choice." Although both authors are eloquent and persuasive when describing the satisfaction gained from a career in science, Wilson's epistolary format excels on this topic. His personal account of the process by which he developed his foundational theories of island biogeography, and of the satisfaction earned from his diligence, are especially compelling on this point.

Overall, both of these books are quick and worthwhile reads for undergraduate students pursuing careers as scientists. While each stands on its own, the strengths and weaknesses of each book establish a synergy between them. In *Advice for a Young Investigator*, Ramón y Cajal offers a more formal exposition of his beliefs about how science should be practiced, which is lacking by comparison in *Letters to a Young Scientist*. However, Wilson's epistolary narrative approach is better suited to conveying the humanizing and inspirational messages of the book. The two books differ in many ways, but they are both successful in their common intent: to inform and inspire the next generation of scientists.

References

1. Ramón y Cajal, S. Advice for a Young Investigator. A Public Domain Book.
2. Wilson, E.O. (2013). Letters to a Young Scientist. New York, NY: Liveright Publishing Corporation.
3. Harrison, J. (2003). [Web Photo]. Retrieved November 1, 2014, from http://upload.wikimedia.org/wikipedia/commons/thumb/9/9d/Plos_wilson.jpg/800px-Plos_wilson.jpg
4. Universidad de Ciencias Médicas de la Habana, Cátedra de Santiago Ramón y Cajal. (2014). [Web Photo]. Retrieved November 1, 2014, from http://instituciones.sld.cu/csrc/files/2012/02/000346020.jpg

Tapping the Mysteries of Drinking Water

Neha Udayakumar

Water: It makes up 71 % of the planet we live on, and about 60 % of the average adult body. But when it comes to the water we drink, what exactly are we getting in addition to good old H_2O?

The last time you drank a cup of water, you probably did not appreciate its deliciousness or fragrance. Yet a lot of effort goes into making sure that the taste and odor of commercial drinking water are well maintained (Virginia Community Colleges System).

While the U.S. Environmental Protection Agency (EPA) constantly evaluates levels of toxicity in drinking water and regularly conducts health surveys in order to refine these regulations based on the health outcomes of consumers, there are no precise regulations on the minute levels of certain compounds that are added to contribute to the water's "aesthetics" (qualities such as taste, odor, and color). Rather, these aesthetic elements, as well as those that relate to certain cosmetic effects (like the tooth discoloration caused by excess fluoride), are described only by "non-enforceable guidelines" and are not regulated by the EPA (American Association for the Advancement of Science 2014) (EPA 2012).

Water purification systems in the U.S., and the force of EPA regulations, focus instead on the removal of several pathogenic and chemical contaminants found naturally in surface and groundwater sources. Some of the most infamous of these contaminants are coliform bacteria (found in animal and human fecal matter), radioactive substances (such as radium, uranium, and thorium), and heavy metals like lead or arsenic (which used to leach into water from lead plumbing) (Scott County Department of Parks, Library and Environment) (United States Geological Survey).

While the EPA concerns itself with what should not be included in water, municipal and commercial water providers are more occupied with ensuring that certain compounds and minerals do find their way into our taps. Frighteningly, emerging research shows that long-term accumulation of some of these compounds can lead to harmful health effects, and that our methods of detecting them are far less sensitive than we thought.

But how do these compounds enter our drinking water even under our well-established water purification systems? Compounds such as geosmin and 2-methylibomeol (MB) have an earthy, musky taste and are produced by actinomycetes or algal blooms found naturally in industrial waste or sewage. Phenols and chlorophenols give a medicinal taste and originate from industrial waste sites. Iron and manganese seep into the water supply from the ground, and provide a metallic taste to our water. Hydrogen sulfide (rotten egg odor) and methane gas (garlic taste) are produced by the metabolic activity of microorganisms.

A water treatment plant in the United States, where water is purified and aesthetic elements are added in order to make it fit for drinking purposes.

Some of these odorous compounds can also be formed as a byproduct of reactions involving treatment chemicals. Chlorine and ammonia are commonly used for water treatment. In addition to experiencing an undesirable bleach-like taste, people drinking water with chlorine, chloramines, or chlorine dioxide may experience irritation of their eyes, nose, and stomach. Another common treatment strategy, the ozonation of water for disinfection, produces fruity-smelling aldehydes.

A Threshold Odor Test and a Flavor Profile Analysis are usually performed on water for evaluating problems in taste and odor. These tests are performed subjectively and involve nothing more than a human tester smelling the water samples. Since the tests are based on human perception, several individual readings must be performed to achieve a measure of accuracy.

For years, a large determining factor for the composition of our drinking water has been taste or odor, rather than a need for certain compounds to promote our health or well-being. Researchers at Virginia Tech found that manganese, though nutritionally beneficial in small amounts, is extremely harmful with chronic exposure at high levels; among other issues, its inhalation has been found to damage the central nervous system. Despite these findings, the EPA still places little

regulation on the amount of manganese allowed in drinking water. Drinking water purification facilities are given much freedom to establish their own manganese levels based on aesthetic factors, as long as they are within the 0.05 mg/L baseline (Lenntech Water Treatment Solutions).

In a study published in January 2014 in the American Water Works Association's journal, Dietrich et al. investigated whether a taste or color difference can in fact be detected at various manganese concentrations. Surprisingly, they found that consumers could not detect manganese even up to 1000 times the maximum amount allowed by the EPA. It is concerning that, given the current subjective methods of compound detection in drinking water, high amounts of manganese and other harmful compounds may be finding their way into our water (Dietrich, A., Griffin, A., & Sain, A. 2014).

Not only is tap water affected, but a study conducted in 2010 shows that even bottled water sometimes contains trace elements at levels significantly higher than what is normally accepted in drinking water. Long-term exposure to these toxins can lead to harmful effects on health. In this sense, it was found that bottled water is not in fact superior to municipal tap water (Cidu, R., Frau, F., & Tore, P. 2010).

Although we rarely think about the smell and taste of water, there are researchers devoting their careers to perfecting it. Recent findings on the pernicious effects of some aesthetic additives, as well as on the inability of current quality control methods to distinguish between safe and unsafe levels of these additives, should give us plenty of reason to consider the aesthetics of our water more carefully. More than ever, there is now a growing need to investigate the mysteries surrounding the monitoring, assessment, and treatment of our water, and to develop a more sophisticated system of detecting dangerous chemicals in it.

References

1. American Association for the Advancement of Science. So... do you know what is in your water? (2014, September 3). Retrieved February 13, 2015, from http://www.eurekalert.org/pub_releases/2014-09/vt-syk090314.php
2. Cidu, R., Frau, F. & Tore, P. (2010). Drinking water quality: Comparing inorganic compounds in bottled water and Italian tap water. Journal of Food Composition and Analysis, 24(2):184-193
3. Dietrich, A., Griffin, A., & Sain, A. (2014). Assessing taste and visual perception of Mn(II) and Mn(IV). American Water Works Association, 106(1): E32-E40. Retrieved from http://www.awwa.org/publications/journal-awwa/abstract/articleid/40068076.aspx
4. Environmental Protection Agency. (2012) An Introduction to Water Quality Monitoring. (n.d.). Retrieved February 13, 2015, from http://water.epa.gov/type/watersheds/monitoring/monintr.cfm
5. Lenntech Water Treatment Solutions. Demiwater and health. (n.d.). Retrieved February 13, 2015, from http://www.lenntech.com/health-risks-demineralized-water.htm
6. KIT Professionals. (2014). [Web Photo]. Retrieved February 13, 2015, from http://kitprofs.com/services/water/
7. Scott County Department of Parks, Library and Environment. Possible Health Effects of Drinking Contaminated Water. (n.d.). Retrieved February 13, 2015, from http://www.co.scott.mn.us/ParksLibraryEnv/water/Pages/PossibleHealthEffectsDrinkingContaminatedWater.aspx
8. United States Geological Survey. Drinking Water Exposure to Chemical and Pathogenic Contaminants. (n.d.). Retrieved February 13, 2015, from http://health.usgs.gov/dw_contaminants/
9. Virginia Community Colleges System. Lesson 9: Taste and Odor. (n.d.). Retrieved February 13, 2015, from http://water.me.vccs.edu/courses/env110/Lesson9_print.htm

science news

A Review of *Lost Antarctica: Adventures in a Disappearing Land*

Roxanne Lockhart

The icy, white, and forbidding continent Antarctica has captivated the imaginations of explorers and scientists for as long as it has been known. Now, UAB's own Dr. James McClintock has offered a way for the public at large to journey to this wondrous land without the cost of extreme weather gear, or even the need to leave home at all. McClintock's book, *Lost Antarctica: Adventures in a Disappearing Land*, is an informative and interesting memoir of his own extensive experiences at the far south of the world.

Dr. McClintock, Endowed University Professor of Polar and Marine Biology at UAB, is one of the world's leading experts on Antarctic marine biology. In the last thirty years, he has led no fewer than fourteen research expeditions to Antarctica. His work on the continent is so well recognized that he is the namesake of "McClintock Point," located on the north side of the entrance to Explorer's Cove on the Ross Sea—and a geographical guarantee that our professor's studies will never be "pointless."

Dr. James McClintock during a research expedition to Antarctica.

The memoir begins with Dr. McClintock describing his first visit to Antarctica, from passing the treacherous Drake Passage to observing the unique ecology. It goes on to describe not only Dr. McClintock's adventures, but also the science of how Antarctic organisms have evolved to survive and even thrive. With the coldest temperatures on planet Earth and three months without sunlight, Antarctica is all but uninhabitable for humans. Despite these conditions, unique wildlife still finds its niches on the continent. To name just a few species, Antarctica is home to leopard seals, whales, penguins, predatory worms, colorful fungi, sea stars, and even 50-foot algae.

In *Lost Antarctica*, Dr. McClintock also thoroughly explains the effects of climate change on this isolated and delicate ecosystem. As temperatures rise and ocean acidification increases, this unique and extremely fragile web of life is rapidly disappearing. Dr. McClintock's eloquent firsthand descriptions, in combination with his scientific expertise, help to make these threats to the continent he loves seem vivid and real even to those of us reading from half a world away. Bill Gates, Co-Founder and Chairman of Microsoft and Co-Chair of the Bill & Melinda Gates Foundation, wrote of the book's impact that "He [McClintock] issues a stark warning about the catastrophe facing this remarkable place—and our globe—from the twin dangers of climate change and ocean acidification. *Lost Antarctica* reminds us of the urgency of finding new energy systems that do not use our atmosphere or oceans as a waste dump."

For those not sated by reading alone, undergraduate and graduate students at UAB have the opportunity to travel to Antarctica each December on expeditions led by Dr. McClintock. Students visit Palmer Station and experience the continent's beautiful ecology firsthand. Undergraduate students must maintain a natural history journal throughout the voyage, recording observations of the myriad of organisms they will surely spot. If you explore with Dr. McClintock, you may find yourself completing assignments by watching a nine-foot leopard seal circling your Zodiac boat, a pod of orcas swimming past, or a playful penguin who waddles by to visit. Students are also able to record temperature changes throughout the journey with the help of the ship's captain and instruments. Particularly lucky travelers may even experience "Lake Drake," which is the name given to the most violent sea in the world, the Drake Passage, on the rare occasions when it is perfectly still. Along the journey, scientists and natural historians from around the world will join the adventure. Each day, students enjoy a scientific or historical presentation about Antarctic Research or Exploration delivered by these experts. Finally, throughout the journey, students observe for themselves the relationships among Antarctica's organisms, the remnants of past explorations, and the negative effects of climate change. Truly, these expeditions are adventures and learning opportunities at a scale that few other institutions can hope to provide.

Even if you are unable to travel to Antarctica through UAB, however, there is still Dr. McClintock's *Lost Antarctica* to transport you to this phenomenal land, in all its beauty, strangeness, and fragility. Its descriptions of adventure in Antarctica are awe-inspiring and thought-provoking, and its scientific perspectives on climate change are enough to create a sense of urgency in anyone who is interested in preventing the disappearance of the continent and its ecosystems.

References

1. "Lost Antarctica." Lost Antarctica. http://www.lostantarctica.com/
2. McClintock, J. (2012). Lost Antarctica: Adventures in a Disappearing Land. New York, NY: MacMillan. Print.
3. "UAB in Antarctica." UAB-CAS-Antarctica-Home. http://www.uab.edu/antarctica/
4. The University of Alabama at Birmingham. (2011). [Web Photo]. Retrieved October 15, 2014 from http://media.al.com/birmingham-news-stories/photo/9490395-large.jpg

"To Catch a Star on Your Fingertips" — A Review of *Madame Curie* (1943)

Marina Triplett

To the modern-day undergraduate researcher, the achievements of renowned scientific figures may seem daunting, and such legendary scientists may themselves appear to have been larger than life. Part of the value and fun of a good science film or book is that it can portray the wonder of what these titanic figures accomplished while still placing them in a human and relatable context. One film that succeeds in finding this balance is director Mervyn LeRoy's Academy Award-nominated *Madame Curie*, a 1943 biographical film depicting the discovery of radium by Marie and Pierre Curie. The film stars the incomparable Greer Garson in the title role and Walter Pidgeon as Pierre Curie in the fourth of nine movies that the pair made together. Both actors were nominated for Academy Awards for their portrayals of the famed Nobel Prize-winning husband and wife.

Marie Sklodowska began her scientific career in a way familiar to many researchers: as an undergraduate with stars in her eyes and dreams of becoming a full-fledged scientist. At the start of the film, Marie is a starving, "invincibly eager" student at the Sorbonne—France's oldest and, at the time, most prestigious university—with a passion for physics and mathematics. After her potential is noticed by one of her professors, she is invited to join the research lab of Pierre Curie, whom she later marries. While working in the lab, Marie becomes captivated by a pitchblende rock that produces large amounts of energy, believing that the emission must be caused by an undiscovered element she names "radium." After years of dedication and research, Marie and Pierre are able to successfully isolate radium from the pitchblende and are awarded the 1903 Nobel Prize for this discovery.

One of the film's greatest achievements is its ability to convey scientific terms to a lay audience and to provide an accurate depiction of the sustained toil that scientific research demands. Though the film was made during the Golden Age of Hollywood, it does not glamourize the research process or ignore the hard science behind the discovery of radium. Rather, it acknowledges the research process as long, arduous, and uncertain, but also rewarding. Unable to obtain funding for their research, the Curies claim a dilapidated, unequipped shed to serve as a laboratory, where they labor for years under extreme conditions with the goal of separating all elements from the pitchblende rock until nothing but radium remains. The science behind each step of the process is explained in a way that is interesting and easy to understand. The movie's most powerful scene depicts the Curies in their "lab" performing thousands of dilutions to accomplish the nearly impossible task of separating barium from radium as the camera slowly pans across a room of thousands of evaporating dishes. This scene perfectly captures the enormous effort and perseverance that the Curies displayed in advancing their project, and it also shows that scientific research requires years of trial and error and that success—despite the storytelling appeal of "Eureka" moments—almost never occurs overnight. Even when discovering that the pitchblende is causing burns on her fingertips that may one day become cancerous, Madame Curie remains undeterred and refuses to give up her dream of isolating radium. After four and a half years, eight tons of pitchblende, and 5,677 crystallizations, radium is finally isolated—and the rest is history.

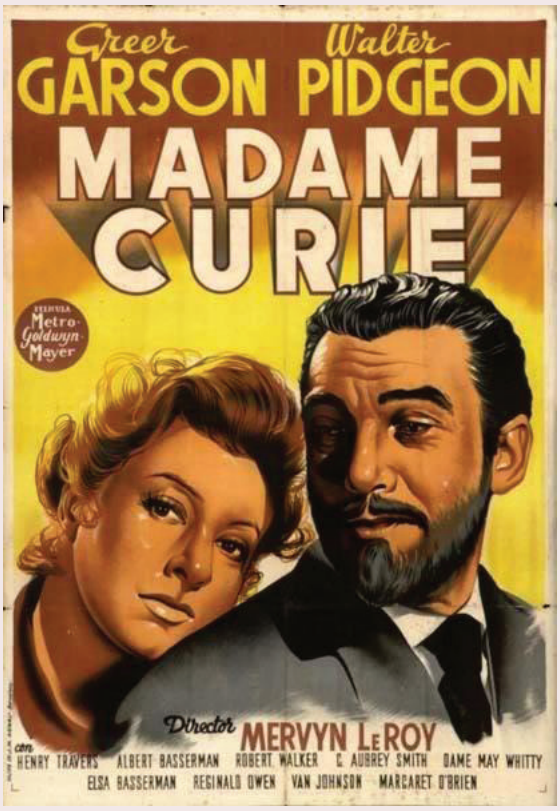

An original movie poster advertising Madame Curie before its 1943 release.

In addition to illustrating the hard work and determination required of a research scientist, *Madame Curie* serves as a commentary on a subject as pertinent today as it was in the early 1900s: the role of women in science and technology. In the time of Marie Curie and in the time during which the film was made, women were widely perceived as being socially inferior to men, and were expected to serve as housewives and mothers. Even in today's society, women scientists

often must overcome discrimination and gender bias in the workplace. In the beginning of the film, Pierre Curie refers to science, by definition, as a constant "struggle against woman." In his apprehension to allow Marie to work in his laboratory, Pierre dramatically refers to women as a "danger," a "distraction," and a "natural enemy of scientists." Though we know this viewpoint to be illogical, we cannot ignore the fact that female scientists throughout history have had to overcome societal obstacles to gain esteem and recognition in their fields. As the number of women pursuing careers in STEM fields continues to grow, the scientific community must remember that recognition should be based on merit, not gender. Even today, women in science often face a unique struggle to maintain a work-life balance, and a pressure to choose between marriage and a family or a scientific career. Some women consider science and marriage to be, as stated by Pierre in the film, "incompatible." Yet *Madame Curie* answers by showing its title character for all she was: a wife, mother, and scientist—an embodied proof that women belong in science.

Just as Curie herself was multifaceted—working at the highest level in both physics and chemistry, and balancing life in the home and lab—LeRoy's film about her is of broad interest: it is well worth watching for anyone who wishes to learn more about science and its history, for aspiring researchers, and especially for women who wish as Curie did to compete in fields that are traditionally male-dominated. And although this year marks the 80th anniversary of Curie's death, her legacy as one of the greatest scientists in history lives on through the film, helping to ensure that her contributions to the fields of physics and chemistry will not be forgotten. As the scientists of the future, it is important that undergraduate researchers understand the scientific discoveries of the past and recognize the important figures in history that have brought us to where we stand today. It is also important that we recognize in Madame Curie the qualities that anyone who hopes to be a great scientist should strive to emulate: persistence, curiosity, and a relentless passion for learning more about the world around us.

A still from the film, showing Greer Garson and Walter Pidgeon as Madame and Pierre Curie attempting the refinement of the pitchblende rock.

References

1. Madame Curie. Dir. Mervyn LeRoy. Perf. Greer Garson, Walter Pidgeon, and Henry Travers. Metro-Goldwyn-Mayer, 1943. Film.
2. Madame Curie Film Poster. [Web Photo]. Retrieved November 22, 2014, from http://imgbuddy.com/madame-curie-movie.asp
3. Madame Curie Film Still. [Web Photo]. Retrieved November 22, 2014, from https://hepburnia.wordpress.com/2012/12/03/madame-curie-dec-3-315-pm-est/

science news

A "Cooler" Approach to Long-Term Organ Preservation

Susmita Murthy

From the first procedure in 1954, the almost miraculous procedure of organ transplantation has been critical to the development of modern medicine and surgery, and it is in wide use today to give individuals a new lease on life. However, clinicians and researchers have encountered several persistent problems with organ transplantation through the last 60 years that have prevented some patients from getting the happy ending they were promised. In addition to donor organ rejection and the perpetual shortage of organs available for transplant, a major issue is the brief lifetime of organs once removed from the donor's body—typically only 24 hours. Because of this short window for usage, thousands of organs go to waste every year. The United Network for Organ Sharing estimates that, on average, 3,881 organs

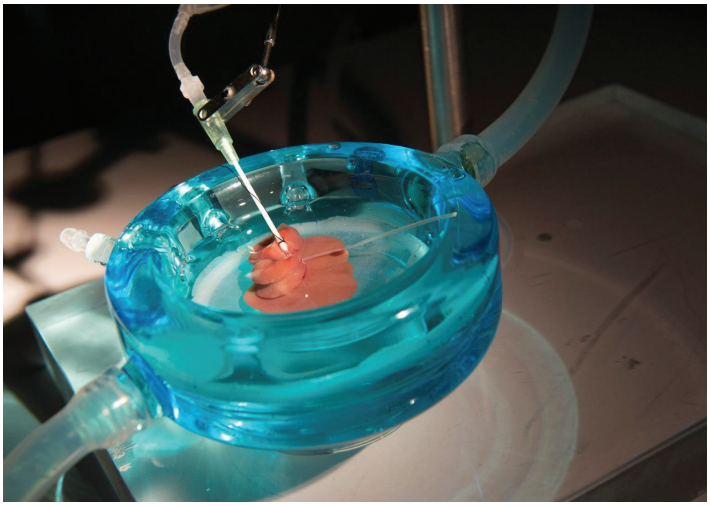

A rat liver being "supercooled" using the machine perfusion system developed at Harvard University.

are discarded every calendar year (Sack, K. 2012). Imagine a world in which such donor organs would never go to waste: one in which organs could be preserved indefinitely before being transplanted into dying patients. This lofty goal is the focus of much of the recent research in the field of organ transplantation.

In 1988, Folkert O. Belzer and James H. Southard from the University of Wisconsin-Madison developed the current, accepted method of organ preservation: a cold storage liquid known as the "UW solution" (Belzer, F.O., & Southard, J.H. 1988). Designed first for pancreas preservation, the solution is often hailed as the best method of organ preservation to date (Guibert, E.E. 2011). The UW solution mimics the body's internal conditions, and the solutes contained in the cold water prevent the organ from undergoing swelling or crenation (a type of undesirable shape change due to osmotic water loss) (Belzer, F.O., & Southard, J.H. 1988). Though the UW solution was a leap forward in organ preservation techniques, it is only able to keep organs viable for up to 24 hours outside of the body (National Institutes of Health 2014). Belzer and Southard also attempted to cool the temperature of their water solution in order to keep the organs viable for longer, but below certain temperatures the solution began to form ice crystals that created holes in the organs (Belzer, F.O., & Southard, J.H. 1988).

To combat this weakness of the UW solution, a team of researchers and doctors at the Massachusetts General Hospital in Boston developed a preservation technique dubbed "supercooling." In this experiment, a rat liver was cooled to about 21 degrees Fahrenheit and, utilizing machine perfusion, a solution was pumped through the organ. This solution consisted of water and a modified glucose compound which lowers the freezing point of the liquid water around the organ and prevents the cell membranes from lysing (Berendsen, T.A., et al. 2014). After this solution was delivered to the liver cells, the organ slowly cooled without freezing. The livers were then stored for a variable number of days, rewarmed, and transplanted into rat subjects. The supercooling technique allowed the researchers to extend the 24-hour organ viability window substantially: in 32 rats transplanted with supercooled livers that were stored for four days, the survival rate was 58 % (Berendsen, T.A., et al. 2014). Even more remarkably, rats that received livers that had been supercooled for three days had a 100 % survival rate (Berendsen, T.A., et al. 2014).

Expanding upon the existing methods of organ preservation, the researchers in Boston have developed a technique that keeps organs viable for up to two days longer than traditional methods. The next step for these researchers will be to test the supercooling technique in larger organisms and various other organs. The longer donor organs can be stored, the better chance there will be to find the best possible match for a patient. Thus, advances in organ preservation will not only reduce waste, but may also help to ameliorate problems with rejection. While the new technique is only the next step towards an approach that might someday allow the preservation of organs for indefinite periods of time, two days, for now, will be more than enough to make the difference between life and death for many patients awaiting transplants.

References

1. Belzer, F.O., & Southard, J.H. (1988). Principles of Solid-Organ Preservation by Cold Storage. Transplantation, (45)4, 673-676.

2. Berendsen, T.A., et al. (2014). Supercooling enables long-term transplantation survival following 4 days of liver preservation. Nature Medicine, (20), 790-793.

3. Guibert, E.E., et.al. (2011). Organ Preservation: Current Concepts and New Strategies for the Next Decade. Transfusion Medicine and Hemotherapy, (38)2, 125-142.

4. Reeves, W., Uygun, K., & Yarmush, M. Harvard University. [Web Photo]. Retrieved December 12, 2014 from http://www.livescience.com/46596-supercooling-technique-liver-preservation.html

5. National Institutes of Health. (2014). NIH-funded researchers extend liver preservation for transplantation. Retrieved October 28, 2014 from http://www.eurekalert.org/pub_releases/2014-06/niob-nre062614.php

6. Sack, Kevin. (2012). In discarding of kidneys, system reveals its flaws. The New York Times. Retrieved October 28, 2014 from http://www.nytimes.com/2012/09/20/health/transplant-experts-blame-allocation-system-for-discarding-kidneys.html?pagewanted=all&_r=0.

The Effects of Politics on the Efficacy and Efficiency of Research

Emily Jennings

The long shadow of global terrorism has been an almost incessant feature of American media coverage for the last decade, even though the chance of dying in the United States as a result of a terrorist attack was only 1 in 20 million from 2007-2011 (Time Magazine 2013). In contrast, the number one cause of death in the United States, heart disease, has garnered substantial media coverage only a couple of times each year. Accounting for 1 in every 4 deaths and a total of 600,000 deaths every year in the United States, heart disease is one of the biggest public health issues our nation has faced to date (Centers for Disease Control 2014). The rising cost of healthcare only serves to exacerbate the problem.

Coronary heart disease alone costs the U.S. $108.9 billion each year (Centers for Disease Control 2014). Many other diseases also contribute greatly to costs in money and health: Alzheimer's disease cost the United States $150 billion in 2014 and is estimated to affect 5.2 million Americans (Alzheimer's Association 2014); cancers are projected to cost the United States $158 billion in 2020 (National Institutes of Health 2011).

The numbers alone demonstrate quite obviously how much more harmful and costly disease is to the average American than terrorism. Despite this, the 2015 United States Fiscal Year Budget included only $135.4 billion proposed for federal research and design (White House Office of Science and Technology 2014), while $495.6 billion was proposed for the Department of Defense. The latter figure is second only to the $710 billion proposed for the Small Business Administration (White House Office of Management and Budget 2014). The purpose of these facts is not to say that the lives of some Americans—those lost to disease rather than defense issues—are more important than others. Rather, given the responsibility of politicians to represent the general public and lead the country with their best interests in mind, it is to point out that more Americans are directly affected by issues related to health and science than by those related to defense, and thus that American spending is in many ways out of line with the realities of the dangers that Americans face. For this reason, it is important that science is adequately represented to politicians.

Scientific investigation is the first step to solving the problems that affect many Americans, because it is through scientific research that medical advances are achieved, reducing the number of Americans affected by diseases as well as the costs of treatment. New treatments and knowledge that result from scientific research, however, do not appear overnight; it takes years of data collection, analysis, and failed experiments to make a scientific breakthrough. Billions of dollars (federal and private) put into research may disappear quickly, but the philanthropic contributions and grants are not wasted. Though not all research leads to new forms of treatment or other breakthroughs, it is precisely the unpredictability and slowness of progress that demands a continuous and patient stream of funding (Dobrunz 2014). This is where the role of a researcher in relation to scientific advances needs a closer look.

An aerial view of the Mark O. Hatfield Clinical Research Center on the Bethesda, MD main campus of the National Institutes of Health. The NIH, which supports much biomedical research in the United States, has had to contend with stagnant budgets in recent years.

Many scientific investigators spend much more time writing grants than they do working in the lab. An interview with Dr. Lynn Dobrunz, a neurobiologist at UAB's Evelyn McKnight Brain Institute, revealed that it has become significantly more difficult to obtain funding within the last 15 years, as the percentage of grant applications funded has dropped from an estimated 25-30 % to an estimated 10 % nationally. This decrease in the chance of receiving funding has caused researchers to spend ever more time writing and refining grant applications. According to Stuart Campbell, a bioengineering professor at Yale University, grant applications must be "basically perfect" to stand a chance in the competition today (Gersten 2014). Dr. Dobrunz agreed with this statement, adding that some researchers dedicate more than half of their time to the grant application process, because multiple grants must be applied for in order to increase the chance of funding.

To further increase the chance of receiving funding, some scientists even go so far as to change the interests of their labs. For example, an article posted by *Yale Daily News* noted that a genetics and dermatology professor at the Yale School of Medicine switched from her interest in researching cancer pathology to researching cancer treatment, an area that was not necessarily where her passion lay, but one in which more funding is available (Gersten 2014). According to Dr. Dobrunz, similar instances have occurred at UAB, including in her own lab: "We started out as a lab studying how the brain works, but are now more focused on disease models, which is still somewhat studying how the brain works, and is still fun." Though some researchers can adapt in this way, a system that forces such homogenization of approaches is not in the best interests of society; history has shown that progress often comes from unexpected directions and basic, curiosity-driven explorations.

Many scientists are willing to sacrifice time spent working in the lab for the purpose of writing grants, while others are not as inclined to step away from the bench. According to Dr. Dobrunz, some scientists decide to find employment at pharmaceutical companies (which can pull the plug on their employees' projects and switch them to new ones at any time) just to avoid spending the majority of their time writing grants. Although these scientists are free from applying for funding, they are often deprived of their intellectual freedom (Dobrunz 2014). Despite the continuous decrease in funding for research, Dr. Dobrunz assures that, "these things are cyclic. When I was in grad school, funding was reduced, but it increased again a few years later."

Although the funding trend is cyclic, the current situation may not follow the previous cycles. According to Dr. Dobrunz, "The problem with this downturn of funding is that it has lasted for so long, and does not seem to be headed toward improving anytime soon." Many talented scientists have either switched to new interests or working environments or left the scientific community for good before they would otherwise have retired, as a pathology professor and the director of graduate admissions for Yale's microbiology program did this past June (Gersten 2014).

The United States can afford neither to lose scientists nor to limit their imaginations and efforts. Scientists need to remain in academia in order to train the next generation of investigators, and they need to be able to devote more time to guiding their lab's research in person if it is to be its most efficient. More funding would solve both of these problems and reduce the pressure towards homogenization. As Dr. Dobrunz explains, "If researchers are spending more time in their labs than writing grants, the research will be more efficient." Now, with a population that is aging and suffering from skyrocketing rates of issues such as obesity and diabetes, it is as critical as ever that politicians be aware of the problems facing America's researchers and patients. For many Americans, quality and length of life depends on it.

References

1. Alzheimer's Association. (2014). Use and Costs of Health Care, Long-Term Care and Hospice. In 2014 Alzheimer's Disease Facts and Figures, 43. Retrieved November 2, 2014 from http://www.alz.org/downloads/Facts_Figures_2014.pdf

2. Centers for Disease Control. Heart Disease Facts. (2014, September 26). Retrieved November 1, 2014 from http://www.cdc.gov/heartdisease/facts.htm.

3. Dobrunz, L. (2014, Oct 22). Interview by E. Jennings.

4. Gersten, J. (2013, April 23). Researchers navigate funding tempest. Yale Daily News. Retrieved October 29, 2014 from http://yaledailynews.com/blog/2014/04/23/researchers-navigate-funding-tempest/.

5. National Institutes of Health. Cancer costs projected to reach at least $158 billion in 2020. (2011, January 12). Retrieved November 2, 2014 from http://www.nih.gov/news/health/jan2011/nci-12.htm.

6. National Institutes of Health. (2014). NIH Campus Photos. [Web Photo]. Retrieved November 2, 2014 from http://www.ors.od.nih.gov/pes/dma/express/Pages/express_aerial.aspx

7. Time Magazine. Numbers: 1 in 20 million. (2013, May 6). Retrieved November 1, 2014 from http://swampland.time.com/2013/05/06/chances-of-dying-in-a-terrorist-attack-number/.

8. White House Office of Science and Technology. (2014, March). The 2015 Budget: Science, Technology, and Innovation for Opportunity and Growth. Retrieved November 1, 2014 from http://www.whitehouse.gov/sites/default/files/microsites/ostp/Fy %202015 %20 R&D.pdf.

9. White House Office of Management and Budget. (2014, March). Department of Defense. In Fiscal Year 2015 Budget of the United States Government, 57. Retrieved November 1, 2014 from http://www.whitehouse.gov/sites/default/files/omb/budget/fy2015/assets/budget.pdf.

Schizophrenia: An Entire Orchestra at Play

Hriday Bhambhvani

Schizophrenia affects about 0.5-1.0 % of the population at any one point in time, and the incidence is fairly homogenous from country to country. Individuals with schizophrenia typically exhibit both positive and negative behavioral symptoms—that is, the presence of some behaviors that are considered abnormal as well as the absence of some that are considered normal. Positive symptoms may include delusions of grandeur, auditory or visual hallucinations, and incoherent thought and speech. Negative symptoms include lack of typical emotional responses, flat affect, and lack of motivation.

The pathophysiology of schizophrenia is not completely understood, though it is generally accepted that the disorder arises as a result of dysregulated neurotransmitter systems. In particular, faulty dopaminergic and glutamatergic neurotransmission has been implicated. Furthermore, the risk of developing schizophrenia is known to be elevated in individuals with certain genetic predispositions. However, the specific genetic architecture underlying schizophrenia is not known.

In a recent study at Washington University in St. Louis School of Medicine, researchers completed a large-scale genetic study including more than 4,000 individuals with schizophrenia and 3,800 healthy individuals for comparison. They identified several specific "gene clusters," which they concluded may be associated with eight distinct phenotypic variants of schizophrenia. By matching any individual's genetic variations with that individual's specific symptoms, the team of researchers was able to delineate these separate classes of schizophrenia, a disease for which attempts at subclassification have historically been difficult and controversial. Specifically, the researchers looked for sets of a certain type of genetic variant known as a single-nucleotide polymorphism (SNP). This ad hoc grouping of SNP sets yielded 42 sets associated with at least a 70 % risk of schizophrenia. In total, 2891 SNPs were analyzed out of a total of 696,788; these 2891 were pre-selected based on their degree of association (p-value < 0.01) with a "global phenotype of schizophrenia" (Arnedo, J., et al. 2014).

Such a separation of schizophrenia into different disorders based on underlying genetic factors is potentially desirable for many reasons. In particular, it may enable prediction of the onset of schizophrenia, and thus increase the ability of healthcare providers to provide effective treatment. This refinement of a broad diagnostic category into subclasses is not a new idea in the field of mental illness; many other psychiatric illnesses are thought to have an underlying heterogeneity similar to that now believed to exist in schizophrenia.

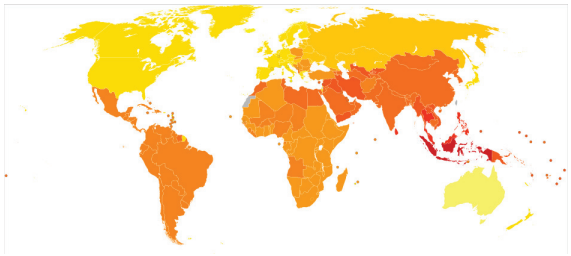

A color-coded world map showing the global disease burden of Schizophrenia in terms of Disability-Adjusted Life Years, i.e., years of "healthy" life lost due either to early death or to living with disease, per 100,000 people. Burden ranges from yellow, at fewer than 185, to red, at more than 295.

Dr. C. Robert Cloninger, one of the principal investigators of the Washington University in St. Louis study, has been widely quoted on his statement regarding the nature of genes: "Genes don't operate by themselves. They function in concert much like an orchestra, and to understand how they're working, you have to know not just who the members of the orchestra are but how they interact." The rise of genome-wide association studies such as Cloninger's have facilitated research regarding the dynamic interplay of genes and "allowed the identification of individual genetic risk loci or at least markers linked to them" (Wray, N.R. & Visscher, P.M. 2010).

Recent work from other labs has complemented this increased understanding of schizophrenia's diagnostic subclasses with an increased understanding of its etiology. A study published in the journal *Nature* this past summer showed as many as 108 genes that may play into the onset and pathophysiology of schizophrenia, though it is difficult to ascertain which of these put otherwise healthy individuals at risk of developing the disorder (Schizophrenia Working Group of the Psychiatric Genomics Consortium 2014).

Often, neuropsychiatric illnesses lack a determinant phenotype. This is particularly true for schizophrenia, a disorder for which there are neither firm diagnostic tests nor a simple neuropathology. As such, large molecular genetic studies are often the most effective approach for identifying risk loci across the wide gamut this disorder runs. Such studies further the possibility of eventually identifying certain clinical syndromes by their underlying etiology. In turn, this makes person-centered treatment of complex disorders an

increasingly plausible mode of day-to-day clinical psychiatry in the near future.

References

1. Arnedo, J., et al. (2014, September 15). Uncovering the Hidden Risk Architecture of the Schizophrenias: Confirmation in Three Independent Genome-Wide Association Studies. Am J Psychiatry. [E-print].

2. Schizophrenia Working Group of the Psychiatric Genomics Consortium (PGC-SCZ). (2014). Biological insights from 108 schizophrenia-associated genetic loci. Nature. In press.

3. World Health Organization. (2004). [Web Photo]. Retrieved October 11, 2014 from http://en.wikipedia.org/wiki/Epidemiology_of_schizophrenia#/media/File:Schizophrenia_world_map_-_DALY_-_WHO2004.svg

4. Wray, N.R. & Visscher, P.M. (2010). Narrowing the boundaries of the genetic architecture of schizophrenia. Schizophr Bull, 36(1), 14-23

science news

A Review of *The Anatomy of Violence: The Biological Roots of Crime*

Tamara Imam

In a world chronically plagued by crime, Adrian Raine's *The Anatomy of Violence: The Biological Roots of Crime* (Vintage Books) offers a unique perspective on the causes of violence in human beings.

The book begins with a critique of nineteenth-century physician and criminologist Cesare Lombroso, whose radical anthropological and criminological theory held that criminals are born as such and can be identified by primitive physical features even before they commit any criminal acts. While Lombroso's theory has been widely rejected as racist and eugenic, Raine claims that Lombroso was not all wrong or, at least, was not pursuing a fruitless goal when he attempted to link criminal behavior and biology. Rather, Raine stakes out a position that is somewhat more nuanced: while stopping well shy of the exaggerated predictive power and coarse classifications of Lombroso, he deviates from the archetypal Freudian explanations of immorality and makes a compelling argument that human tendencies towards violence have a biological component that cannot be ignored, even if it does not tell the whole story.

In the classic nature vs. nurture argument, we have often heard that genetic inheritance influences a person's demeanor. Studies of identical twins reared in disparate environments reveal that a large number of them exhibit very similar behaviors and lead very similar lifestyles, including with respect to criminal activity. Raine advances on this common knowledge by bringing together and discussing a list of specific genes, such as monoamine oxidase A (MAOA) or the "warrior gene," that have been correlated with violent behaviors.

Raine also makes a case for a physiological basis of violence in humans. Where most criminology is focused on discrepancies in brain function between violent offenders and normal controls, Raine goes several steps further by examining other vital organs such as the heart.

The author, Adrian Raine, at his University of Pennsylvania office. Raine is the Richard Perry University Professor and Chair of the Department of Criminology and also holds appointments in the Departments of Psychology and Psychiatry.

At times, however, Raine overestimates statistical relationships when doing so is convenient and in the interest of his book. At several points, he suggests that the findings he discusses represent direct causal relationships rather than correlations, without offering any compelling data or hypotheses on a causal pathway. Low resting heart rate, according to Raine, is characteristic of psychopaths and in some way explanatory of their behavior. Such misrepresentations, while unfortunately not uncommon in popular science writing, are regrettable for the way that they cloud the public's understanding of research.

Raine concludes *The Anatomy of Violence* with a description of a hypothetical society set in 2034 that treats violence as a disease characterized by obvious biomarkers, not unlike cancer. He envisions a world in which a number of brain imaging and physiological tests are used as diagnostic tools for potential psychopaths who can then be treated proactively—before they become violent offenders. Surely this is an intriguing idea, even if its achievement by 2034 is more than a bit optimistic.

For its occasional exaggerations, *The Anatomy of Violence* is

not a book that one can read once and simply put back on the shelf to collect dust. It is fresh, controversial, and sure to spark debate among readers.

References

1. Raine, A. (2014). The Anatomy of Violence: The Biological Roots of Crime. New York, NY: Vintage Books.
2. Faculdade Unidas de Feira de Santana. [Web Photo]. Retrieved December 3, 2014 from http://www.fufs.edu.br/noticia.php?codnoticia=359

science news

Understanding and Detecting Frontotemporal Dementia

Aashka Patel

Through the biological functioning of the brain, an organ like any other, all our decisions, actions and perceptions are generated and mediated. From birth, the brain allows us to coordinate and perform complicated tasks, as well as take part in learning, speaking, and interpreting the world around us. As the human brain ages past middle life, however, it gradually starts to deteriorate and become more susceptible to neurodegenerative diseases. One such disease with a particularly great impact is frontotemporal dementia (FTD).

FTD, part of the larger category of dementias, itself serves as an umbrella term used to describe any neurodegenerative disease that affects the frontal lobe and results in cognitive decline. The age of onset and progression of the disease are variable, but it typically strikes its victims at a younger age and causes their deaths sooner than Alzheimer's Disease, the largest single cause of dementia. Multiple forms of FTD exist, but the three major forms are behavior variant FTD, semantic primary progressive aphasia, and agrammatic primary progressive aphasia. Of these, behavior variant FTD is the most common. It is linked to impulsivity, personality changes, disinhibition, apathy, lack of empathy, repetitive compulsive behavior, and dietary changes (Rascovsky, K., et al. 2011). The semantic variant of primary progressive aphasia features a loss of word comprehension as its primary symptom. One example of such a deficit in a semantic primary progressive aphasia patient would be for him or her to forget the word "match," but remember the object it represents and its function—making fires. The other aphasic FTD variant, agrammatic, includes speech problems that worsen over time, leading eventually to mutism.

The onset of FTD is strongly influenced by genetics. Seven different genetic links to FTD have been found, of which three are thought to be the predominant contributors. These genes—GRN, tau, and C9ORF72—are associated with half of all cases. The protein product of GRN is Progranulin, which is found in neurons and microglia, the computational and immune cells of the brain, respectively (Filiano, A.J., et al. 2013). Microglia are present in areas where inflammation is present, and Progranulin is known to have anti-inflammatory

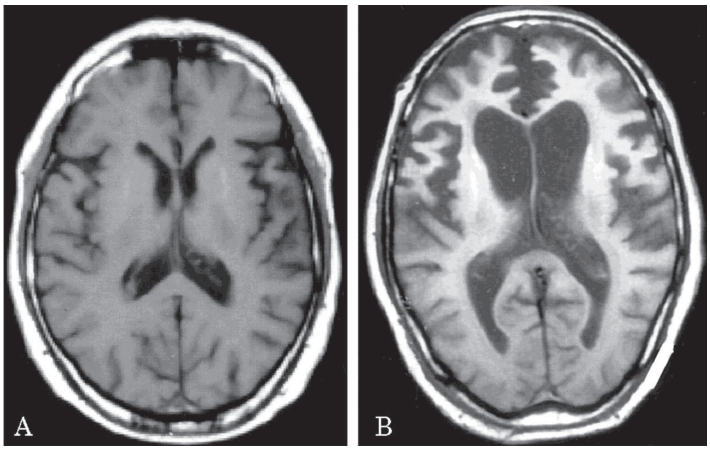

Two radiographs of the brain of a man suffering from FTD, obtained using Magnetic Resonance Imaging. The left panel, taken at age 37, shows essentially normal anatomy. The right panel, taken three years later at age 40, shows the profound, relatively rapid, and relatively early-onset atrophy associated with FTD.

properties and to be secreted as a growth factor. Its absence or deficiency has been linked to FTD. Tau, a microtubule binding protein produced by the tau gene and believed to be dysfunctional in Alzheimer's Disease, also gathers abnormally in the brains of FTD patients (Roberson, E.D. 2012). C9ORF72, also known as C9, has only been associated with FTD relatively recently, and its dysfunction in the disease is not yet well understood (Arrant, A.E. 2014).

In order to study FTD, mouse models are often used. Though mice obviously differ from humans in many respects, their brains show patterns of expression for many proteins that are very similar to those in human brains, and they provide for a faster, easier, and more controllable way to study human disease by analogy (Roberson, E.D. 2012).

At UAB, Dr. Erik Roberson's lab is involved in using mouse models to determine a phenotype that will help doctors and patients to identify FTD even before its cognitive symptoms first become noticeable. Through their research, they have

determined that retinal thinning is an indication of possible FTD (Ward, M.E. 2014). Specifically, a deficiency of the protein TDP-43 (TAR DNA/RNA binding protein 43) in the nuclei of neurons is associated with retinal thinning; by using mouse models to probe this connection, the Roberson lab was able to link the loss of TDP-43 to FTD (Ward, M.E. 2014). Because Progranulin knockout mice studied in the Roberson lab showed a pathology resembling FTD, as well as TDP-43 deficiencies and retinal thinning, it is possible that retinal thinning can come into use by clinicians as a valuable, easy to observe, and early sign of impending FTD in humans.

Giving healthcare professionals the ability to predict and diagnose neurodegenerative diseases such as FTD earlier and with greater accuracy is a vital step forward in providing care for these devastating and relatively common diseases. Furthermore, awareness of such advances allows patients to gain a peace of mind regarding their health, and feeds public support for further research initiatives that may one day provide cures and preventions for FTD and other diseases.

References

1. Arrant, A.E. Postdoctoral fellow in the Roberson lab, UAB. (2014). [Personal Communication]
2. Filiano, A.J., et.al. Dissociation of Frontotemporal Dementia–Related Deficits and Neuroinflammation in Progranulin Haploinsufficient Mice. (2013). The Journal of Neuroscience (33)12, 5352-361.
3. Neurology. [Web Photo]. Retrieved February 1, 2015 from http://www.neurology.org/content/55/8/1224.figures-only
4. Rascovsky, K., et.al. Sensitivity of Revised Diagnostic Criteria for the Behavioural Variant of Frontotemporal Dementia. (2011). Brain: A Journal of Neurology, (134)9, 2456-477.
5. Roberson, E.D. Mouse Models of Frontotemporal Dementia. (2012). Annals of Neurology, (72)6, 837-49.
6. Ward, M.E. Early Retinal Neurodegeneration and Impaired Ran-mediated Nuclear Import of TDP-43 in Progranulin-deficient FTLD. (2014). Journal of Experimental Medicine, (211)10, 1937-945.

narrative

Research in a Setting that Hits Home

Ramsha Farrukh[1], Emil Kurian[2], and Jessica Maya[2]

[1]Department of Neurobiology, University of Alabama School of Medicine, Birmingham, AL, USA
[2]Department of Biology, University of Alabama at Birmingham, Birmingham, AL, USA

Birmingham is a town that owes a lot to carbon and to the energy that's released when it is combusted in the form of coal. That includes the city's two principal nicknames: the Magic City, for its rapid growth centered around heavy industry; and the Steel City, for the products that flowed out of its foundries and into the factories and infrastructure of the South and beyond. Yet harnessing this fossil fuel energy also became—and continues to be—dangerous for Birmingham. We learned first-hand about this issue at the intersection of history, science, medicine and economics as we explored some residential areas in North Birmingham that are surrounded by coke factories. Coke is a byproduct of a coal burning process that seeks to remove the volatile compounds from coal, making it richer in carbon, but also releases harmful toxins like sulfur dioxide, benzene, and particulate matter into the air. From a biological and chemical standpoint, we knew that benzene is a carcinogen at high enough doses, particulate matter causes lung irritation, and high concentrations of sulfur dioxide can lead to lung inflammation. But as we ventured into the communities of North Birmingham, hearing stories of serious health ailments that seemed to be unlike those faced by any other populations we knew, we began to learn to see these lessons from our classes in real and human terms. This mix of engagement with our local communities and application of our scientific knowledge also helped us to understand the critical thinking skills that are necessary to sort out the many connections involved in any real-world issue of health, science and policy.

Since the environmental movement began to gain ground in mainstream America in the 1960s and 1970s, citizens, scientists, and industrial leaders have increasingly realized that unmitigated pollution is not a sustainable or desirable system. As a result, the array of technologies available to reduce pollution and remediate environments has grown rapidly in the last few decades. However, our experiences in North Birmingham reminded us of an important fact: technology alone, without economic motivation and political will to implement it, cannot solve the pollution problem. Since the 1970s, the Clean Air Act has provided regulations regarding the maximum amount of certain types of emissions that can be created in a given area and forced industries that exceeded these regulations to incorporate technology such as scrubbers, which are used to remove particulates and gases from industrial exhausts in a selective manner. In many parts of the country with histories of industry and pollution similar to Birmingham's, such as North Carolina, air monitors have also been used to record the levels of specific pollutants over time. Many companies, however, see the implementation of these protective measures as a financial burden; in North Birmingham, a number of coal companies refused even to

install scrubbers until the EPA intervened, long after these technologies should have begun curbing the pollution of our communities. Such a lack of responsibility and concern within these companies directly affects the communities that lie just down the street, where their employees and others live. Scientific and engineering innovation can only do so much. Without the infrastructure, effective regulations from the government, and a sense of stewardship on the part of polluters, communities built around heavy industries will continue to pay a price.

The enforcement of regulations, the implementation of technologies, and even the initial scientific discoveries, in turn, all rely on steady and substantial public funding, as well as pressure on political leaders. Our experiences in North Birmingham allowed us to see all of these connections in action and led us to develop a long-term plan for resolving the pollution problem modeled off of the Central Dogma of biology. This dogma states the process involved in creating biomolecules from DNA to RNA to protein. In comparison, our Central Dogma of action on pollution is a process that moves in stages from awareness to advocacy to implementation. The first step in addressing the pollution problem is to raise awareness of it, educating people and getting them to acknowledge the reality and significance of the issue at hand. As awareness increases and the ill effects of pollution continue to accumulate, advocacy and pressure will grow, and political and economic systems will respond by bringing more resources to bear on the problem. Moving beyond this simple conceptual framework, we sought to implement it on a local scale. To this end, we conducted a general survey of pollution awareness using the undergraduate students of UAB as a population. Of the 200 students we surveyed, a majority did not know the extent to which pollution is a problem in Birmingham, nor the extent to which pollution can travel from its source. This lack of understanding raised concerns about scientific literacy and awareness of current events, and we plan to focus next on measuring the scientific literacy of the UAB undergraduate population. As we continue to move through this data-collection process, we will have opportunities to refine and specify our conceptual model and will begin to understand how a pollution-mitigation approach might be tailored to work best in Birmingham.

Often in scientific research we assume that the most pressing and important problems are the most publicized ones and those that are largest in scale. However, when we step out into our very own communities, we realize that local problems can be just as urgent and complicated, and also demand significant thought and effort. The issue of pollution in Birmingham is multi-faceted and interfaces with government, economics, and medicine. Therefore, its solution will require a diverse array of professionals working together to tackle the problem. As a broad-based research and medical center with major ties to its surrounding communities in the forms of healthcare, investment, and employment, UAB is uniquely situated to contribute to this effort. Its students, faculty, and administrators should consider how they can help by bringing their talents and resources to bear on improving our communities and turning Birmingham into a positive example of environmental change and responsibility for the rest of the country and world.

short report

Hydrolysis Studies of cis-Disubstituted Tetracarbonylmolybdenum(0) Complexes with Binaphthol-based Chlorophosphite Ligands

Rachel Davidson, Samantha D. Hastings, and Gary M. Gray

Department of Chemistry, University of Alabama at Birmingham, Birmingham, AL, USA

Abstract

Catalysts are used in industry to increase efficiency in large-scale production of chemical products. Hydroformylation reactions involve the conversion of alkenes to aldehydes through the addition of carbon monoxide. This process involves the use of a transition metal catalyst.

Asymmetric catalysts are of particular interest because they are used in the pharmaceutical industry to produce racemically pure products. Transition metal complexes with axially chiral (binaphthoxy-based) phosphite ligands are some of the best complexes for producing an enantiomeric excess in hydroformylation reactions of alkenes. Model metal complexes containing these ligands are of interest in identifying possible structure-activity relationships.[1-8]

This report describes the characterization of cis-disubstituted tetracarbonylmolybdenum(0) complexes with binaphthol-based chlorophosphite ligands, which can be considered the parent for many of the complex ligands used in the catalysts. To determine the effect of altering the biaryl groups, the complex has been compared to the biphenol chlorophosphite analog.[9] The hydrolysis of cis-$Mo(CO)_4$(**1**)$_2$ is in some ways similar to the hydrolysis of the biphenol-based analog in that the observed product, when excess reagents are used, is the dianion and that an equilibrium exists between the

monoanion of the hydrolysis product and the dianion of the hydrolysis product. However, cis-$Mo(CO)_4$(**1**)$_2$ does not appear to be as reactive towards water, as no product is formed when stoichiometric ratios of reagents are added. Additionally, the equilibrium between monoanion and dianion may lie more towards the dianion for this complex.

Introduction

Transition metal-catalyzed asymmetric synthesis is often used in industry to produce racemically pure products. This process is increasingly important, as the U.S. Food and Drug Administration requires that pharmaceuticals be racemically pure before they are approved. Many of the catalysts that perform asymmetric transformations well consist of phosphorus-based ligands containing binaphthol moieties. A common precursor of many of these ligands is phosphochloridite ester (**1**), shown in Figure 1. The coordination chemistry of the precursor and the reactions of the coordinated ligands have not been studied in detail.

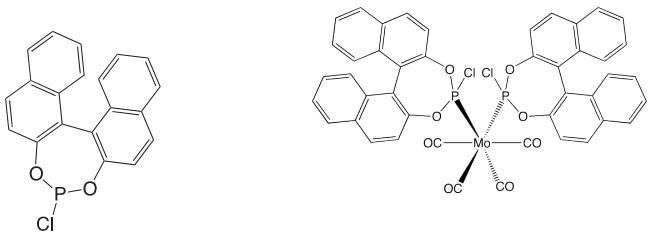

*Figure 1. Chlorophosphite ligand (**1**) and its model complex, cis-$Mo(CO)_4$(**1**)$_2$.*

Although transition metal complexes in catalytic cycles cannot easily be characterized due to their transient natures and low concentrations, model complexes such as those discussed in this paper can give insight into the effects of changes in ligand environment on reactivity. Complexes of the type $Mo(CO)_{6-n}$(P-donor ligand)$_n$ (n = 1, 2) are excellent model complexes for this type of characterization because the molybdenum(0) center is inert, allowing for the formation of stable products that can be studied by nuclear magnetic resonance (NMR) spectroscopy and X-ray crystallography. Additionally, the P-C coupling in the ^{13}C NMR resonances of the carbonyl ligands allows the coordination geometry of the molybdenum center to be determined.[10]

These model complexes may also have other applications. They could be used as sensors for mercury(II) in solution because the cis-trans isomerization reaction requires only catalytic amounts of mercury(II) chloride in order to proceed. Potentially interesting organometallic polymers could also be created using these compounds. The chloride groups on the chlorophosphite ligands are still reactive and could be displaced with nucleophiles to form polymer chains. These polymers could then undergo cis-trans isomerization in order to change the properties of the polymer or could potentially be cross-linked. These molecules are also interesting in that they can serve as molecular gyroscopes when the tetracarbonylmolybdenum(0) center has a trans coordination geometry. The tetracarbonylmolybdenum(0) center can then freely rotate, while the P-donor ligands remain stationary.

The model complex, cis-$Mo(CO)_4$(**1**)$_2$ (Figure 1), has previously been synthesized and reported by our group.[10] Racemic 1'1-bi-2-naphthol was used in the synthesis of the chlorophosphite ligand (**1**), and both diastereomers of the model complex were obtained. These were separated by fractional crystallization, and X-ray crystal structures of the two diastereomeric products were obtained. The crystal structures showed intramolecular pi-pi interactions for both diastereomers with stronger interactions seen in the cis-RR/SS diastereomer. The cis-RS diastereomer shows intermolecular pi-pi stacking. Images of the crystal structures for both diastereomers are shown in Figure 2.[10]

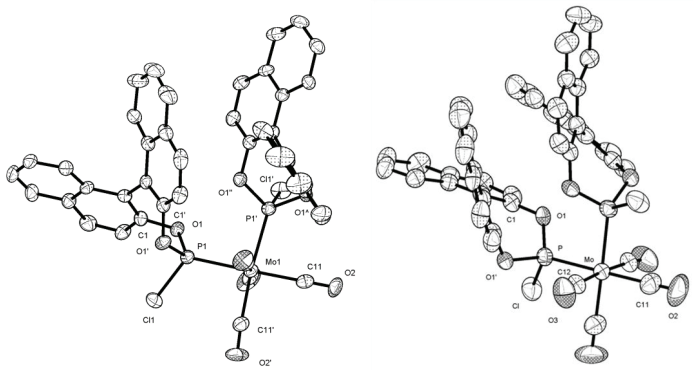

cis-RS *cis*-RR/SS

*Figure 2. Crystal Structures of both the RS and the RR/SS diastereomers of cis-$Mo(CO)_4$(**1**)$_2$ previously reported.[10]*

In this paper we report further characterization of both diastereomers of this complex through comparison of the hydrolysis of these complexes to those of their previously reported biphenoxy analogs using ^{31}P NMR spectroscopy.[9]

Materials and Methods

All reactions were performed under nitrogen. Triethylamine and tetrahydrofuran were dried by distillation from Na/benzophenone. Glassware was flame dried or dried in an oven before use. The starting material, cis-$Mo(CO)_4$(**1**)$_2$, was synthesized using methods previously described in the literature.[10] Hydrolysis reactions were followed by $^{31}P\{^1H\}$ NMR spectroscopy on a Bruker DRX400 spectrometer using chloroform as the deuterated solvent. The $^{31}P\{^1H\}$ NMR spectra were calibrated using an external 85 % phosphoric acid reference.

A solution containing 0.0311 g (0.0342 mmol) of cis-$Mo(CO)_4$(**1**)$_2$ in 0.055 mL of tetrahydrofuran, triethylamine (13.0 µL, 0.0932 mmol), deionized water (1.0 µL, 0.056 mmol) and 0.1 mL of chloroform-*d* was added to an NMR

tube. The NMR tube was sealed with Teflon tape and a cap, and the hydrolysis reaction was monitored using $^{31}P\{^{1}H\}$ NMR spectroscopy. The ^{31}P NMR resonances of the two diastereomers of cis-$Mo(CO)_4$(**1**)$_2$ were observed at 193.64 ppm and 192.78 ppm. When little reaction was observed after 5 h and 5 min, an additional 13.0 µL (0.0932 mmol) of triethylamine and 1.0 µL (0.056 mmol) of water were added. Because the reaction continued to go slowly, 26.0 µL (0.186 mmol) of triethylamine and 2.0 µL (0.11 mmol) of water were added after 24 h and 6 min. After 48 h and 7 min, the ^{31}P NMR resonances of the two diastereomers of cis-$Mo(CO)_4$(**1**)$_2$ could no longer be observed, and two new ^{31}P NMR resonances were observed at 166.93 ppm and 166.73 ppm. The volatile components in the NMR tube were removed by blowing a stream of nitrogen through the tube. Next, chloroform and tetrahydrofuran were added to dissolve the solid residue, and then 0.50 mL of a 6.84×10^{-5} M aqueous acetic acid solution was added. The solvent was then removed once more using a stream of nitrogen. Solvent was added again, and new resonances appeared at 176.58 ppm and 176.00 ppm. Throughout the reaction, a blue precipitate formed. This precipitate was suspected to be an oxidized molybdenum compound. At different times throughout the reaction, no peaks were observed on the NMR spectra. We speculate that, when mixtures of species were present in solution, exchange occurred.

Results and Discussion

It was anticipated that the hydrolysis of cis-$Mo(CO)_4$(**1**)$_2$ might be similar to that of the biphenoxy analog of the complex cis-$Mo(CO)_4$(2,2′-$C_{12}H_8O_2PCl)_2$.[9] The reaction scheme presented in Figure 3 is therefore a comparison to that obtained for the analog. The $^{31}P\{^{1}H\}$ NMR spectra in Figure 4 show that, when excess triethylamine and water were added to the cis-$Mo(CO)_4$(**1**)$_2$, the $^{31}P\{^{1}H\}$ NMR resonances for the two diastereomers of this complex at 193.64 ppm and 192.78 ppm completely disappear, and a new set of narrow $^{31}P\{^{1}H\}$ NMR resonances are observed significantly upfield at 166.93 ppm and 166.73 ppm. To gain insight into the nature of this product, one equivalent of acetic acid was added to the solution. This addition caused the narrow $^{31}P\{^{1}H\}$ NMR resonances at 166.93 ppm and 166.73 ppm to disappear and a new set of broad resonances at 176.58 ppm and 176.00 ppm to appear. This behavior is consistent with the narrow upfield resonances belonging to the dianion of the hydrolysis product (complex B, shown in Figure 3) and the broad, downfield resonances resulting from an exchange between the dianion and monoanion (complex C, shown in Figure 3) of the hydrolysis product. The effect of the addition of excess reagents can also be compared to results from a previous paper describing the hydrolysis reaction of cis-$Mo(CO)_4(Ph_2PCl)_2$.[11] The hydrolysis of this complex in the presence of excess triethylamine and water resulted in the formation of only the monoanion. Comparing the three analogs, it is not unexpected that the binaphthol analog being investigated would react more similarly to the biphenoxy compound. The differences in these reactivities likely relate to the ability of the intramolecular hydrogen bond in the monoanion to be broken to form the dianion from the monoanion. With the biphenoxy and binaphthoxy compounds, it would be expected that this process would be easier, as these are more electron-withdrawing ligands.

For the equilibrium between the monoanion and the dianion, shown in Figure 3, both the biphenoxy and the binaphthoxy analogs resulted in the formation of monoanion when a stoichiometric amount of acetic acid was added to the dianion complex. After this addition, the ^{31}P NMR spectrum for the previously reported biphenoxy analog showed a sharp peak indicating the formation of only the monoanion. In contrast, after the addition of the acetic acid, the ^{31}P NMR spectrum of the binaphthoxy analog showed a broad peak consistent with the exchange between dianion and the monoanion. This observation would suggest that it is harder to re-protonate the dianion of the binaphthoxy complex than it is to reprotonate the dianion of the biphenoxy complex and that the equilibrium between the monoanion and the dianion may lie toward the monoanion to a greater degree for the biphenoxy analog than it does for the binaphthoxy analog. An attempt was made to form the monoanion directly from the reaction of cis-$Mo(CO)_4$(**1**)$_2$ with a stoichiometric amount of water and triethylamine, but no reaction was observed. This behavior is quite different from that of the biphenoxy analog, for which this reaction yielded the corresponding monoanion.

Increasing the temperature of the reaction in order to sharpen the peaks was considered; however, this reaction was not attempted, as it has been previously shown that the hydrolysis products can decompose upon heating. Additionally, for the biphenoxy analogs, it was observed that the equilibrium could be pushed by adding excess triethylamine to the monoanion.[9] This reaction has not yet been attempted for the $Mo(CO)_4$(**1**)$_2$ complex.

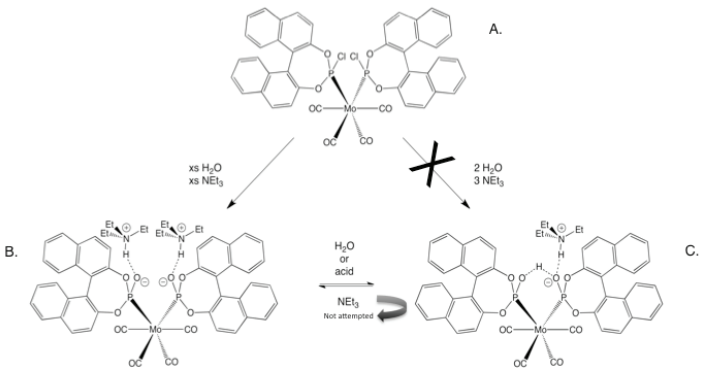

*Figure 3. Hydrolysis of cis-$Mo(CO)_4$(**1**)$_2$, A, to yield either the dianion of the hydrolysis product, B, or the monoanion product of the hydrolysis product, C.*

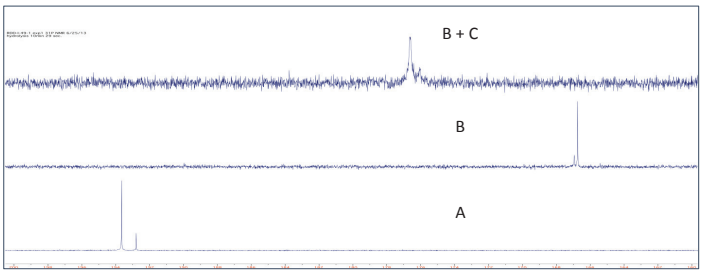

*Figure 4. $^{31}P\{^{1}H\}$ NMR spectra of cis-Mo(CO)$_4$(**1**)$_2$, A bottom, its dianion hydrolysis product, B center, and an exchanging mixture of the monoanion hydrolysis product, C, and the dianion hydrolysis product, B + C top.*

Conclusion

As expected, the hydrolysis reactions of cis-RS and RR/SS exhibit some similarities to those of the biphenoxy analogs in that the addition of excess triethylamine and water results in the formation of the dianion product. This product appears to be in equilibrium with the monoanion, as adding stoichiometric amounts of acid can push the equilibrium towards the monoanion. The results differed from those observed for the biphenoxy analog of the compound in that the formation of the monoanion directly from stoichiometric ratios of the reagents was not observed. It is likely that Mo(CO)$_4$(**1**)$_2$ is less reactive towards hydrolysis.[12] Additionally, the equilibrium between the monoanion and the dianion products of hydrolysis may lie more towards the dianion for the binaphthoxy analog than it does for the biphenoxy analog.

References

1. Darensbourg, D., & Graves, A. Correction. Steric contributions to the solution dynamics involving phosphorus ligand dissociation in substituted derivatives of molybdenum hexacarbonyl. *Inorg. Chem.* 18, 2336–2336 (1979).
2. Diéguez, M., Pàmies, O., Ruiz, A., Castillón, S., & Claver, C. Chiral diphosphites derived from d-glucose: New ligands for the asymmetric catalytic hydroformylation of vinyl arenes. *Chemistry - A European Journal*. 7, 3086–3094 (2001).
3. Cserépi-Szúcs, S., Tóth, I., Párkányi, L., & Bakos, J. Asymmetric hydroformylation of styrene using rhodium and platinum complexes of diphosphites containing chiral chelate backbones and chiral 1,3,2-dioxaphosphorinane moieties. *Tetrahedron: Asymmetry*. 9, 3135–3142 (1998).
4. Buisman, G. J. H., et al. Chiral cooperativity in diastereomeric diphosphite ligands: Effects on the rhodium-catalyzed enantioselective hydroformylation of styrene. *Organometallics*. 16, 2929–2939 (1997).
5. Nozaki, K. et al. Highly enantioselective hydroformylation of olefins catalyzed by rhodium(I) complexes of new chiral phosphine−phosphite ligands. J. Am. *Chem. Soc*. 119, 4413–4423 (1997).
6. Deerenberg, S., Kamer, P. C. J., & van Leeuwen, P. W. N. M. New chiral phosphine−phosphite ligands in the enantioselective rhodium-catalyzed hydroformylation of styrene. *Organometallics*. 19, 2065–2072 (2000).
7. Cobley, C. J. et al. Synthesis and application of a new bisphosphite ligand collection for asymmetric hydroformylation of allyl cyanide. J. *Org. Chem*. 69, 4031–4040 (2004).
8. Kadyrov, R., Heller, D., & Selke, R. New carbohydrate bisphosphites as chiral ligands. *Tetrahedron: Asymmetry*. 9, 329–340 (1998).
9. Byrd, H., Harden, J. D., Butler, J. M., Jablonsky, M. J., & Gray, G. M. Unusual hydrolysis reactions of cis-bis((2,2′-biphenylylene) phosphochloridite ester)tetracarbonylmolybdenum(0). *Organometallics*. 23, 3239–3245 (2004).
10. Hastings, S. D., Owens, S. B., Jr., & Gray, G. M. Synthesis, characterization, and coordination of chiral 1,1′-bi-2-naphthenephosphorchloridite ester with molybdenum. (2013).
11. Gray, G. M., & Kraihanzel, C. S. Reactions of coordinated ligands. *Journal of Organometallic Chemistry*. 146, 23–37 (1978).

short report

Isolation and Characterization of LtDan, a Novel Phage Infecting *Acinetobacter guillouiae*

Emil Kurian, Jessica Maya, Katrina Sahawneh, Sarah Swalley, Edwin Tsay, Beth Tuttle, Neha Udayakumar, Justin Wimberly, Tiffany Colburn, Jordan Gallardo, Alex Johnson, Sean McMahon, Brenna Nye, Brooke Pruitt, Surabhi Rao, Sarahanne Davidson, and Denise Monti

Department of Biology, University of Alabama at Birmingham, Birmingham, AL, USA

Abstract

Acinetobacter baumannii is a major cause of nosocomial infections worldwide and is one of the multi-drug resistant ESKAPE pathogens (*Enterococcus faecium, Staphylococcus aureus, Klebsiella* sp., *Acinetobacter baumannii, Pseudomonas aeruginosa,* and *Enterobacter* sp.) listed by the Centers for Disease Control and Prevention as a serious infectious disease threat. Research is urgently needed to develop new antimicrobials to treat drug-resistant *Acinetobacter* infections. Full genome sequencing has significantly enhanced efforts to better understand the bacterial host, yet little is known about the viruses (phages) that naturally infect *Acinetobacter*. The UAB Phage Genomics research team isolated and characterized a

novel bacteriophage, LtDan, infecting the bacterial species *Acinetobacter guillouiae*. Our data show that LtDan is similar to a previously characterized phage, ZZ1, infecting *Acinetobacter baumanii*. Overall, our work demonstrates the ability to isolate and characterize phages from the host *Acinetobacter guillouiae* and is the first step in developing a library of phages capable of infecting *Acinetobacter*.

Keywords: Bacteriophage, *Acinetobacter*, Phage therapy, Nosocomial infections, Antibiotic resistance

Introduction

Acinetobacter is a genus of bacteria that consists of 27 known species of gram negative, ubiquitous, non-motile, non-fermentative, coccobacilli that are found in soil, water, sewage, health care environments, and even on human skin.[1] Some strains of *Acinetobacter* are opportunistic pathogens, especially in immunocompromised patients, and play a significant role in nosocomial infections.[2] Several studies indicate an increase in *Acinetobacter* anti-microbial resistance.[3] Moreover, the bacterium's ability to survive long term in hospital environments makes this specific pathogen particularly dangerous in the healthcare setting.[4] Recently, infections caused by *Acinetobacter* have even spread from the hospital environment to the general public as cases involving healthy individuals of various ages have been reported after natural disasters and in war settings. *Acinetobacter baumanii* infections have also been implicated in wound infections among veterans serving in Vietnam, the Iran-Iraq conflict, and OPERATION Iraqi Freedom.[5] As antibiotics continue to be used to treat infections, resistance will likely become more prevalent.

One alternative to antibiotics in treating *Acinetobacter* infections is phage therapy. Bacteriophages, viruses that infect and lyse bacteria, were discovered in 1916 and were first used as therapeutic agents in 1919.[6] Phage therapy was then used for over 20 years before the discovery of antibiotics proved to be a cheaper and easier alternative.[6] Phage therapy has gained recent attention as the number of antimicrobial-resistant pathogens continues to rise and new therapeutics are needed. Phages may be an attractive treatment alternative because they are specific to certain bacterial strains and do not harm human cells.[1,4] Although more research is needed before the therapeutic use of phages can be approved by the Food and Drug Administration, phages have already been authorized as food additives to prevent foodborne illnesses caused by bacteria.[1]

To date, very few phages infecting the host strain *Acinetobacter* have been isolated and characterized. A novel *Acinetobacter guillouiae* phage, LtDan, was recently isolated and characterized by the 2013–2014 Phage Genomics team at the University of Alabama at Birmingham. Phage LtDan was isolated from a creekbed sediment sample taken from Griffin Creek in Homewood, Alabama, USA. Following isolation, a series of five experiments was performed to characterize LtDan. These experiments included temperature and pH stability, bacterial host range, effects of varying divalent cation concentrations, and latency period, defined as the duration of time needed for the phage to infect and then lyse the host bacteria.

Materials and Methods

Host Selection

Acinetobacter guillouiae was selected as the target host for phage isolation because it is readily available from the American Type Culture Collection (ATCC 11171) at low cost. It is in the same genus as the pathogen *Acinetobacter baumanii*, yet it is a BSL1 pathogen and can be safely used in a wide variety of student laboratory settings.

Temperature Stability

Aliquots of 500 µL of phage LtDan were stored for 24 h at various temperatures (−80 °C, −20 °C, 4 °C, 25 °C, 30 °C, 37 °C, 45 °C, and 65 °C). After storage, a standard ten-fold viral titer assay was performed. The virus was then plated with *Acinetobacter guillouiae* and incubated for 24 h at 30 °C. Virus viability was determined by comparing phage titer before and after incubation.

pH Stability

100 µL of LtDan phage lysate (2.6×10^8 pfu mL^{-1}) was added to 5 mL of pH-adjusted phage buffer, and samples were incubated at room temperature for 1 h. Ten-fold serial dilutions of each sample were prepared, and 50 µL from each was used to infect 500 µL of *Acinetobacter guillouiae*. This suspension was mixed with 4.5 mL of top agar and directly plated. Plates were incubated for 24 h at 30 °C, and plaques were counted to determine phage titer.

Host Range

Ten different bacterial strains (*Acinetobacter baumannii, Acinetobacter guillouiae, Acinetobacter calcoaceticus, Bacillus cereus, Bacillus megaterium, Escherichia coli, Staphylococcus aureus, Staphylococcus epidermis, Enterobacter aerogenes,* and *Proteus mirabilis*) were used to test the host range of LtDan. Approximately 500 µL of each bacterial strain was mixed with 4.5 mL of 1x nutrient broth (Difco Cat#213000) top agar and plated on nutrient broth plates. After solidification, 10 µL of ten-fold serial dilutions of LtDan (10^7 pfu mL^{-1}) was spotted onto the lawn. Plates were incubated for 48 h at 30 °C and checked for the presence of plaques.

Divalent Cations: $MgCl_2$ and $CaCl_2$

To determine the effect of divalent cation concentration on viral infectivity, several dilutions of phage LtDan were plated in top agar containing 5 different concentrations of $MgCl_2$ (0 mM, 1 mM, 5 mM, 10 mM, and 25 mM). Briefly, several dilutions of a high-titer stock of phage LtDan (7.6×10^7 pfu mL^{-1}) were plated with 500 µL *Acinetobacter guillouiae* and 4.5 mL 1x Luria Broth (LB, Difco Cat#241420)

top agar containing $MgCl_2$. Samples were gently mixed, plated on petri dishes, and incubated for 24 h at 30 °C. Individual plaques (20 to 200) were counted to measure phage infection titer. This procedure was repeated using the alternate divalent cation, $CaCl_2$.

Latency Period

Acinetobacter guillouiae was grown in a shaking incubator at 30 °C until its optical density at 600 nm was 0.4 to 0.6. Approximately 50 mL of bacteria was pelleted, re-suspended in 500 µL LB, and incubated with 500 µL of 1×10^{-8} phage LtDan for 1 min. Phage-infected bacteria was pelleted and re-suspended in 100 mL LB medium. A 10 µL sample was pulled out. The infected bacteria were placed in a shaking incubator at 30 °C, 225 rpm for 4 h. Samples were taken every 20 min for 4 h and stored at 4 °C until plating. A phage titer assay was used to evaluate viral titer at each time point.

Results and Discussion

After repeated experimentation, we were able to isolate LtDan using phage titer assays by plating phage and bacteria directly into a petri dish without the presence of bottom agar. In normal phage isolation protocols, a 3 mL to 5 mL layer of phage, bacteria, and top agar is plated directly over bottom agar in the petri dish. We found LtDan was only productively infectious when bottom agar was not present. Various concentrations of top agar (0.5 % to 2 % weight/volume) were tested to determine whether the density of the top agar affected the ability of the virus to infect the host. We did not find any difference in viral infectivity with varying concentrations of agar, but always lost infectivity of the virus with the presence of bottom agar. Further studies are ongoing to determine why the presence of bottom agar seemingly prevents productive phage infection of the host.

To confirm that we had indeed isolated a single population of virus, electron microscopy (EM) was performed. All phages visualized by EM on the prepared grid shared similar morphological characteristics. LtDan had an icosahedral capsid with diameter 86.8 nm and the apparent lack of a tail. While the capsid size is not atypical for phage, the lack of a defined tail structure is unique. Additional detailed imaging will be needed to determine precisely whether LtDan lacks a tail entirely or has a very short, stubby tail (Figure 1). Analysis of the genomic sequence of the virus may also be informative in determining whether LtDan is a tailless phage.

Phage viability can differ dramatically among viruses infecting the same species and is an important consideration when selecting a phage as a potential candidate for phage therapy. To assess the viability of LtDan, we subjected high titer preparations (500 µL) of the virus to varying conditions including temperature and pH. The viral titer of LtDan was found to be stable through a wide temperature range of −80 °C to 37 °C (Figure 2). Infectivity was reduced at the higher temperatures tested, likely as a result of protein denaturation. In comparison, a previously characterized phage infecting a clinical isolate of *Acinetobacter baumannii*, ZZ1, was stable when tested at 4 different temperatures (50 °C, 60 °C, 70 °C, and 80 °C). LtDan also maintains infectivity in a pH range of 5 to 11 (Figure 3), which is a broader range of infectivity than that of ZZ1 (pH 5 to 9).[6]

For many phages, infection can only occur in the presence of a divalent cation. Divalent cations create a charge-neutral medium, which allows for attachment of the phage to the host-cell surface.[8] We examined whether LtDan required the presence of a divalent cation for productive infection. Initial isolation studies were performed using 5 mM $CaCl_2$ in accordance with protocols used to isolate other phages that have been historically difficult to isolate from environmental samples, including *Arthrobacter*- and *Rhodococcus*-specific phages. We found that LtDan was able to productively infect *Acinetobacter guillouiae* independent of $CaCl_2$ and $MgCl_2$ concentration (Figure 4). Moreover, we found that LtDan could productively infect *Acinetobacter guillouiae* in the absence of any divalent cations.

Latent time of infection is the period of time required for the production of virus after initial infection. To determine whether the apparent lack of a tail affects the rate of viral attachment and infection, we determined the viral latent time of infection for LtDan. LtDan has a latency period of nearly 120 min (Figure 5) in comparison to a 9 min latency period for phage ZZ1.[6] Possible reasons for the slow latent time of infection in LtDan include a mismatch of host specificity, an alternate entry mechanism, and non-optimized buffering.

Small-scale host range experiments were performed using a high titer stock of LtDan. Hosts selected were readily available in the laboratory and all were categorized as BSL1 or BSL2 pathogens. LtDan was able to productively infect *Acinetobacter guillouiae*, but was not able to productively infect other *Acinetobacter* species (Table 1) or other common pathogens, such as *Escherichia coli*.

Taken together, we have isolated, for the first time, a novel phage of the host *Acinetobacter guillouiae*. Our work shows that LtDan is infectious over a wide range of conditions, but may have very limited host-range. Future work involves full-genome sequencing, annotation of the phage genome, and acquisition of a larger panel of *Acinetobacter baumanii* clinical isolates to better define host range.

Acknowledgements

We acknowledge the 2013–2014 Phage Genomics Team, Dr. Denise Monti, Sarahanne Davidson, and Roxanne Lockhart, for their contributions to the project. We also thank the Science Education Alliance of the Howard Hughes Medical Institute and the Department of Biology at the University of Alabama at Birmingham for their support of this work.

References

1. Tayabali, A., Nguyen, K., Shwed, P., Crosthwait, J., Coleman, G. & Seligy, V. Comparison of the virulence potential of Acinetobacter strains from clinical and environmental sources. *PLOS ONE*. 7, 1–11 (2012).

2. Yang, H., Liang, L., Lin, S., & Jia, S. Isolation and characterization of a virulent bacteriophage AB1 of Acinetobacter baumannii. *BMC Microbiology*. 160, 101–131 (2010).

3. Yong, D., Shin, HB., Kim, YK., Cho, J., Lee, WG., Ha, GY., Choi, TY., Jeong, SH., Lee, K., & Chong, Y. Increase in the Prevalence of Carbapenem-Resistant Acinetobacter. *US National Library of Medicine*. 52, 84–93 (2014).

4. Bergogne-Bérézin, E., & Towner, K. Acinetobacter spp. as nosocomial pathogens: Microbiological, clinical, and epidemiological features. *Clinical Microbiology Reviews*. 2, 148–165 (1996).

5. Gourdine, E. & Wortman, W. Acinetobacter baumanni infections among patients at military medical facilities treating injured U.S. service members, 2002–2004. *CDC MMWR Weekly*. 53, 1063-1066 (2004).

6. Jin, J., Li, Z., Wang, S., Wang, S., Huang, D., Li, Y., Ma, Y., Wang, J., Liu, F., Chen, X., Li, G., Wang, X., Wang, Z., & Zhao, G. Isolation and Characterization of ZZ1, a novel lytic phage that infects Acinetobacter baumannii clinical isolates. *BMC Microbiology*. 12, 156 (2012).

7. Herman, N.J., & Juni, E. Isolation and characterization of a generalized transducing bacteriophage for Acinetobacter. *Journal of Virology*. 13, 46–52 (1974).

8. Chhibber, S., Kaur, T., & Kaur S. Essential role of calcium in the infection process of broad spectrum methicillin-resistant Staphylococcus aureus bacteriophage. *Journal of Basic Microbiology*. 54, 775-780 (2014).

Addendum: Figure and Table Legends

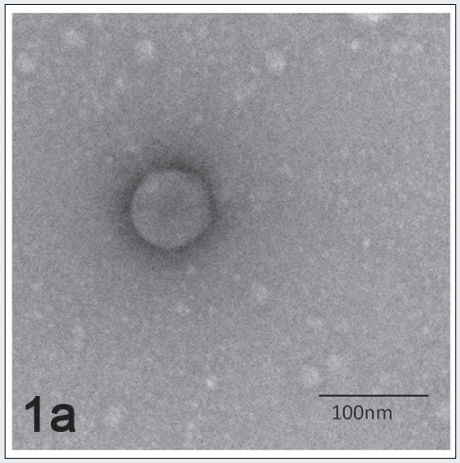

Figure 1. Electron microscope image of phage LtDan. LtDan was isolated from a water sample taken from Griffin Creek, Homewood, Alabama, USA. A concentrated viral preparation was stained with 1 % uranyl acetate and imaged by the UAB HRIF Electron Microscope Core.

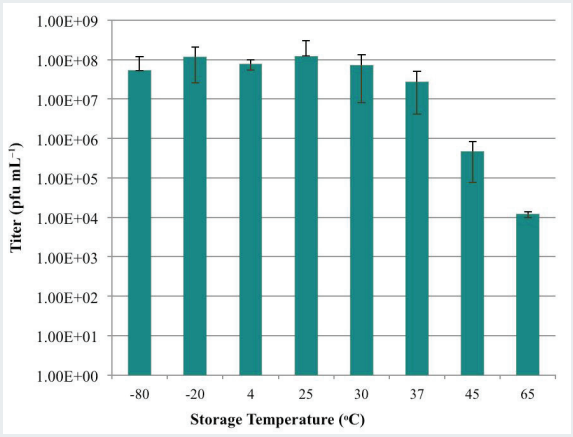

Figure 2. Temperature stability of LtDan. LtDan was stored for 24 h at varying temperatures. Viral titer was then determined by standard phage titer assay.

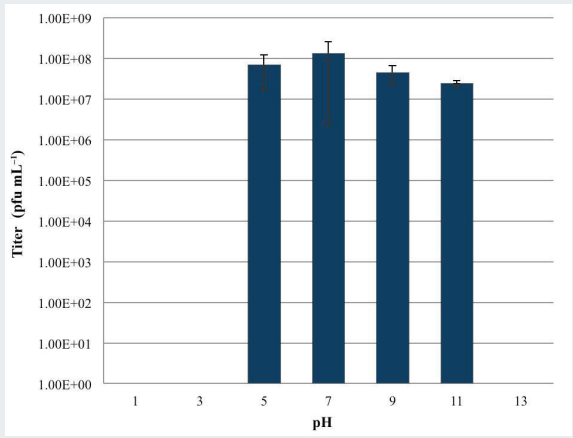

Figure 3. pH stability of phage LtDan. Phage LtDan was incubated in phage buffer of varying pH for 1 h. The number of infectious phage particles was then determined. Viral infectivity was not detected at pH 1, 3, or 13.

Bacterial Strain	Infected by LtDan
Acinetobacter guillouiae	Yes
Acinetobacter baumannii	No
Acinetobacter calcoaceticus	No
Bacillus cereus	No
Escherichia coli	No
Staphylococcus aureus	No
Staphylococcus epidermis	No
Enterobacter aerogenes	No
Proteus mirabilis	No

Table 1. Host range of phage LtDan. Phage LtDan was plated with 10 different bacterial strains, and the presence of plaques is noted below.

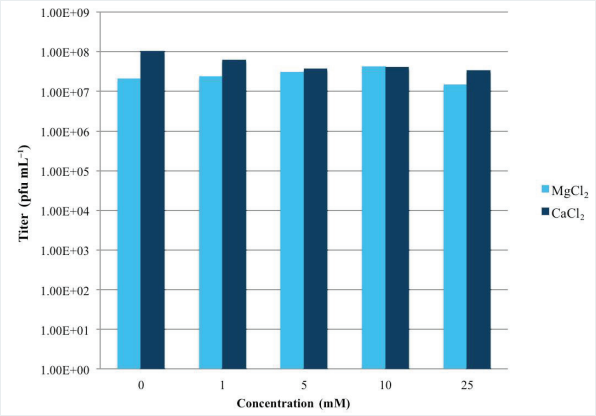

Figure 4. Effect of divalent cation concentration on titer of phage LtDan. Differing concentrations of $MgCl_2$ and $CaCl_2$ were plated with high titer stock of LtDan and incubated for 24 h at 30 °C. Viral infectivity was determined by standard phage titer assay.

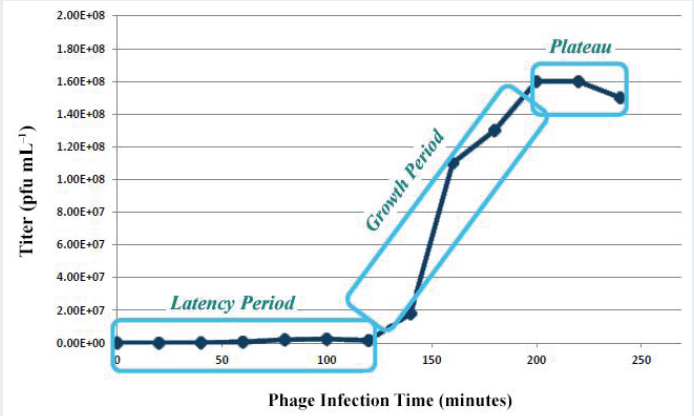

Figure 5. Growth curve for LtDan. Phage LtDan was incubated with Acinetobacter *and assayed for viral infectivity every 6 min for 4 h using a standard phage titer assay.*

short report

Platelet-Activating Factor (PAF) and Lung Inflammation: Effects of Hyperoxia

Alana C. Jones[1,2], Tamas Jilling[3], and Namasivayam Ambalavanan[3]

[1]Howard University, Washington D.C., USA
[2]PARAdiGM Program, University of Alabama at Birmingham, Birmingham, AL, USA
[3]Neonatal Physiology Laboratory, Division of Neonatology, Department of Pediatrics, University of Alabama School of Medicine, Birmingham, AL, USA

Abstract

Hyperoxia exposure is a common treatment in preterm neonates with respiratory distress, but may contribute to lung injury.[1] Hyperoxia-induced inflammation may contribute to the adverse effects of hyperoxia on lung development and function. Platelet-activating factor (PAF) is a potent mediator in the inflammatory response and has been shown to be a factor in respiratory inflammation.[1] The objective of this study was to determine whether PAF contributes to hyperoxic lung injury, using an *in vitro* model system. Untreated, PAF-treated, and PAF-receptor (PTAFR) antagonist (CV6209)-treated Mouse Lung Epithelial (MLE)-12 cells and the RAW 264.7 macrophage cell line were exposed to hyperoxia (85 % O_2) or air for 0, 8, 24, & 48 h. Following RNA isolation, cDNA was prepared and then probed for gene expression of inflammatory cytokines *(CXCL1, IL-1*β*,* and *TNF*α*)*, enzymes required for PAF biosynthesis *(PLA2G2A, PLA2G2E, PLA2G4A,* and *LPCAT2)*, and enzymes that render PAF biologically inactive *(PLA2G7* and *LPCAT1)*. In MLE, PAF induced a time-dependent increase of *CXCL1, PLA2G4A,* and *LPCAT2* gene expression and suppressed *PLA2G7* and *LPCAT1* gene expression. Hyperoxia-induced *CXCL1, PLA2G7*, and *LPCAT1* gene expressions were completely abolished by the PTAFR antagonist at all time points. We conclude that PAF may contribute to hyperoxia-induced inflammation in the lung. Further studies are needed to determine the *in vivo* alteration in PAF and its signaling during hyperoxia in human disease.

Keywords: Hyperoxia, Platelet-activating factor, Inflammation, Lung injury

Introduction

Premature, low birth weight (PLBW) neonates who do not reach full lung development *in utero* are prone to develop respiratory distress, which can decrease their ability to absorb all the oxygen they need from room air (normoxia). This problem is commonly resolved by exposing these babies to high concentrations of oxygen (hyperoxia; ≥85 % O_2). However, prolonged hyperoxia exposure can cause lung injury, e.g., bronchopulmonary dysplasia, a disease in which lung tissue scars from inflammation.[2] Thus, hyperoxia-induced inflammation may adversely affect lung development and

function even though it administers the necessary O_2 to prevent neonatal brain injury.

Platelet-activating factor (PAF, 1-*O*-alkyl-2-acetyl-*sn*-glycero-3-phosphocholine), a phospholipid mediator of various functions, is one of the primary units involved in the inflammatory response. Its most common synthesis pathway is an enzymatic remodeling: phosphatidylcholine (PC) is converted to lyso-PC by a set of PLA2s, which LPCAT2 then converts to PAF (Figure 1). Its degradation is the reverse: PAF-acetylhydrolase (PAF-AH, coded by *PLA2G7*) converts PAF to lyso-PC, which LPCAT1 converts to PC. Although PAF is known to contribute to respiratory ailments such as anaphylaxis and asthma,[3] its role in hyperoxia-induced inflammation is yet to be determined. Furthermore, while its biosynthesizing and degrading enzymes are understood to operate in an equilibrium-like mechanism, it is not understood whether hyperoxia-induced inflammation, if mediated by PAF, is regulated by gene expression or enzymatic activity. The objectives of this study were to confirm that PAF is a mediator in hyperoxia-induced inflammation, determine whether its inflammatory pathway is regulated by gene expression of PAF's synthesis and degradation enzymes, and analyze the effect of PAF-receptor (PTAFR) antagonist on PAF inhibition during hyperoxia in both epithelial cells and macrophages. A clear understanding of this issue is critical in explaining the role of PAF in hyperoxia-induced inflammation, as well as the potential role of PTAFR antagonists in treatment approaches to hyperoxia-induced lung injury.

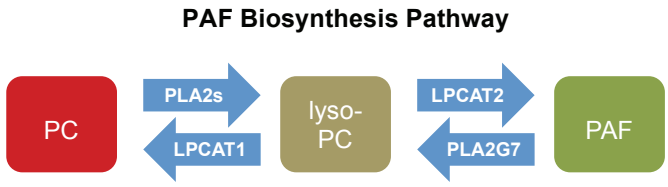

Figure 1. PAF Mechanism

Materials and Methods

Cell cultures

In T-75 flasks, 2 mL MLE-12 (P-22) and 1 mL RAW 264.7 macrophage cell line (P-4) were grown to ≥60 % confluence in 15 mL complete media. The cells were trypsinized, removed from the flasks, and split into 6-well plates (3 plates/flask) with 1 mL complete media per well. After ≥8 h of incubation (5 % CO_2, 37 °C) and the cells had attached to the well surface, 1.5 mL low serum media replaced the complete media, and the cells were allowed to develop to ≥80 % confluence.

Untreated (UT) hyperoxia exposure

For each cell line, 3 plates were incubated in hyperoxia (85 % O_2, 5 % CO_2, 37 °C) for 0, 8, & 24 h (Figure 2). RNA buffer lysates (RA1 with 1 % β-Mercaptoethanol; 600 µL per well) were prepared from 3 wells per plate with RA1 solution and mechanical cell detachment. Protein buffer lysates (89 % T-PER, 10 % PI, 1 % PMSF; 300 µL per well) were prepared from the remaining wells and stored at −80 °C for later analysis.

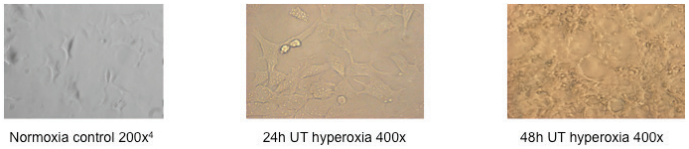

Figure 2. MLE-12 Cell Pictures

Treated hyperoxia exposure

For each cell line, 2 wells per plate were treated with vehicle (0.1 % EtOH), cPAF (1 µM), and PTAFR antagonist CV6209 (5 µM) for a total of 3 treatments per plate. The well plates were incubated in normoxia for 6 h followed by hyperoxia for 0, 18, & 42 h for total treatment times of 6, 24, & 48 h. RNA buffer lysates were prepared from each well.

RNA isolation & quantification, cDNA synthesis, and qPCR.

RNA was isolated from the buffer lysates (QIACube, RNeasy Mini DNAse digest protocol) and quantified (QIAgility & Rotor Gene-Q). From each RNA sample 500 ng cDNA were synthesized via RT-PCR. The samples were probed for gene expression of *CXCL1, IL-1β, TNFα, PLA2G2A, PLA2G2E, PLA2G4A, PLA2G7, PTAFR, LPCAT1,* and *LPCAT2* via qPCR, and data analysis was performed.

Results

Confirmation of inflammation

The cDNA was probed for inflammatory cytokines *CXCL1*, *IL-1β*, and *TNFα* to confirm the presence of inflammation. In MLE, *CXCL1* expressed a 2.1 ± 0.11 fold increase at 8 h, 8.5 ± 0.43 (UT) and 3.3 ± 1.1E-2 (vehicle) fold increases at 24 h, and 6.68 ± 0.37 fold increase at 48 h. However, AFR antagonism completely abolished expression at 24 h and 48 h to 1.1 ± 0.10 fold and 0.82 ± 7.2E-2 old, respectively (Figure 3). In macrophages, *CXCL1* was affected transiently by hyperoxia, with increased expressions 1.9 ± 1.1 fold at 8 h, 1.1 ± 0.62 (UT) and 5.9 ± 1.4 (vehicle) fold at 24 h, and 3.1 ± 1.3 at 48 h. PTAFR antagonism yielded inconclusive results, with increased expression 11. ± 0.26 fold at 24 h and decreased expression 3.1 ± 0.61 fold at 48 h (Figure 4). *IL-1β* expression was too low for accurate analysis in MLE but in macrophages expressed a time-dependent decrease 0.71 ± 0.25 fold at 8 h, 0.29 ± 0.11 (UT) and 0.56 ± 5.2E-3 (vehicle) fold at 24 h, and 0.43 ± 0.10 fold at 48 h. PTAFR antagonism further abated expression 0.31 ± 3.6E-2 fold at 24 h and 0.21 ± 4.3E-2 fold at 48 h (Figure 5). *TNFα* expression was too low for accurate analysis.

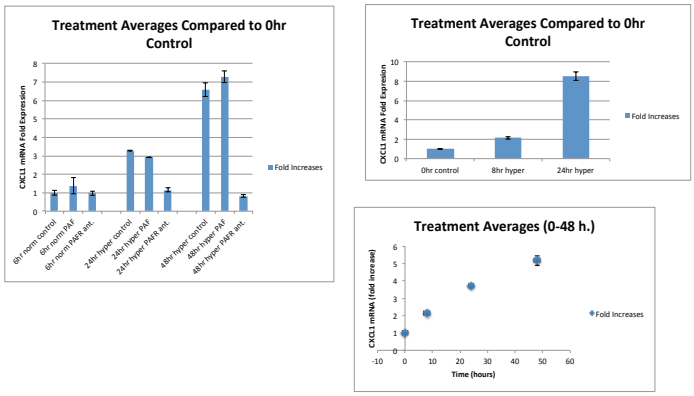

Figure 3. MLE-12 CXCL1

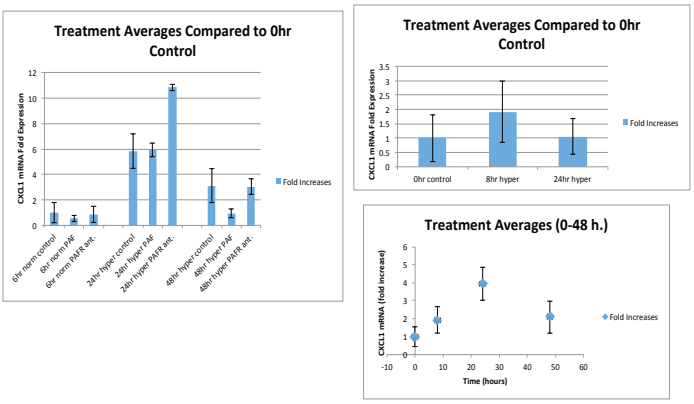

Figure 4. Macrophage CXCL1

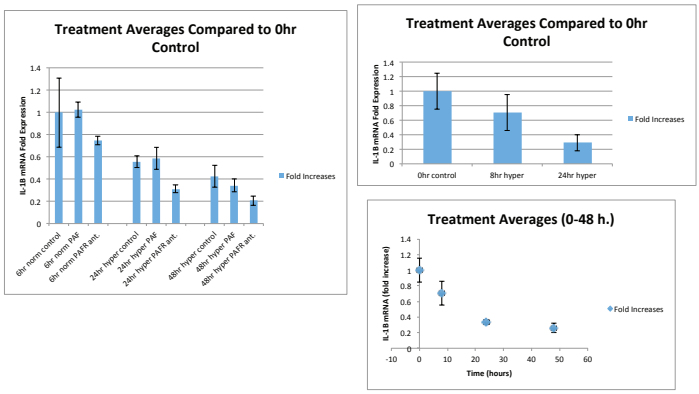

Figure 5. Macrophage IL-1β

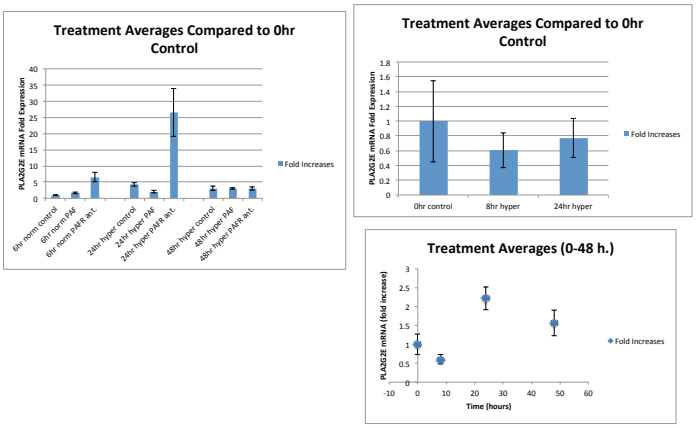

Figure 6. MLE-12 PLA2G2E

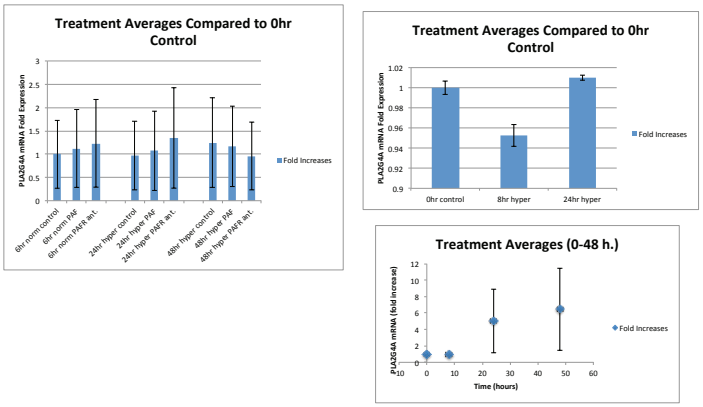

Figure 7. MLE-12 PLA2G4A

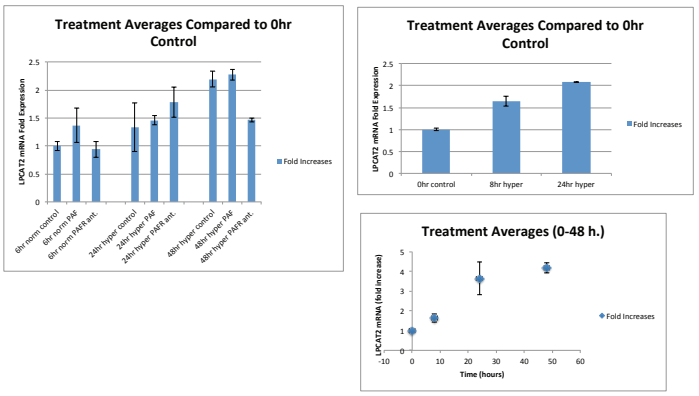

Figure 8. MLE-12 LPCAAT2

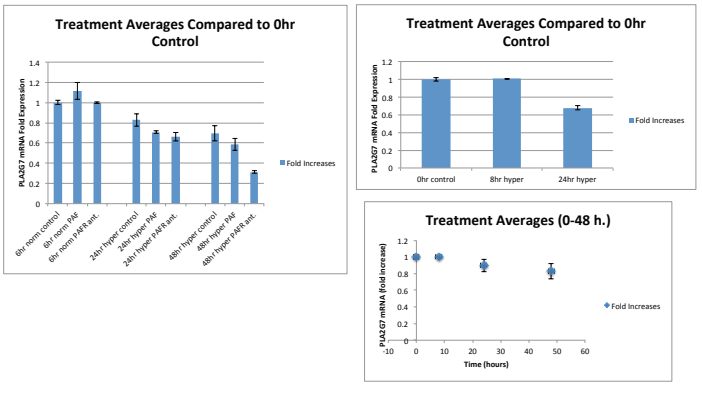

Figure 9. MLE-12 PLA2G7

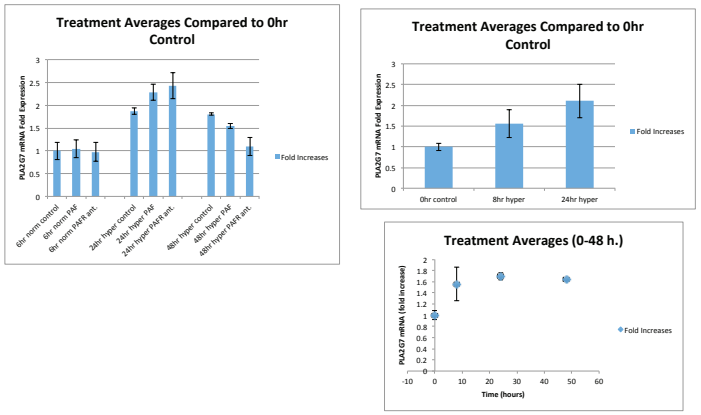

Figure 10. Macrophage PLA2G7 q

Expression of PAF's synthesizing enzymes

The cDNA was probed for *PLA2G2A, PLA2G2E, PLA2G4A,* and *LPCAT2* to analyze the expression of PAF-synthesizing enzymes that convert PC to lyso-PC and lyso-PC to PAF. In MLE, *PLA2G2A* expression was too low for accurate analysis, and *PLA2G2E* expression exhibited no trend, with fluctuating expressions 0.60 ± 0.23 fold at 8 h, 0.77 ± 0.26 (UT) and 4.4 ± 0.60 (vehicle) fold at 24 h, and 3.1 ± 0.68 fold at 48 h. PTAFR antagonist was inconclusive, and did not appear to impact expression, with 26 ± 7.4 at 24 h and 3.1 ± 0.54 fold increased expression at 48 h (Figure 6). *PLA2G4A* expression remained relatively constant in MLE, with expressions 0.95 ± 1.1E-2 fold at 8 h, 1.0 ± 2.7E-3 (UT) and 0.97 ± 0.74 (vehicle) fold at 24 h, and 1.24 ± 0.96 fold at 48 h. PTAFR antagonist treatment seemed to have little effect, with 1.3 ± 1.1 and 0.96 ± 0.73 fold expression at 24 h and 48 h, respectively (Figure 7). *LPCAT2* expression showed a time-dependent increase in MLE 1.5 ± 0.15 fold at 8 h, 1.9 ± 1.5E-2 (UT) and 1.3 ± 0.42 (vehicle) fold at 24 h, and 2.1 ± 0.16 fold at 48 h. PTAFR antagonism further suppressed expression 1.7 ± 0.27 fold at 24 h and 1.4 ± 3.5E-3 at 48 h (Figure 8).

Expression of PAF's degrading enzymes

The cDNA was probed for the expression of *PLA2G7* and *LPCAT1* to analyze the expression of enzymes involved in degrading PAF to lyso-PC (PAF-AH) and lyso-PC to PC (LPCAT1). In MLE, *PLA2G7* expression illustrated a time-dependent decrease 1.0 ± 8.2E-3 fold at 8 h, 0.67 ± 2.4E-2 (UT) and 0.83 ± 6.2E-2 (vehicle) fold at 24 h, and 0.70 ± 7.7E-2 at 48 h. PTAFR antagonism further diminished expression to 0.66 ± 4.1E-2 fold at 24 h and 0.31 ± 1.1E-2 fold at 48 h (Figure 9). In macrophages, *PLA2G7* was affected transiently with expressions 1.6 ± 0.33 fold at 8 h, 2.1 ± 0.41 (UT) and 1.9 ± 6.8E-2 (vehicle) fold at 24 h, but declined to 1.8 ± 0.20 fold at 48 h. PTAFR antagonism also transiently affected expression, with a 2.4 ± 0.28 fold at 24 h and 1.1 ± 0.20 fold increases at 48 h (Figure 10). *LPCAT1* expressed a time-dependent decrease in MLE 0.95 ± 1.0E-2 fold at 8 h, 0.48 ± 2.2E-2 (UT) and 0.51 ± 2.6E-2 (vehicle) fold at 24 h, and 0.37 ± 1.4E-2 fold at 48 h. PTAFR antagonism further abated expression to 0.30 ± 3.9E-2 fold at 24 h and 0.17 ± 8.6E-3 fold at 48 h (Figure 11).

Expression of PTAFR

The cDNA was probed for *PTAFR* to determine whether hyperoxia or PTAFR antagonist affected the expression of PAF receptors. The data were inconclusive for MLE, but in macrophages *PTAFR* was transiently affected, with increased expression 1.3 ± 7.3E-2 at 8 h and decreased expressions 0.76 ± 5.4E-2 (UT) and 0.43 ± 2.5E-2 (vehicle) fold at 24 h and 0.76 ± 1.3E-2 fold at 48 h. PTAFR antagonism diminished expression to 0.32 ± 6.7E-3 fold at 24 h and 0.33 ± 7.5E-3 fold at 48 h (Figure 12).

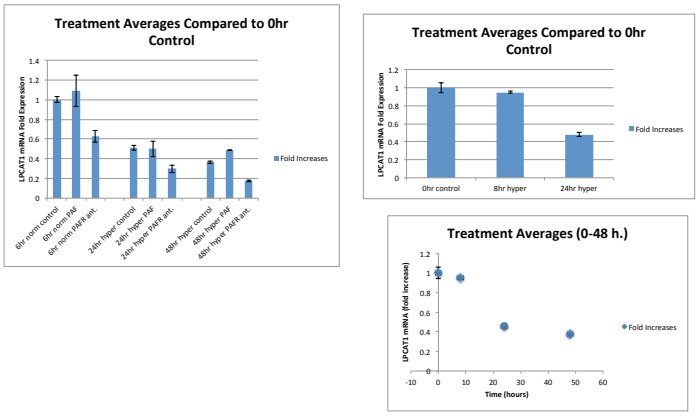

Figure 11. MLE-2 LPCAT1

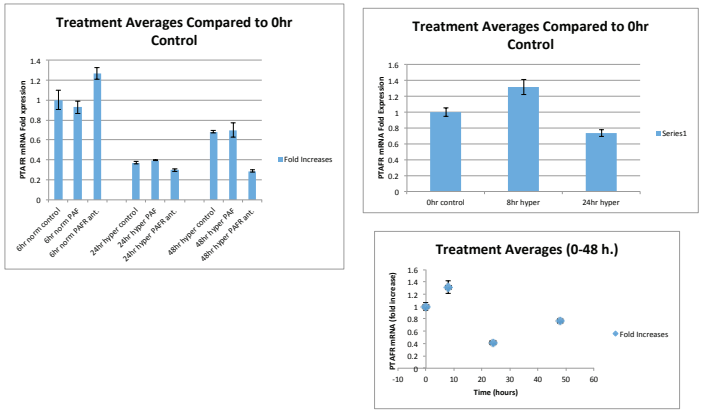

Figure 12. Macrophage PTAFR

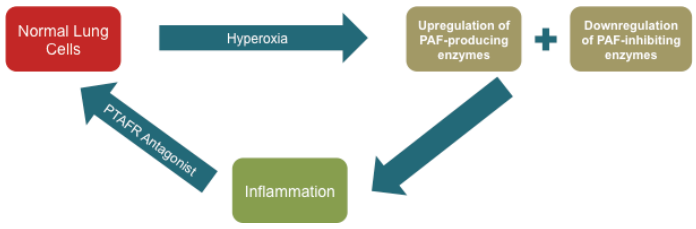

Figure 13. Conclusions

Statistical Analysis

Data were expressed as the mean expression ± standard deviation (SD) and are represented in the figures. UT cells with and without hyperoxia (positive and negative controls) experiments were performed in duplicate, and qPCR was performed in duplicate. *PTAFR* was probed in triplicate. Statistical analysis was performed using Microsoft Excel, and significance of difference was determined to be fold increase/decrease values >0.20 ($p < 0.80$ or $p > 1.2$).

Discussion & Conclusions

Based on the data, we conclude that hyperoxia-induced inflammation is mediated by PAF and that treatment with PTAFR antagonist ameliorates the PAF overexpression seen in hyperoxia. Data from qPCR not only suggest that hyperoxia

affects PAF-synthesizing enzymes on a case-by-case basis, but also reveal a time-dependent downregulation of PAF-degrading enzymes (Figure 13).

Once we confirmed the presence of inflammation in the cells by probing for inflammatory cytokines *CXCL1, IL-1β*, and *TNFα* (with *CXCL1* giving the greatest confirmation in epithelial cells and *IL-1β* in macrophages), we were able to probe for PAF-synthesizing genes. *PLA2G2A*, *PLA2G2E*, and *PLA2G4A* were responsible for the expression of the enzymes involved in converting phosphatidylcholine (PC) to lyso-PC. However, fold increases of the *PLA2s* were relatively small when compared to other biosynthesizing genes probed in the analysis. While the *PLA2s*' lyso-PC synthesis yielded variant results, *LPCAT2*—the protein-coding gene responsible for converting lyso-PC to PAF—clearly expressed a time-dependent increase and confirmed our hypothesis of elevated PAF. These data indicate that PAF's contribution to hyperoxia-induced inflammation may predominantly be mediated in the final stage of PAF synthesis—increased lyso-PC conversion to PAF rather than PC to lyso-PC.

The data also suggest that PAF's elevated levels in hyperoxia-induced inflammation may not exclusively occur through regulation of gene expression, but also through regulation of enzymatic activity. Even though *LPCAT2* experienced a time-dependent increase in expression, the *PLA2s*' expressions were only transiently affected or, in some cases, unaffected. Increased enzymatic activity may be the primary mediator in converting PC to lyso-PC instead of gene upregulation. Further assays and enzymatic studies are needed test this hypothesis. This evidence could also lead to further investigation into why some enzymes' gene expressions were upregulated while other enzymes expressed at normal levels even though we observed overall increased activity in PAF biosynthesis.

Once we confirmed upregulation of PAF-synthesizing enzymes, we probed for PAF-degrading enzymes, expecting to observe a time-dependent decrease in expression. Both *PLA2G7*, which codes for PAF-acetylhydrolase (PAF-AH)—the enzyme that degrades PAF to lyso-PC—and *LPCAT1*, which codes for the LPCAT1 enzyme that degrades lyso-PC to PC, presented time-dependent decreases and confirmed that hyperoxia shifts PAF/PAF-AH equilibrium to the right, resulting in inflammation.

Even though PTAFR antagonism had transient effects on individual gene expressions of PAF-related enzymes, it indicated an overall decrease in both PAF biosynthesis and degradation. By blocking the receptors where PAF could bind, the PTAFR antagonist decreased the overall expression of PAF-related enzymes. PTAFR antagonism drastically diminished expression of inflammatory cytokines (e.g., *CXCL1*), indicating that it could be a possible treatment *in vivo*. However, because PAF is involved in numerous bodily functions, inhibiting it to reduce inflammation may have adverse effects, just as hyperoxia can have adverse effects on neonates in respiratory distress.

Platelet-activating factor is a complex mediator and has multiple functions, one of which was analyzed in this study. Hyperoxia is equally complex: lack of it can cause brain damage in some cases but excess of it can further damage already-weakened lungs. A clear understanding of how the two work together is necessary for the development of treatments that can potentially ameliorate hyperoxia-induced inflammation in PLBW neonates. Next steps include more *in vitro* studies with other types of cells that are present in the lung, as well as studies to determine PAF's alteration and signaling *in vivo*, with the long-term goal of improving clinical treatment in order to give preterm neonates with diminished respiratory function the oxygen they need without hindering their lung development and function.

Acknowledgements

I would like to thank the Neonatal Physiology Lab in the Division of Pediatrics at the University of Alabama at Birmingham: Nelida Olave, Brian Halloran, and Changchun Ren for their technical training and supervision; and Mesheika James and Thea Nicola for their valuable insight in the undertaking of the research summarized here. This research was partially supported by the PARAdiGM Program (NIH/NHLBI R25HL120883), sponsored by the Medical Scientist Training Program at the University of Alabama School of Medicine.

References

1. Pagano A., & Barazzone-Argiroffo, C. Alveolar cell death in hyperoxia-induced lung injury. *Ann NY Acad Sci.* 1010, 405-416 (2003).
2. Zoban, P., & Černý, M. Immature lung and acute lung injury. *Physiol Res.* 52, 507-516 (2003).
3. Ishii, S., & Shimizu, T. Platelet-activating factor (PAF) receptor and genetically engineered PAF receptor mutant mice. *Progress in Lipid Research.* 39, 41-82 (2000).
4. Hamilton, R.F., et. al. The effect of size on Ag nanosphere toxicity in macrophage cell models and lung epithelial cell lines is dependent on particle dissolution. *Int. J. Mol. Sci.* 15, 6815-6830 (2014).
5. Tibboel, J., Joza, S., Reiss, I., et al. Amelioration of hyperoxia-induced lung injury using a sphingolipid-based intervention. *Eur Resp J.* 42, 776-784 (2013).
6. Salluh, J.I., Pino, A.V., Silva, A.R., et al. Lung production of platelet-activating factor acetylhydrolase in oleic acid-induced acute lung injury. *Prostaglandings, Leukotrienes and Essential Fatty Acids.* 77, 1-8 (2007).
7. Jehle, R., Schlame, M., Büttner, C., et al. Platelet-activating factor (PAF)-acetylhydrolase and PAF-like compounds in the lung: Effects of hyperoxia. *Biochimica et Biophysica Acta.* 1532, 60-66 (2001).

Forebrain-specific SIRT1 Knockout is Sufficient to Produce Selective Spatial Memory Impairments

Daniel Gilliam[1,2], Frankie Heyward[1], and J. David Sweatt[1]

[1]Department of Neurobiology, University of Alabama School of Medicine, Birmingham, AL, USA
[2]Department of Chemistry, University of Alabama at Birmingham, Birmingham, AL, USA

Abstract

Empirical evidence has established that obesity in humans can have adverse effects on memory. Rodent models have successfully recapitulated these obesity-induced memory deficits. One model, the diet-induced obesity (DIO) phenotype, has previously been shown to exhibit selective spatial memory deficits. DIO mice show intact performance on novel object recognition (NOR) and contextual fear conditioning tasks but impaired performance on the object location memory (OLM) task. Because OLM is known to more heavily recruit the hippocampus than NOR and contextual fear conditioning tasks, these results corroborate earlier findings that pathology associated with obesity can lead to impaired hippocampal function. In addition, hippocampal gene expression profiles have established that DIO mice exhibit reduced expression of several learning and memory genes, including the NAD^+-dependent lysine deacetylase SIRT1. The current study sought to establish whether SIRT1 depletion in the hippocampus drives the selective spatial memory impairments observed in DIO mice by using a Cre-ERT2/loxP SIRT1 knockout model. Here we report the development of a validated model of inducible, forebrain-specific SIRT1 knockout and that SIRT1 depletion in the forebrain is sufficient to evoke obesity-associated selective spatial memory impairments.

Keywords: Obesity, SIRT1, Spatial memory, Cre-ERT2

Introduction

Over the past few decades, obesity has emerged as an epidemic in the developed world. Currently 34 % of adults in the United States meet the criteria for obesity, defined by a body mass index greater than 30 kg m^{-2}, and an additional 32 % are considered overweight.[1] Because obesity presents with many systems-wide negative health effects, the rising prevalence of obesity represents a serious public health concern. The consequences of obesity extend even to the brain, as demonstrated by converging epidemiological studies that establish obesity as an independent risk factor for cognitive decline and memory impairment.[2,3]

An association between obesity and cognitive impairment is established, but the cellular and molecular connection remains unclear. Attempts to study altered neurophysiology in rodent models of obesity have been informative. For instance, a mouse model of hyperphagia-induced obesity and diabetes leads to impaired hippocampal synaptic plasticity, altered hippocampal dendritic spine morphology, reduced dentate gyrus neurogenesis, and deficits in spatial memory.[4] Such results demonstrate that obesity could affect learning and memory by impairing the hippocampus, but the molecular mechanisms are still unknown.

A clinically relevant model of obesity-associated cognitive deficits can be generated by increasing caloric intake in wild type mice. Maintaining mice on a high fat diet produces a model of diet-induced obesity (DIO) that reliably exhibits impairments in specific types of hippocampus-mediated spatial learning.[5] DIO mice have been shown to have selective impairments in the object location memory (OLM) test, a spatial learning task known to heavily recruit the hippocampus.[6] Intriguingly, the same DIO mice showed no impairments in novel object recognition (NOR) and contextual fear conditioning tasks, suggesting that heavily hippocampus-dependent OLM spatial learning is disproportionately affected by obesity. Analysis of these mice showed decreased expression of several genes canonically implicated in learning and memory, including *Sirt1*, which encodes the NAD^+-dependent lysine deacetylase SIRT1.[5]

Alterations in hippocampal SIRT1 are particularly interesting because SIRT1 has an established role in energy expenditure and fat mobilization in extraneural tissue, thus representing a potential mediator of the cognitive effects of obesity.[7,8] Previous studies have identified *Sirt1* as permissive for learning and memory.[8] Both *Sirt1* overexpression and activation have been shown to promote learning, memory, and synaptic plasticity.[9] However, it remains an open question whether SIRT1 reductions in the hippocampus are the cause rather than an effect of obesity-associated hippocampal impairment. The purpose of this study was to investigate the role of SIRT1 in obesity-associated cognitive deficits by determining whether induced SIRT1 depletion in the forebrain of adult mice is sufficient to replicate the spatial learning deficits observed in DIO mice.

To date, no study has investigated the behavioral effects of SIRT1 knockout exclusively in the forebrain. However, an efficient method to achieve forebrain-specific SIRT1 knockout is available via an application of the inducible Cre-ERT2/

loxP knockout system, an established technique for targeted protein knockout. This system relies on a specific protein complex, Cre-ERT2, which consists of Cre recombinase bound to a mutated ligand binding domain of a human estrogen receptor. This complex does not bind its natural ligand, 17β-estradiol, but can be activated by other estrogen receptor ligands, including tamoxifen.[7] The gene for Cre-ERT2 can be placed under the regulatory control of a specific gene promoter, localizing Cre-ERT2 expression to a target cell population.

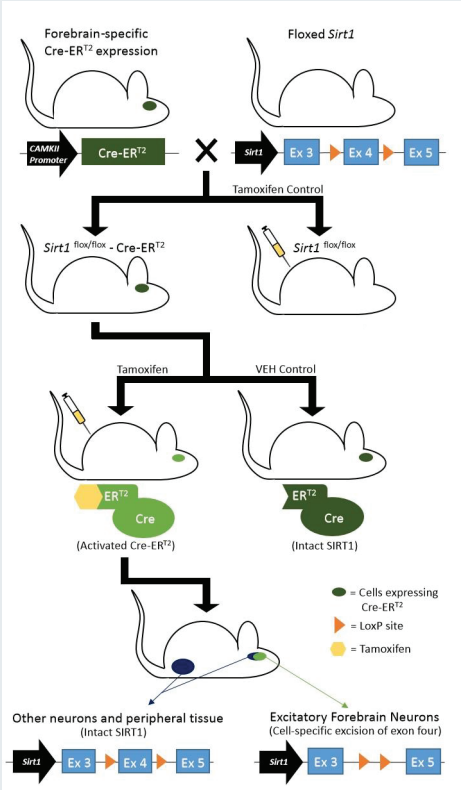

Figure 1. Overview of the CAMK2a*-Cre-ERT2 model of inducible, forebrain-specific SIRT1 knockout. The knockout model created for this study consists of mice harboring both Cre-ERT2 under the control of* CAMK2a *and a floxed version of exon four of the* Sirt1 *gene. Because* CAMK2a *is robustly expressed in excitatory hippocampal neurons,[10] SIRT1 knockout is achieved in these cells. VEH control indicates the control group receiving injections of the vehicle medium (corn oil) with no tamoxifen.*

In this study, forebrain specificity was achieved by placing Cre-ERT2 expression under regulatory control of *CAMK2a* (calcium/calmodulin-dependent protein kinase II alpha promoter), a gene expressed throughout the forebrain and highly expressed in CA1 pyramidal neurons in the hippocampus.[10] In these cells, the recombinase complex should remain in the cytoplasm until activated by tamoxifen. Once activation occurs, the complex should translocate to the nucleus and excise a segment of the *Sirt1* gene targeted for knockout that is flanked by inserted nucleotide sequences known as loxP sites.[11] A gene segment is referred to as "floxed" when it is flanked by loxP sites inserted in the same orientation. This system results in cell-specific ablation of a gene target following systemic tamoxifen administration, enabling inducible gene knockout with temporal and spatial specificity. Importantly, this model circumvents the limitations of germline SIRT1 deletion, namely embryonic lethality and the potential developmental abnormalities due to complete lack of SIRT1. A diagram of the knockout system developed for this study is given in Figure 1.

Materials and Methods

Creating a Forebrain-Specific Inducible SIRT1 Knockout Mouse Model

The Cre-ERT2 protein complex consists of a Cre recombinase bound to a mutant form of the ligand binding domain of the human estrogen receptor. This modified receptor does not bind 17β-estradiol, but will bind other estrogen receptor ligands, including tamoxifen.[7] Forebrain specificity in this model was achieved by using mice with Cre-ERT2 expression under regulatory control of the *CAMK2a* promoter. These mice were crossed with mice with a *Sirt1* transgene containing loxP sites flanking exon four, which encodes the catalytic domain. This breeding scheme produced *Sirt1*$^{flox/flox}$-Cre-ERT2 mice, which would undergo forebrain-specific deletion of the catalytic domain of SIRT1 when treated with tamoxifen. To induce knockout, a five-day regimen of tamoxifen injections was followed beginning at 10 weeks to 16 weeks of age. Mice received 0.08 mg of tamoxifen per gram of body weight via intraperitoneal injection once every 24 h for five consecutive days. Control groups include *Sirt1*$^{flox/flox}$ without Cre receiving tamoxifen, and mice with Cre-ERT2 wild type *Sirt1* receiving tamoxifen injections. No difference was found between the controls, so both groups are combined in the control groups shown in the results. To prevent infection, the injection site was sanitized with 70 % ethanol prior to injection. There was a two-week waiting period post-injection before the mice were used for behavior or tissue collection for downstream analysis. Mice were closely monitored for any adverse reactions to the treatment throughout the injection regimen and waiting period.

Novel Object Recognition Task

The experimental apparatus consisted of a box divided into four separate, identical open arenas (dimensions 39 cm and 19 cm, height 21 cm). Blackened cardboard was used to cover the four walls of each arena. Prior to testing, the animals were acclimated to the general environment by being placed in a nearby storage room in the behavioral facility and allowed to acclimate for one h. Four mice at a time were carried to the NOR testing room in cages fitted with a blackened foam sleeve. The mice were habituated to their individual arenas for 25 min. Habituation was performed on three consecutive days. During the training phase, mice were placed into their arena in the presence of two identical, novel objects and

allowed to explore for 20 min. Following a 24 h retention period, the mice were returned to their arenas, in which one of the original objects was replaced by a novel one, and were allowed to explore for five min. The two objects used were the head of a toothbrush and a single square Lego® block. The initial objects and their location within the arena was balanced between groups.

Objection Location Memory Task

The object location task paradigm began 24 h after the NOR test was completed. The experimental apparatus contexts were identical to the ones previously used for NOR except for the addition of visual cues (electrical tape) on two arena walls. During the OLM training phase, mice were placed in their respective arenas in the presence of two identical objects and allowed to explore for 15 min. The objects were all two-inch long light bulbs fixed to a stabilizing base. After a 24 h retention period, mice were returned to the apparatus, by which time one of the objects was displaced to a novel spatial location. The mice were allowed to explore for five min. Both the object being displaced and the spatial location of the displaced object were balanced between groups.

Scoring NOR and OLM performance

All phases of NOR and OLM were recorded using TopScan (Clever Sys, Reston, VA). In both tasks, each group's ability to recognize the novel object was determined by dividing the mean time exploring the novel object by the mean of the total time exploring the novel and familiar objects during the test session. This value was multiplied by 100 to convert to a percentage preference for the novel object ($T_{novel}/[T_{novel} + T_{familiar}] \times 100$).

In both tasks, objects were rinsed with ethanol between trials and before the first trial to remove residual odors. The first two min of each test phase were hand-scored by a researcher blinded to the experimental conditions. Mice were deemed to be interacting with an object when facing the objects with the tip of the nose in close proximity to the object.

Results

Validation of the Forebrain-Specific Inducible SIRT1 Knockout

To interpret the behavioral data, it was necessary to validate the model on a molecular level. Molecular assays were performed on hippocampus tissue collected from SIRT1 knockout mice and littermate controls.[5] *Sirt1* expression was measured via qRT-PCR using primers designed to amplify exon four, which is the segment flanked by loxP sites and which should not be present if knockout is achieved.[5] SIRT1 protein levels were also measured from hippocampal tissue via Western Blot.[12] Induced knockout of SIRT1 in the hippocampus of adult mice was confirmed by significant reductions in both hippocampal *Sirt1* mRNA and hippocampal SIRT1 protein in knockout mice relative to controls (Figure 2).

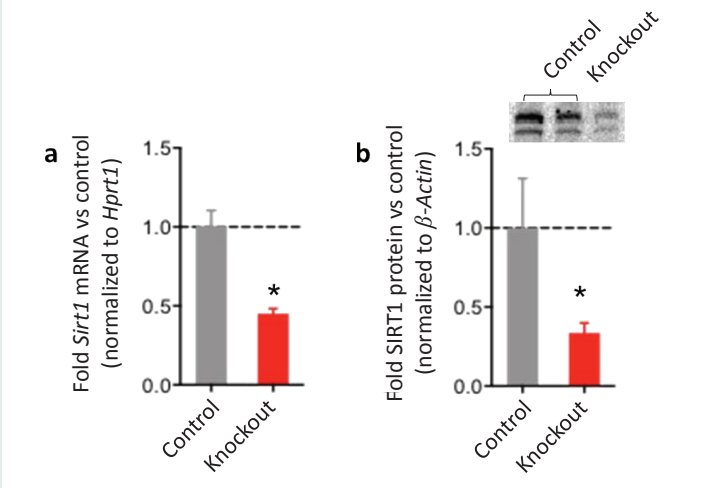

Figure 2. Confirmation of induced SIRT1 knockout in the hippocampus. (a) Using qRT-PCR primers specific for exon four of Sirt1, *it was shown that knockout mice have reduced* Sirt1 *mRNA expression in whole-hippocampus compared to their control littermates (n = 2 to 4 per group, Student's two-tailed t-test $t_4 = 7.052$, **$p < 0.01$). (b) Western blot analysis of SIRT1 (N-term) in hippocampus tissue revealed that knockout mice have reduced SIRT1 protein expression compared to their control littermates (n = 2 to 4 per group, Student's two-tailed t-test $t_4 = 3.101$, $p < 0.05$). Error bars indicate SEM.*

SIRT1 forebrain knockout mice exhibit a selective deficit in hippocampus-dependent spatial learning

To rule out the possibility of differences in ambulation between SIRT1 knockout and control mice, the total distance traveled during an open field test was measured for both groups. No significant difference was found in ambulation between the two groups (Figure 3A). We next sought to assess whether SIRT1 depletion in the hippocampus is sufficient to recapitulate the selective spatial memory impairments observed in the DIO phenotype. The first behavioral test performed was the novel object recognition (NOR) task. Both the control and SIRT1 knockout groups spent more time interacting with the novel object than with the learned object, and no significant difference between the two groups was found (Figure 3B). The next behavioral test performed was the object location memory task, a spatial variant of the NOR task that is known to recruit the hippocampus more heavily than NOR.[6] Using the OLM paradigm, it was found that SIRT1 knockout mice exhibit a selective impairment in hippocampus-mediated spatial learning relative to controls (Figure 3C).

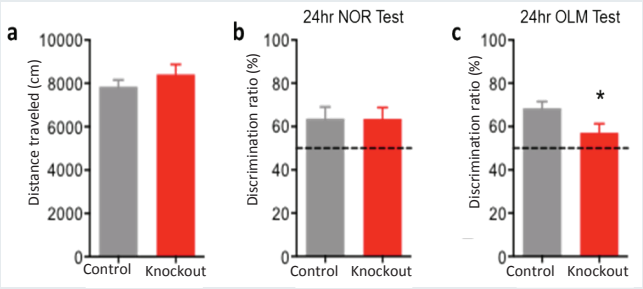

*Figure 3. SIRT1 depletion within the forebrain is sufficient to produce a selective deficit in hippocampus-dependent spatial memory. (a) During the 30 min open field trial, control and knockout mice ambulated for a similar distance (n = 14 to 19 per group, Student's two-tailed t-test t_{31} = 0.9593, p = 0.3463). (b) Control and knockout mice did not significantly differ in their performance on the 24 h test of novel object recognition (NOR) (n = 14 to 19 per group, Student's two-tailed t-test t_{31} = 0.0123, p = 0.9903). (c) Knockout mice exhibited impaired object-location memory (OLM) that was significantly different from that of control mice (n = 14 to 19 per group, Student's two-tailed t-test t_{31} = 2.058, *p < 0.05). The perforated lines (a-c) denote performance indicative of random chance (50 %). Error bars indicate SEM.*

Discussion and Conclusion

Through an inducible knockout model of SIRT1, we have demonstrated that depletion of SIRT1 in excitatory forebrain neurons of adult mice is sufficient to establish deficits in a heavily hippocampus-dependent spatial learning task without impairing performance for less hippocampus-dependent tasks. These results demonstrate that SIRT1 knockout is sufficient to replicate the impaired behavioral phenotype of DIO mice.[5] Furthermore, these observations potentially implicate SIRT1 in the molecular mechanisms subserving at least one modality of spatial learning. An alternative explanation of these results is that SIRT1 is not itself involved in the molecular processes underlying spatial learning, but reduced SIRT1 negatively affects hippocampal physiology in such a way as to evoke mild deficits in heavily hippocampus-dependent tasks. This interpretation decouples SIRT1 from direct involvement in learning and memory but does not undermine its potential role as the mediator between obesity and cognitive impairment.

Our current experiments are aimed at identifying learning and memory genes that exhibit altered expression in the context of SIRT1 knockout and characterizing changes in their epigenetic status relative to controls. The forebrain-specific SIRT1 knockout model developed in this study opens several avenues for such experiments. Because of SIRT1's function as a lysine deacetylase and a transcriptional regulator, it is reasonable to hypothesize that downstream effects of SIRT1 dysregulation in the context of obesity will lead to altered gene expression profiles for genes known to be involved in learning and memory. This hypothesis is bolstered by the reported observation of decreased expression of *PP1*, a gene commonly implicated in learning and memory, in the hippocampus of DIO mice. Identifying the downstream effects of hippocampal SIRT1 depletion in terms of gene expression and locus-specific epigenetic alterations is the crucial next step for investigating the role of SIRT1 in learning and memory and in obesity-associated cognitive deficits. In addition, if obesity is causing hippocampal SIRT1 dysregulation, there must be an unknown upstream pathway leading to dysregulation of SIRT1. Future studies will need to determine which obesity parameters may lead to SIRT1-mediated hippocampal dysfunction.

References

1. Carvajal, R., Wadden, T. A., Tsai, A. G., Peck, K., & Moran, C. H. Managing obesity in primary care practice: A narrative review. Ann N Y *Acad Sci.* 1281, 191-206 (2013).
2. Cohen, R. A. Obesity-associated cognitive decline: Excess weight affects more than the waistline. *Neuroepidemiology.* 34, 230-231 (2010).
3. Cournot, M., Marquie, J. C., Ansiau, D., Martinaud, C., Fonds, H., Ferrieres, J., & Ruidavets, J. B. Relation between body mass index and cognitive function in healthy middle-aged men and women. *Neurology.* 67, 1208-1214 (2006).
4. Stranahan, A. M., Norman, E. D., Lee, K., Cutler, R. G., Telljohann, R. S., Egan, J. M., & Mattson, M. P. Diet-induced insulin resistance impairs hippocampal synaptic plasticity and cognition in middle-aged rats. *Hippocampus.* 18, 1085-1088 (2008).
5. Heyward, F. D., Walton, R. G., Carle, M. S., Coleman, M. A., Garvey, W. T., & Sweatt, J. D. Adult mice maintained on a high-fat diet exhibit object location memory deficits and reduced hippocampal SIRT1 gene expression. *Neurobiol Learn Mem.* 98, 25-32 (2012).
6. Murai, T., Okuda, S., Tanaka, T., & Ohta, H. Characteristics of object location memory in mice: Behavioral and pharmacological studies. *Physiol Behav.* 90, 116-124 (2007).
7. Xu, F., Gao, Z., Zhang, J., Rivera, C. A., Yin, J., Weng, J., & Ye, J. Lack of SIRT1 (Mammalian Sirtuin 1) activity leads to liver steatosis in the SIRT1+/- mice: A role of lipid mobilization and inflammation. *Endocrinology.* 151, 2504-2514 (2010).
8. Price, N. L., Gomes, A. P., Ling, A. J., Duarte, F. V., Martin-Montalvo, A., North, B. J., & Sinclair, D. A. SIRT1 is required for AMPK activation and the beneficial effects of resveratrol on mitochondrial function. *Cell Metab.* 15, 675-690 (2012).
9. Gao, J., Wang, W. Y., Mao, Y. W., Graff, J., Guan, J. S., Pan, L., . . . Tsai, L. H. A novel pathway regulates memory and plasticity via SIRT1 and miR-134. *Nature.* 466, 1105-1109 (2010).
10. Feil, R., Wagner, J., Metzger, D., & Chambon, P. Regulation of Cre recombinase activity by mutated estrogen receptor ligand-binding domains. *Biochem Biophys Res Commun.* 237, 752-757 (1997).
11. Tsien, J. Z., Chen, D. F., Gerber, D., Tom, C., Mercer, E. H., Anderson, D. J., . . . Tonegawa, S. Subregion- and cell type-restricted gene knockout in mouse brain. *Cell.* 87, 1317-1326 (1996).
12. Miller, C. A., Campbell, S. L., & Sweatt, J. D. DNA methylation and histone acetylation work in concert to regulate memory formation and synaptic plasticity. *Neurobiol Learn Mem.* 89, 599-603 (2008).

The IRES Experience: Producing Nanofibers and the Ultimate Czech Adventure

Catherine Ritchey

Department of Biomedical Engineering, University of Alabama at Birmingham, Birmingham, AL, USA

Not every 20 year old can say she has friends in the Czech Republic. In fact, it's safe to say that many 20 year olds in the US are not even entirely sure where the Czech Republic is. But thanks to the International Research Experience for Students (IRES) program I had the opportunity to join in summer 2014, I don't have either of these problems: over the course of several weeks in the Czech Republic, IRES allowed me to absorb myself in both a research experience and a culture that were completely different from anything I have experienced in America.

My research in Liberec, Czech Republic focused on needleless centrifugal spinning (NCS) of polymer nanofibers. NCS is a cost-efficient and effective method for the formation of fibers, with significant potential applications in a range of fields, especially medicine and tissue engineering. However, the success of NCS is heavily influenced by the properties of polymer solutions and particular spinning systems. Our study focused on testing the spinnability of different polymer solutions while varying solution composition and angular velocity of spinning. Polyvinyl Butyral (PVB) was determined to be the best solution for the system we used, and our studies focused on this polymer specifically to understand the parameters affecting its spinnability. The goal was to determine which conditions and solutions are optimal for spinning fibers on an NCS device.

NCS is a very simple process, and it takes less than a minute to generate a usable sample. Each morning we headed to the lab by 9:00 AM, spun samples for about an hour, then mixed the solutions for the following day's samples. Solutions had to mix overnight, so the only experimentation left to do for the day was to view samples under the scanning electron microscope (SEM). I was especially excited to use the SEM (albeit always under close supervision), because I knew it was a learning experience I could apply in my future studies. We collected some really interesting SEM pictures of our nanofibers, and I also had the opportunity to analyze the fiber diameters and structures.

A particular goal of the research was to determine which polymer solutions spin well via force spinning, and which do not work with this system. We initially focused our attention on aqueous solutions. We performed spins while varying angular spin velocity, concentration, and molecular weight for several aqueous solutions—Polyvinyl alcohol (PVA), PVB, and Polyvinylpyrrolidone (PVP)—as well as for solutions of PVB and PVP dissolved in a mixture of ethanol and water. We concluded that our centrifugal spinning system was not capable of spinning aqueous solutions, which we hypothesized was due to the slow evaporation rate of the water along with other factors determined by the polymer and the concentration of the solution. With PVA, the aqueous solutions formed mainly droplets, with very few fibers. Tests with PVB and PVP yielded similar results. We then attempted to spin a range of polymers in different solvents: PVB+ PVP in ethanol; Polyacrylonitrile in Dimethylformamide; and Polyethylene oxide, Polycaprolactone (PCL), and different weight ratios of PCL and PVB in chloroform and ethanol. The best results for nanofiber formation were achieved with PVB in ethanol, so we chose to move forward with this system. Finally, we varied weight concentration and spinning velocity to look for any trends associated with these factors. With our limited time-frame, we only noticed a basic trend: fiber diameter increases with weight concentration (Image 1).

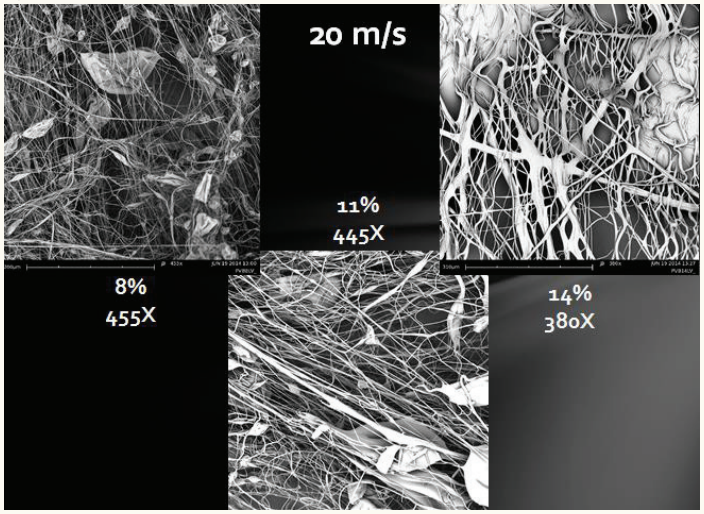

Image 1. SEM Pictures of 8 %, 11 %, and 4 % of PVB spun at 20 m s^{-1}.

After several hours of analyzing samples and collecting images, the Ph.D. students who were our supervisors would end our workday early—around 2:00 PM—and take us on a uniquely Czech adventure they had planned for us. Before my visit, I could not have imagined how beautiful our host

country would be or how much there would be to see and do outside of the lab. One day, we hiked 19 miles through Česky Raj, also known as Bohemian Paradise. We passed small waterfalls, beautiful flowers, and even some chateaus, castles, and a pantheon (Image 2). I had also never imagined that visiting castles and chateaus could become commonplace for me, but it did! Some other highlights of the afternoon explorations were the three beautiful lakes we visited close to Liberec, where we spent a few lovely afternoons swimming and tanning. One afternoon, our supervisors took us to the triple point, where Germany, the Czech Republic, and Poland meet. I took a nap in all three countries at the same time! Afternoons like these made the research we did during the day even more exciting, because we were always looking forward to what was coming after-hours.

Both in and out of the laboratory, my experience was incredibly rewarding and exciting. I learned a remarkable amount and had a wonderful time both working and taking in a new culture, and I would strongly encourage any students interested in travel and research to consider participating in programs such as IRES. Finally, I would like to thank Dr. Andrei Stanishevsky (UAB), who made participation in IRES possible for UAB students, along with Lenka Blažková and Eva Košťáková, my research mentors during my stay. I also gratefully acknowledge the support for the IRES program provided by the grant OISE-1261154 from the National Science Foundation.

Image 2. The beautiful town hall in Liberec—a castle in itself!

Characterization and Development of $BaZrO_3$/NiO Composites for Use as Anodes in Proton Conducting SOFCs

Islam Khan[1], Kelly Dillon[2], Amber Genau[2], and Renato Camata[1]

[1]Department of Physics, University of Alabama at Birmingham, Birmingham, AL, USA
[2]Department of Materials Science and Engineering, University of Alabama at Birmingham, Birmingham, AL, USA

Abstract

Solid oxide fuel cells (SOFCs) are devices that directly convert chemical into electrical energy through oxidation of a fuel. Currently, there is intense interest in developing new kinds of SOFCs that can reduce the typical 800 °C to 1000 °C operating temperature of existing cells to the more manageable 400 °C to 600 °C range, which can be achieved by using doped perovskite-type $BaZrO_3$ protonic conductors as the electrolyte. However, no effective anode materials that are compatible with $BaZrO_3$ have yet been demonstrated. The focus of this work is on developing and characterizing anode materials suitable for integration with $BaZrO_3$-based electrolytes, to enable the next generation of SOFCs. The anode material selected for study was $BaZrO_3$-Ni cermet (ceramic and metal). Samples were created by mechanically mixing $BaZrO_3$ and NiO powders, followed by pressing into cylindrical pellets (0.5 inch in diameter), and sintering at various temperatures. Hypothesizing that the properties of the initial composite $BaZrO_3$-NiO have a strong influence on the properties of the $BaZrO_3$-Ni obtained after reduction in hydrogen, we studied NiO and $BaZrO_3$-NiO composites as a first step to characterizing these complex materials. Grain growth and porosity were observed in BaZrO3-NiO using optical microscopy image analysis, and results showed that 1400 °C to 1600 °C is a suitable sintering temperature range for these composites, with the porosity in their microstructures remaining relatively constant beyond 1500 °C. Electrochemical impedance spectroscopy (EIS) that was carried out on NiO as a reference indicated that there are multiple factors that contribute to the impedance in its structure, and possible sources for each factor are discussed.

Keywords: Solid oxide fuel cells (SOFCs), Anode, Barium zirconate ($BaZrO_3$), Nickel oxide (NiO), Electrochemical impedance spectroscopy (EIS)

Introduction

Today, most of the world's energy is obtained from fossil fuels. However, fossil fuels are slowly being depleted. As the world ages and the population grows, the balance between supply and demand of energy shifts. The modernization and industrialization of previously underdeveloped countries increases further the demands for energy currently obtained from fossil fuels by the method of combustion, creating more air pollution. The rate of growth of world demand for energy is much faster than the rate of replenishment of traditional energy sources. The urgency to fulfill the demand for energy and the increased awareness of global warming has prompted research seeking alternative energy sources that are affordable, reusable, and less harmful to the environment.

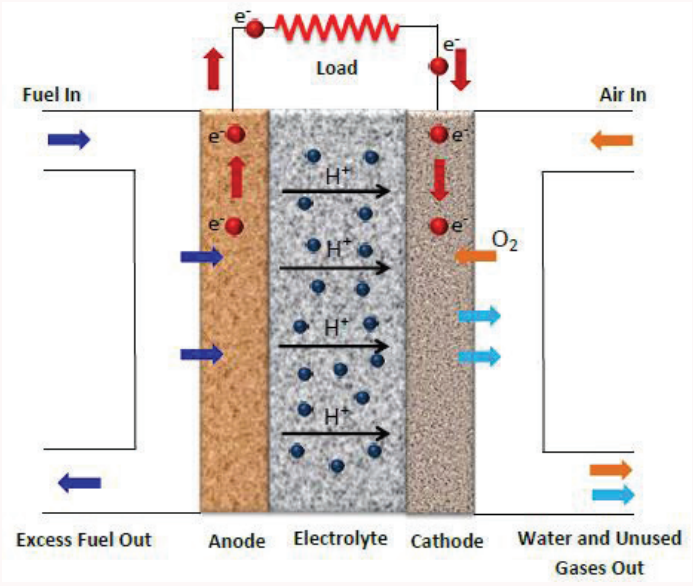

Figure 1. Schematic diagram of a protonic solid oxide fuel cell (SOFC).

One alternative is the use of fuel cells, which are devices that convert chemical energy into electrical energy directly through various mechanisms. One type of fuel cell is the solid oxide fuel cell (SOFC) which uses an oxide material as the electrolyte and oxidation of the fuel to convert energy from chemical to electrical form.[1] Hydrogen fuel and oxygen are used in SOFCs to generate electric current with water as a byproduct (Figure 1). As H_2 molecules in the gas phase enter the anode and pass through porous networks, a chemical reaction takes place at the triple phase (anode, electrolyte, and H_2) boundary regions. Due to high temperature, H_2 molecules are split into H^+ ions (protons) and electrons. The O_2 molecules from air entering through the cathode on the opposite side of the fuel cell combine with these electrons

and the protons that have diffused through the electrolyte to form water as the end product. A continuous conversion to electrical energy can be obtained through a constant flow of electrons, provided that a continuous source of H_2 and air is fed to the fuel cell.

Solid oxide fuel cells have a number of advantages over fossil fuels. They are highly efficient, sustainable, and produce lesser quantities of greenhouse gases.[2] Compared to the efficiency of gasoline internal combustion in a car engine, which is about 20 – 25 %, fuel cells used in a vehicle can have an energy conversion efficiency of about 64 %, which is significantly higher. The most established SOFC technology is based on a yttria-stabilized zirconia (YSZ) electrolyte, which requires the cell to operate at high temperatures (800 °C to 1000 °C).[3,4] These high operating temperatures demand expensive materials for the fuel cell interconnectors, cause thermal stress, require long start-up times, and require substantial energy inputs to heat the cell up to the operating temperature.[5] Consequently, there is a need to reduce the operating temperature to support the use of SOFCs for widespread applications. There is an intense interest in developing new kinds of SOFCs that can reduce the typical 800 °C to 1000 °C operating temperature of existing cells to the more manageable 400 °C to 600 °C temperature range. This can be achieved by creating better electrolytes or better electrodes within the SOFCs that can operate at a lower temperature.[1]

Materials science research has been mainly focused on oxygen-ion conductor electrolyte alternatives to YSZ for many years. However, in recent years, interest has been driven toward proton-conducting ceramics, in particular oxides with perovskite-type structure ABO_3 in which the A site contains alkaline earth elements and the B site contains tetravalent elements.[5] It has been reported that proton-conducting oxides perform well in intermediate temperatures (400 °C to 700 °C) and display higher conductivity measurements along with a lower activation energy compared to the standard oxygen-ion conducting electrolytes.[6]

The main focus of this research is to investigate possible anode materials for proton-conducting SOFCs. An ideal anode for SOFCs is a good electrical conductor for the transfer of electrons, has a porous structure that allows the H_2 to pass through the anode structure and react at the anode's interface with the electrolyte, and has a similar coefficient of thermal expansion (CTE) to that of the electrolyte in order to have lattice compatibility. The most common anodes in the SOFC community are made of an electrolyte-NiO composite material.[7] The electrolyte-NiO composites are reduced in H_2 to remove the oxygen atoms in the NiO to form an electrolyte-Ni composite material which is composed of a ceramic and a metal, commonly known as cermet. The reason electrolyte-Ni cermet is used as an anode is because Ni has a high CTE compared to that of most electrolytes being used in fuel cells and this would result in uneven thermal expansion and contraction at the anode/electrolyte interface. This electrolyte-Ni combination of $BaZrO_3$-Ni greatly lowers the CTE of the anode which shows compatibility with the electrolyte, thus enabling anode-supported SOFCs to be made.

Doped barium cerate ($BaCeO_3$) and doped $BaZrO_3$ are the two most investigated proton-conducting materials. Unlike doped $BaCeO_3$, $BaZrO_3$ has shown high chemical stability against H_2O and CO_2 and high proton conductivity.[6] Thus, the usage of $BaZrO_3$ as a high temperature proton conductor is common among researchers. We hypothesize that the properties of the intermediate composite materials $BaZrO_3$-NiO have a strong influence on the final properties of the $BaZrO_3$-Ni cermet anode. Our goal is to study these composite materials and develop a good anode material with good electronconductivity, controlled porosity in the microstructure, and CTE compatibility with the electrolyte in SOFCs.

Materials and Methods

$BaZrO_3$ and NiO (BZ/NiO) composite pellet samples were made using a mechanical mixing method. The BZ powders used had a density of 5.52 g mL^{-1} at 25 °C and had a particle size of less than 10 µm. The NiO powders used had particle sizes of 12 µm to 22 µm. A mortar and pestle was used to thoroughly mix the two powders, then the mixture was pressed using a 12.7 mm I.D. pressing die set and hydraulic press. The pressure applied on the powder mixtures was 12000 psi (82.737 MPa). The samples were then placed in a furnace and sintered in air at 1500 °C for 5 h. Each side of the pellet samples was polished using a metallographic polishing machine: silicon carbide sandpaper with grit size 800 was used, followed by sandpaper with grit size 1200, and finally a polishing cloth with 1 µm diamond paste. Multiple pellet samples with different ratios by weight were made using this procedure. Optical microscopy was used to take images of the surfaces of the composite sample. Images with magnifications of 200x and 500x were obtained. With the intention to look closer at the microstructure of the composite sample, scanning electron microscopy (SEM) was used to carry out back-scattered electron (BSE) imaging as well as secondary electron (SE) imaging on the sample. Energy-dispersive x-ray (EDX) spectroscopy was used to carry out an elemental analysis on the different phases that appeared on the surfaces of the samples.

Furthermore, five BZ/NiO pellet samples with 40/60 ratio by weight were made using the same procedure except that the sintering temperature was varied from 1300 °C to 1700 °C in 100 °C increments while keeping all other parameters constant. The samples were polished using the same procedure as before, and images of both sides of each sample were obtained using optical microscopy. Twenty

images, ten from each side, of each of the samples were used for the purpose of measuring the porosity as a function of temperature. Using image analysis software Image-Pro Plus, a color threshold was applied on the images to visually highlight the dark regions on the images that represented the pores. This highlighted area was used to measure the percentage of porosity per unit area for each of the selected areas of the sample. The porosity percentage of each of the five samples was estimated by calculating an average of the porosity percentages of all twenty images per sample and the results were compared and analyzed. A pure BZ pellet sample and a pure NiO pellet sample were also made using the same procedure. The sintering temperature used for both pellet samples was 1500 °C, and the sintering time was 5 h. X-ray diffraction (XRD) analysis was carried out on the pure BZ, the NiO, and 40/60 BZ/NiO pellet samples sintered at 1300 °C and 1500 °C. This analysis was carried out in order to test the purity of the sintered composite pellets by comparing the diffraction patterns of BZ and NiO reference data obtained from the American Mineralogist Crystal Structure Database (AMCSD) with that of the BZ, NiO and the two 40/60 BZ/NiO pellet samples that were obtained by taking XRD measurements.

A pure NiO pellet sample with particle size 0.5 µm to 1.5 µm was made as a reference by using hot press (350 °C for 2 h) followed by sintering at 1500 °C for 5 h. In order to create contacts on the composite sample as well as the pure NiO sample, Ni was deposited on both sides of each sample using pulsed laser deposition (PLD). The pellets were then placed between two electrodes, and a staircase potentio electrochemical impedance spectroscopy (SPEIS) sweep was carried out on each of them to measure their electrical properties. The frequency was varied in the range 1 Hz to 7 MHz, and the voltage was varied in the range 0 V to 10 V in 0.5 V increments.

The complex plane of Nyquist plots (Re(Z) vs –Im(Z)) obtained from the Electrochemical Impedance Spectroscopy (EIS) was thoroughly analyzed. A mathematically equivalent circuit model was used to fit the model data on the measured data and values of resistances were obtained. A bode plot (|Z| vs frequency) was also obtained and the capacitance for each voltage was obtained using the equivalent circuit model. A capacitance versus voltage graph (C vs. V) was obtained followed by the reciprocal of capacitance square versus voltage graph ($1/C^2$ vs. V). The slope of this graph was used to calculate the charge carrier concentration in the NiO using the following equation:

$$n = \frac{2}{q\varepsilon A^2 \frac{1}{\frac{d}{dV}\left(\frac{1}{C^2}\right)}} \qquad (1)$$

Results and Discussion

The images of the 60/40 BZ/NiO sample obtained using optical microscopy showed the presence of three different phases of materials along with pores in their microstructures. The porosity in the microstructure was a defect that resulted from the incomplete densification of the powder particles during sintering. Figure 2a shows one of these images in which the brighter regions were in the NiO phase, and the grey regions were in the BZ phase. There were also dark grey regions whose phase was unknown at first. EDX spectroscopy analysis on those regions gave the same elemental composition as the grey regions that were in the BZ phase. The SE detector was divided into quadrants, and subtraction of two opposite quadrants was used to obtain topographical images that show the surface of the composite pellet to be fairly smooth except at the dark grey regions where shallow holes occurred. It was hypothesized that the depth of these holes resulted in those regions appearing darker in both the optical microscope and SEM images.

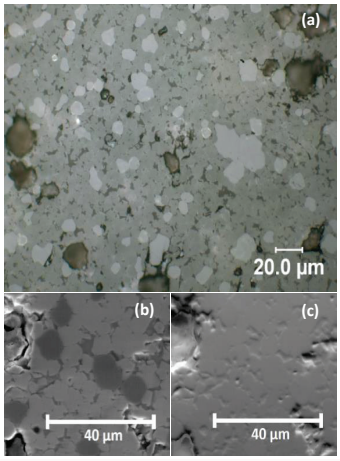

Figure 2. (a) Optical microscopy image of 60/40 BZ/NiO sintered at 1500 °C for 5 h showing the different phases. (b) Scanning electron microscopy (SEM) image in secondary electron mode. (c) Topographical image obtained using back-scattered electron mode in SEM.

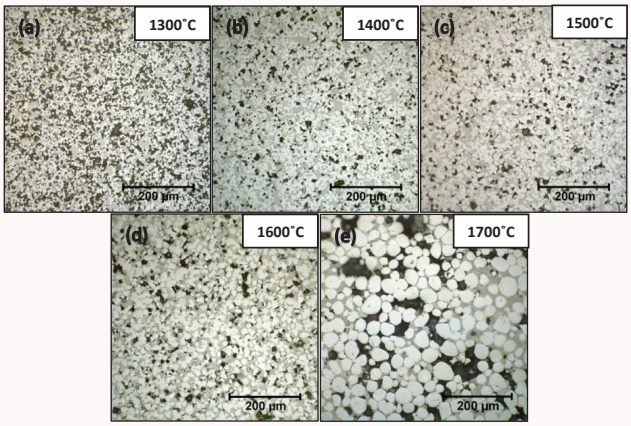

Figure 3. Optical microscopy images of 40/60 BZ/NiO sintered for 5 h at (a) 1300 °C (b) 1400 °C (c) 1500 °C (d) 1600 °C and (e) 1700 °C.

As seen in Figure 3, optical microscopy analysis of the five 40/60 BZ/NiO samples that had been sintered at different temperatures showed that the samples sintered at higher temperatures had a larger grain growth as well as less porosity per unit area compared to the samples that had been prepared at lower temperatures. It was noted that even though the same procedure was used to polish both the samples, the sample sintered at a higher temperature appeared shinier on the surface, possibly due to the reduction in porosity. The larger grain growth and higher densification at the higher temperature were expected since there was more thermal energy available for atomic diffusion to take place in the microstructure. The sample sintered at 1700 °C showed evidence of non-uniformity in porosity in the microstructure of the composite. The BZ phase was observed to be more concentrated at certain areas, leaving large pores behind. Figure 3 shows images of the five samples obtained using optical microscopy at a magnification of 200x.

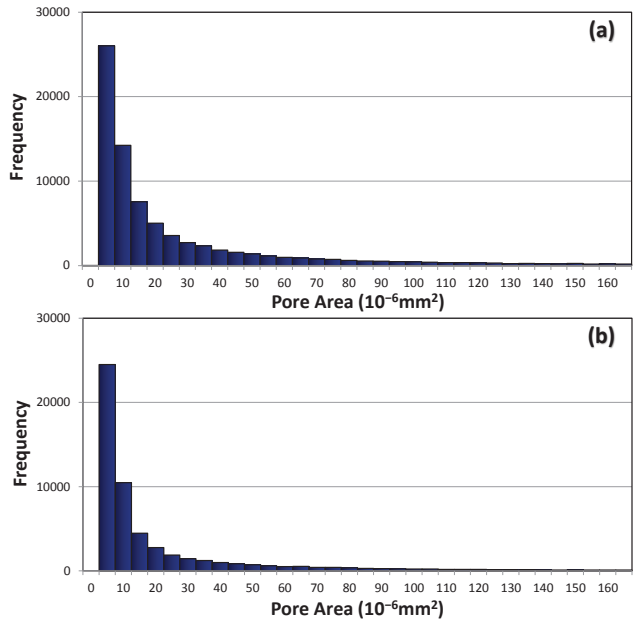

Figure 4. Pore area distribution of 40/60 BZ/NiO samples sintered at (a) 1300 °C and (b) 1500 °C.

The porosity of each side of the 40/60 BZ-NiO samples was measured using image analysis. The samples sintered at 1300 °C, 1400 °C, 1500 °C, 1600 °C, and 1700 °C showed an average porosity of 28.3 % ± 2.4 %, 10.2 % ± 1.4 %, 16.9 % ± 2.3 %, 17.0 % ± 1.0 %, and 16.8 % ± 3.7 %, respectively. These results show that the porosity appears to be highly uniform across each of the samples sintered at lower temperatures. Figure 4 displays the pore size distribution for the two samples that were sintered at 1300 °C and 1500 °C. About 94 % of the pores were 1.65 × 10^{-4} mm^2 or smaller for the sample sintered at 1300 °C, and 96 % of the pores were 1.65 × 10^{-4} mm^2 or smaller for the sample sintered at 1500 °C. The porosity in the composites has been summarized in a histogram in Figure 5. The histogram shows that the porosity decreases with the increase in temperature, but beyond 1500 °C the porosity percentage remains relatively constant with the increase in temperature. The high standard deviation in the porosity percentage measurements for the sample sintered at 1700 °C also indicates the non-uniformity of pores in the composite microstructure.

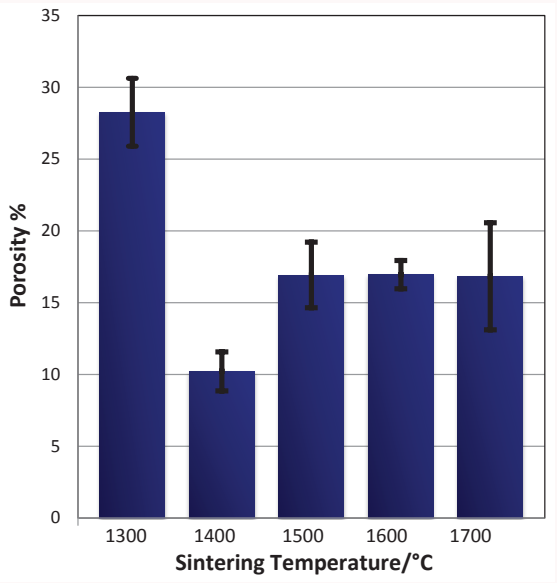

Figure 5. Histogram showing porosity percentage of 40/60 BZ/NiO as a function of sintering temperature. The error bars represent standard deviation.

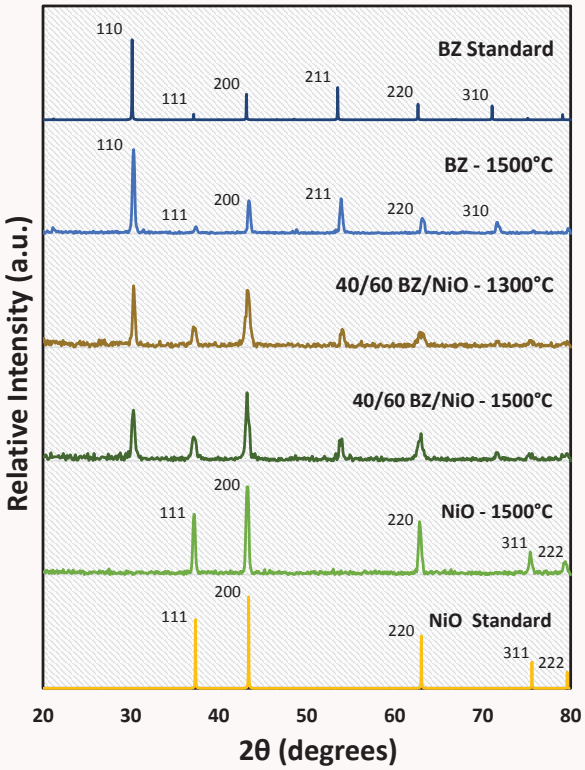

Figure 6. XRD patterns of BZ, NiO and 40/60 BZ/NiO composites sintered at different temperatures with reference data obtained from AMCSD.

The XRD patterns of the four pellet samples along with the reference XRD patterns of BZ and NiO obtained from the AMCSD are shown in Figure 6. Results show that the BZ and NiO pellet samples prepared by firing at 1500 °C for 5 h had the same phases as in the reference XRD patterns, indicating that there were no changes in phase during the sintering process. The XRD patterns of the two 40/60 BZ/NiO composite pellet samples fired at 1300 °C and 1500 °C cannot be differentiated. In both cases, the peaks appear only at those values of 2θ at which the peaks appear for the BZ and NiO pellet samples. This indicates that the two phases in the composite, BZ and NiO, retained their phases after they had been sintered, which also indicates that there are no reactions taking place between the two phases in the composite or between the composites and the air present in the furnace during the sintering process.

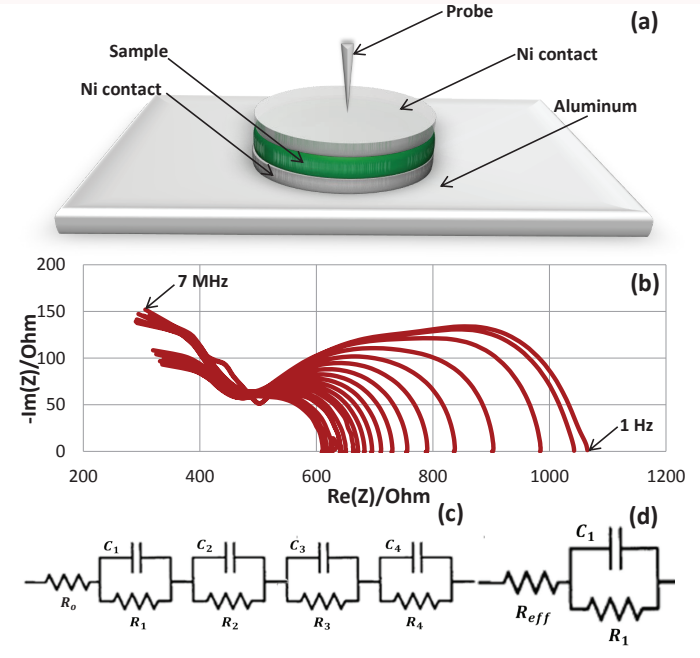

Figure 7. (a) Graphic showing the system used for taking impedance measurements. (b) Complex-impedance plane plot for the NiO. (c) Equivalent circuit model used to measure resistance and capacitance. (d) Simplified equivalent circuit model assuming the polarization is due to the electrode/NiO interface.

The electrical properties of a material are commonly studied by measuring the magnitude of opposition to electric current through it. NiO is known as a p-type semiconductor with a wide band gap that conducts a negligible amount of current at room temperature.[9,10] However, an alternating current (AC) can be conducted through a dielectric (insulating material) by the polarization mechanism. Like resistance is the opposition to direct current (DC), impedance is the opposition to AC that provides valuable information regarding the electrical properties of a dielectric material. Figure 7a shows a schematic of the system that was used to take impedance measurements on the samples. In EIS, an electrical stimulus (known voltage or current) over a range of frequencies is applied and the response of the system is observed. Different polarization mechanisms in a system are only activated at certain frequencies. The complex-impedance plane/Nyquist plot for the pure NiO sample pellet with Ni contacts on both sides was obtained (Figure 7b). In a typical Nyquist plot, each polarization in the system corresponding to different dielectric mechanisms gives rise to a semicircle with a single time constant. Impedance measurements on BZ/NiO composites proved to be too difficult to comprehend since there are two phases of materials in the structure. Therefore, the system was simplified by taking impedance measurements on pure NiO samples that only contained one phase. The complex-plane plot of NiO is complicated compared to typical plots which have clearly defined semicircles. Looking at the results, four overlapping indistinct semicircles can be observed with some difficulty. Mathematically equivalent circuit models can be designed to give similar plots as a real system that produces semicircles in a Nyquist plot. Figure 7c shows the equivalent circuit model that was used to fit the curve on the measured data.

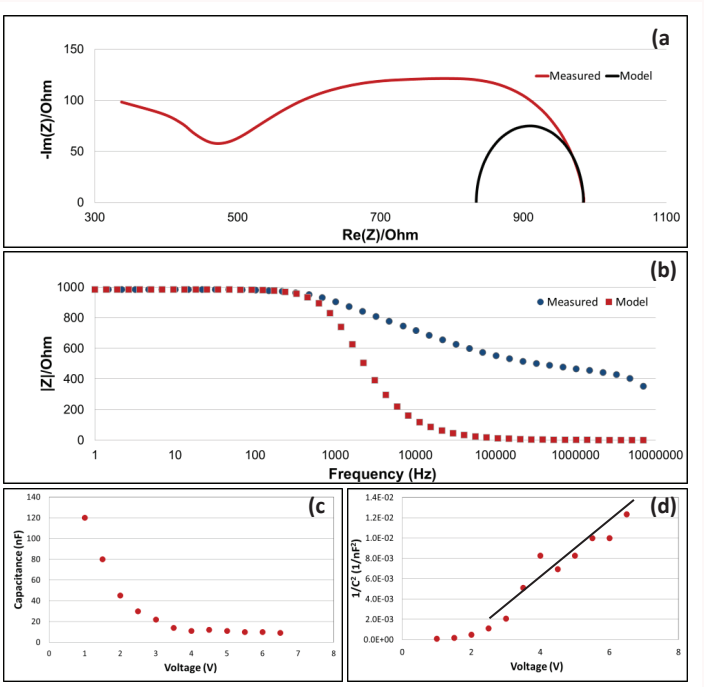

Figure 8. (a) Electrical circuit model used to fit complex plane plot on measured data to obtain resistance. (b) Model used on bode plot to measure capacitance. (c) Graph showing capacitance vs voltage. (d) Graph showing $1/C^2$ vs voltage graph the slope of which can be used to measure charge carrier concentration.

It is known that the polarization that takes place at a metal-semiconductor interface is activated at a lower frequency range. Possible sources for the other impedance can be attributed to bulk conductivity resistance and grain boundary contributions. The semicircle at the lowest frequency

also intercepts the x-axis in the Nyquist plot at 90°. Given the complexity of the Nyquist plot of NiO, an attempt for simplification was made by only taking into consideration the semicircle at the lowest frequency, which is assumed to be the polarization taking place at the Ni-NiO interface. When a metal makes a contact with a semiconductor, a barrier is formed at the metal-semiconductor interface and it is known as a Schottky barrier. Figure 9a displays the assumed band diagram of p-type semiconductor NiO indicating the vacuum energy E_{Vac}, conduction energy E_C, Fermi energy E_F, valence band E_V, electron affinity χ, work function φ, and band gap E_g in which the acceptor impurities in NiO contribute hole levels in the semiconductor band gap which shifts the Fermi level downwards at a point about halfway between the acceptor levels and the valence band. The Ni is assumed to have a higher work function, which is the energy difference between the vacuum level and the Fermi level, compared to the NiO. When they are brought into contact, their Fermi levels would align as a brief transient current flow would take place from the Ni to NiO assuming the Ni has a higher work function. The electrons that flow from the Ni to NiO get bounded to fixed positions in the NiO. This can also be seen as the NiO having an excess of positive holes and, upon contact with Ni, the holes "flow" from the NiO to the Ni, leaving negative charges behind. This flow of charges creates a depletion layer, and the accumulation of positive charges in Ni and of negative charges in NiO, both at the boundary, creates a capacitor. Figure 9b shows band diagrams of the Ni and NiO after they have been brought into contact and a Schottky barrier is created.

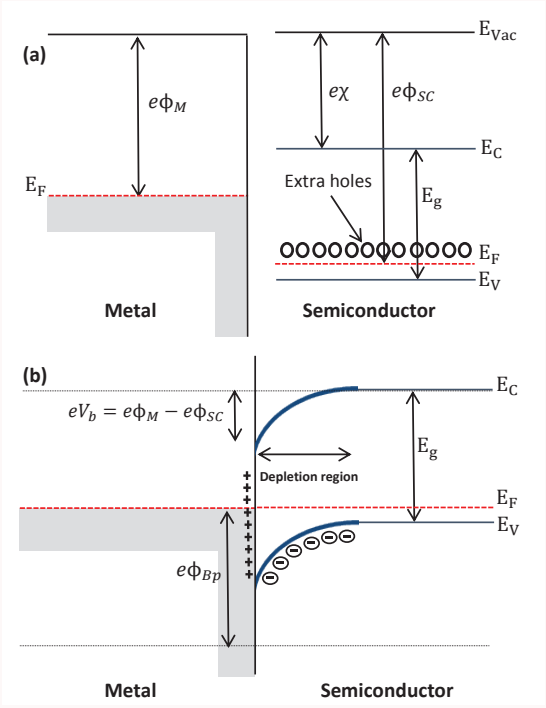

Figure 9. (a) Ni and NiO band diagrams before contact. (b) Schottky barrier after Ni and NiO are brought into contact.

The capacitor created at the Ni-NiO interface has an electric field pointing from the positive to negative charges. In the parallel plate capacitor, the capacitance resists any change in voltage and remains constant; however, the capacitance at the metal-semiconductor junction does not remain constant since the width of the depletion layer varies with the applied voltage. The increase in reverse bias adds more electrons on the NiO side of the barrier which raises its Fermi level. This increase in voltage increases the width of the depletion region. This width of the depletion region is also the separation distance between the two average planes of charges. Capacitance is inversely proportional to the distance between the planes of charges, and therefore the capacitance of the Ni-NiO Schottky barrier should decrease with the increase in voltage.

Using the simplified equivalent circuit model and method of fitting curve, the resistance for each forward bias voltage was measured and it was noted that the resistance decreased with the increase in voltage. These resistance values were used to fit the curve on the bode plot and the capacitance for each forward bias voltage was also measured. A capacitance against voltage graph was plotted and the results show that the capacitance due to the Ni-NiO interface decreases with the increase in voltage (Figure 9c), an outcome which agreed with the predictions. This shows that the assumed band diagram of the Schottky barrier is possibly correct. Furthermore, a $1/C^2$ against voltage was plotted and using the slope of this curve and Eq. 1, the charge carrier concentration in NiO was found to be 2.94×10^{10} cm^{-3} at room temperature. This is a reasonable value of charge carrier concentration for a typical semiconductor.

Conclusions

The goal of this research was to study the factors contributing to the properties of anode materials and develop a better anode for use in SOFCs. In order to reach this goal, the microstructure and electrical properties of potential materials for use in SOFCs, in particular SOFCs with solid ceramic $BaZrO_3$ electrolytes, were studied. An electrolyte-Ni cermet is generally used for anode materials because it shows good electrical conduction, catalytic activity, and CTE compatibility. $BaZrO_3$/NiO composite materials are commonly prepared by a mechanical mixing method followed by sintering at high temperatures and reducing the NiO to Ni to produce the $BaZrO_3$/Ni cermet. The microstructure and electrical properties of the $BaZrO_3$/NiO composite material plays a crucial role in the properties of the cermet and hence its function as an anode in the SOFCs. A BZ/NiO composite with 60/40 weight ratio was prepared by mechanically mixing the powders and sintering at 1500 °C for 5 h. Optical microscopy image analysis and SEM imaging showed that there are two phases (BZ and NiO) in the microstructure with the presence of porosity, which is a defect that is beneficial for use in anodes in fuel cell applications. Porosity percentage

as well as pore size distribution of five 40/60 BZ/NiO pellet samples that were sintered at different temperatures were analyzed and compared. Results show that the porosity in the samples that were sintered at lower temperatures appeared to be highly uniform but at high temperatures there is non-uniformity in the porosity in the microstructure. Uniformity in porosity is important for fuel cell applications since the fuel in gas phase needs to pass through the anode uniformly across the anode for good performance. The sample sintered at 1300 °C showed high porosity percentage which would affect the conductivity of the composite. Therefore, 1400 °C to 1600 °C is a suitable sintering temperature range for preparation of these composite materials. XRD patterns of the samples were compared with reference XRD patterns of BZ and NiO obtained from the AMCSD, and results showed that the two phases do not undergo any phase change during the sintering process and that no reaction of the two BZ/NiO composite phases takes place with each other or with air when they are being sintered. Impedance measurements on the BZ/NiO proved to be too complex to comprehend due to the presence of two phases in its structure, and therefore impedance analysis was carried out on NiO with Ni contacts on both sides that showed there are four or more sources of impedance in the system. Possible sources of impedances in the system are bulk conductivity resistance, grain boundary contributions, and Ni-NiO interface resistance. Using SPEIS, the polarization at the Ni-NiO junction was investigated and results showed that the charge carrier concentration in the NiO in the sample is about 2.94×10^{10} cm^{-3} at room temperature. The semicircles that are attributed to the Ni-NiO interface can now be subtracted from the data and the other sources of impedance investigated. Using a similar method as used for the Ni-NiO interface polarization, the values of resistance and capacitance of the other impedance contributors can be measured. A basic understanding of the BZ/NiO composites has been achieved by this research project and the next stage is to reduce this composite to BZ/Ni cermet in H_2 and study its properties. This reduction process would increase the porosity in the microstructure as oxygen atoms would be taken away from it. The porosity percentage measured in the BZ/NiO composite should be proportional to the porosity of the cermet after reduction, but the new material produced would have an electrical conductor Ni in it and would therefore have very different electrical properties compared to those of the composite. Studying the properties of the cermet would be the next step in order to develop good anode materials.

Acknowledgements

Support for this project was provided by the UAB College of Arts and Sciences Interdisciplinary Innovation Team Award entitled, "A New Interdisciplinary Research Thrust in Ceramic Materials for Clean Energy Applications with Broad Student Participation." The authors would like to thank Zack Lindsey, Eric Remington, Alex Skinner, William Warriner, and Elis Rivera for their technical assistance and support with experiments.

References

1. Fabbri, E., Bi, L., Pergolesi, D., & Traversa, E. Towards the next generation of solid oxide fuel cells operating below 600 °C with chemically stable proton-conducting electrolytes. *Advanced Materials*. 24, 195-208 (2012).
2. Traversa, E., & Boudghene Stambouli, A. Solid oxide fuel cells (SOFCs): A review of an environmentally clean and efficient source of energy. *Renew. Sustain. Energy Rev*. 6, 433-455 (2002).
3. Singhal, S. C. Advances in solid oxide fuel cell technology. *Solid State Ionics*. 135, 305-313 (2000).
4. Steele, B., & Heinzel, A. Materials for fuel-cell technologies. *Nature*. 414, 345-352 (2001).
5. Fabbri, E., Pergolesi, D., & Traversa, E. Materials challenges toward proton-conducting oxide fuel cells: A critical review. *Chem. Soc. Rev*. 39, 4355-4369 (2010).
6. Bi, L., Fabbri, E., Sun, Z., & Traversa, E. Sinteractive anodic powders improve densification and electrochemical properties of BaZr0.8Y0.2O3-o electrolyte films for anode-supported solid oxide fuel cells. *Energy and Environmental Science*. 4, 1352-1357 (2011).
7. Bi, L., Fabbri, E., Sun, Z., & Traversa, E. BaZr(0.8)Y(0.2)O(3-delta)-NiO Composite anodic powders for proton-conducting SOFCs prepared by a combustion method. *Journal of the Electrochemical Society*. 158, B797-B803 (2011).
8. Morin, F. J. Electrical properties of NiO. *Phys. Rev*. 93, 1199-1204 (1954).
9. Hufner, S., Steiner, P., Sander, I., Reinert, F., & Schmitt, H. The optical gap of NiO. Z. *Phys. B - Condensed Matter*. 86, 207-215 (1992).

research paper

Quantitative Mapping of Cytochrome C Oxidase Metabolic Activity in the Developing Brain of Rats Bred for High Versus Low Depression-like Behavior

Samantha Golf[1,2], C.R. McCoy[3], S.A. Stringfellow[3], M. Melendez-Ferro[4], E. Perez-Costas[4], N.L. Jackson[3], and Sarah Clinton[3]

[1]Department of Neurobiology, University of Alabama School of Medicine, Birmingham, AL, USA
[2]Department of Chemistry, University of Alabama at Birmingham, Birmingham, AL, USA
[3]Department of Psychiatry, University of Alabama School of Medicine, Birmingham, AL, USA
[4]Department of Psychology, University of Alabama at Birmingham, Birmingham, AL, USA

Abstract

Individual differences in temperament in humans can increase risk for psychiatric disorders like depression and anxiety. Our laboratory utilized a rat model of temperamental differences to study neurobiological factors that underlie emotional behavior differences. Rats that were selectively bred for low novelty exploration (Low Responders, LR) also displayed high levels of anxiety- and depression-like behavior compared to High Novelty Responder (HR) rats. Previous microarray studies in developing HR/LR brains have revealed numerous differences in gene expression in the early postnatal hippocampus, including marked changes in genes related to metabolic processes. The present study builds on that earlier work by examining activity of cytochrome c oxidase (COX), one of the enzymes responsible for ATP production and a correlate of metabolic activity, in brain tissue from seven-day-old HR/LR rat pups. We focused on postnatal day seven (P7) because at this age robust differences in HR/LR expression of metabolic genes occurred. Our analysis focused on three brain regions known to regulate emotional behavior: the amygdala, the hippocampus, and the prefrontal cortex. We found that P7 LR rats display higher COX activity in the amygdala compared to HRs while no differences were found in the prefrontal cortex. Within the cornu ammonis region of the hippocampus, we found increased COX activity in the cellular and molecular layers of HR vs. LR pups. Our results shed light on how the brain develops differently in rats known to express high vs. low anxiety/depression-like behavior, highlighting particularly robust differences in the amygdala and hippocampus during the first week of life.

Introduction

Individual differences in temperament and emotional reactivity play a formative role in humans' ability to cope with stress and predispose certain individuals to psychiatric disorders such as depression and anxiety.[1] Our lab uses a rodent model of temperamental differences to study the neurobiological basis of emotional behavior differences. Sprague Dawley rats that were selectively bred to display low behavioral response to novelty (Low Responders, LR) also exhibit high anxiety- and depression-like behavior compared to High Novelty Responder rats (HRs).[2] These behavioral traits emerge in early life, and previous microarray studies have revealed widespread differences in gene expression in the developing HR vs. LR brain.[3] Numerous genes were found to be altered in the developing hippocampus and amygdala of HR/LR rats during the first two weeks of life (i.e., as assessed at postnatal days seven and 14), with particularly marked changes occurring in genes involved in metabolic processes (McCoy, C.R., Clinton, S., et al., unpublished data). For example, our bioinformatics analyses used the Kyoto Encyclopedia of Genes and Genomes (KEGG) pathway analysis tool to identify the top ten molecular pathways that differed in the postnatal day seven (P7) HR vs. LR brain (Table 1). In bold, Table 1 shows that three of the top 10 differentially enriched pathways are related to metabolism, including genes involved in the electron transport chain, glycolysis/gluconeogenesis, and the TCA cycle.

While dysregulation of monoamine neurotransmission has long been hypothesized to underlie the pathophysiology of depression,[4] others have postulated a possible role for mitochondrial dysfunction in the illness.[5] This hypothesis is based in part on the fact that depression and other affective disorders are highly co-morbid with metabolic disorders. Moreover, these two classes of disorders share many symptoms, such as fatigue, cognitive deficits, and psychomotor retardation.[5] A recent study even showed that mitochondrial dysfunction and monoamines, specifically serotonin, may be linked through monoamine-dependent regulation of phosphorylated glucocorticoid receptor and its transcriptional control of the mitochondrial genes for cytochrome c oxidase (COX).[6] Whether these processes are overlapping or provide separate mechanisms of action, it is important to gain a deeper understanding of their roles in shaping emotional behavior.

Given that most neurons in healthy tissue are postmitotic cells, they do not experience continuous turnover and rebirth; thus, neurons engage in metabolic activity almost exclusively

KEGG pathway analysis		
Top 10 Pathways	ratio of enrichment	adjusted p-value
Metabolic pathways	43/1169	1.38E-13
Protein processing in ER	17/164	3.50E-12
Phagosome	15/185	2.31E-09
Gap junction	10/89	1.02E-07
Glycolysis / Gluconeogenesis	9/78	3.76E-07
Alzheimer's disease	13/212	5.94E-07
Oocyte meiosis	10/115	6.99E-07
Pathways in cancer	15/319	1.39E-06
Lysosome	9/124	1.14E-05
Citrate cycle (TCA cycle)	5/30	4.00E-05

Table 1. Enrichment for metabolic genes within the group of genes that were differentially expressed in the HR vs. LR postnatal day seven hippocampus or amygdala. A previous study used genome-wide expression profiling to ascertain mRNA expression differences in the postnatal day seven brains of HR/LR rats. Bioinformatics analysis of those gene lists using Kyoto Encyclopedia of Genes and Genomes (KEGG) pathway analysis identified an enrichment of several metabolic pathway-related genes. Enrichment analysis was performed on genes that differed between HR/LR rats, with data altered by p< 0.05, fold change> 1.5, and corrected for false discovery rate. The ratio of enrichment is the number of regulated genes in a particular pathway to the total number of genes in the pathway. The adjusted p-value was generated by the pathway analysis tool.

to meet functional demands. As a result, metabolic activity serves as an ideal indicator of neuronal activity levels. To produce energy, neurons are heavily reliant upon oxidative metabolism, a process that requires COX. COX is the terminal mitochondrial enzyme in the electron transport chain and plays an essential role in establishing the proton gradient, ultimately leading to ATP production (Figure 1). Thus, COX activity levels are highly predictive of metabolic activity levels and can be used to estimate relative metabolic activity levels within different regions of the brain.[7]

The present study assessed COX enzymatic activity in brain tissue from seven-day-old HR/LR pups, focusing on three key limbic brain areas known to regulate emotional behavior: the amygdala, the hippocampus, and the prefrontal cortex. The postnatal day seven time point was chosen because at this age prominent differences in the HR/LR expression of metabolic genes were found in our earlier microarray study (McCoy, C.R., Clinton, S., et al., unpublished data). Based on prior gene expression data together with a previous study reporting lower COX activity in the brains of infant (one-day-old) rats predisposed to learned helplessness behavior,[8] we hypothesized that P7 LR pups, prone to "anxiety and depression," would exhibit diminished COX activity in one or more emotionally-relevant brain regions compared to HR pups.

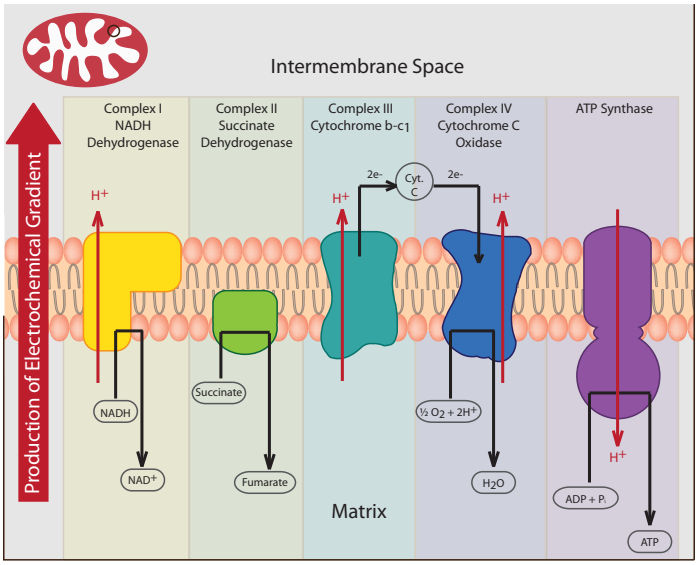

Figure 1. Cytochrome c oxidase (Complex IV) plays an integral role in oxidative energy metabolism. As a transmembrane spanning protein of the inner mitochondrial membrane, COX facilitates the production of an electrochemical gradient by catalyzing the transfer of electrons from its substrate to metabolic water. This process is coupled with the oxidative phosphorylation of ADP, leading to the production of ATP. As a result of this tight coupling in neurons, ATP generation exclusively occurs after energy has been spent through neuronal activity. [7]

Materials and Methods

Animals and Tissue Collection

To generate HR and LR offspring for this study, adult HR male/female rats and adult LR male/female rats from our in-house breeding colony were mated. At birth (P0), litters were culled to six male and six female pups. A subset of the offspring were sacrificed on P7 (n=8 per phenotype) by rapid decapitation.

Brains were removed, flash frozen with isopentane cooled to −30 °C, and then stored at −80 °C until further use. Brains were cryostat sectioned at 15 µm, collected every other section, mounted onto slides in parallel series of 10 slides, and stored at −80 °C until further processing.

Cytochrome C Oxidase Histochemistry

The COX enzymatic assay was performed as previously described by Melendez-Ferro et al.[9] Slides from each rat were removed from –80 °C storage and warmed to 23 °C (RT) for 15 min. Tissue sections were incubated in the reaction medium (described below) at 37 °C in the dark for 120 min. Preliminary experiments showed that the 120 min incubation was optimal for our P7 brain tissue samples. The reaction medium was a solution that consisted of the following chemicals: 22.4 mg cytochrome c (Sigma-Aldrich, St. Louis, MO, USA; C3131), 115.23 mg diaminobenzidine (DAB, Sigma-Aldrich, D5637), 4.5 g sucrose (Sigma-Aldrich, S0389), and 12.51 mL of a 1 % aqueous nickel(II) ammonium sulfate solution (Sigma-Aldrich, A1827) mixed in 100 mL of 0.1 M HEPES buffer (Sigma-Aldrich, H3375) at pH 7.4.[9] To terminate the COX enzymatic reaction, sections were immersed in 4 % paraformaldehyde in 0.1 M phosphate buffer (PB) at pH 7.4 for one h at RT. Sections were then rinsed in PB, dehydrated in ethanol, cleared in xylene, and plated onto coverslips. In preliminary studies, negative control sections were immersed in 4 % paraformaldehyde in 0.1 M PB at pH 7.4 for 60 min at RT. Then, slides were rinsed in PB and incubated in a 10 mM sodium azide solution in PB for 17 h at RT to inactivate COX. After again rinsing in PB, the sections were incubated with the experimental slides. The negative control showed no evidence of nonspecific staining in brain regions of interest, though low amounts of staining were observed on the perimeter of the tissue.

To more accurately assess differences in COX activity between groups and between different brain regions, a standard dot blot of known COX protein concentrations (0.03 µg to 2 µg) was generated as described by Melendez-Ferro et al.[9] These known standards were loaded onto a nitrocellulose membrane using vacuum and a slot-blot microfiltration apparatus (Bio-Rad, Hercules, CA, USA; 170-6542). This dot blot was created the same day as the reaction in the incubation medium and was imaged within a few days after drying.

Image Acquisition and Analysis

Slides containing rat brain tissue processed for COX histochemistry and the dot blot membrane containing COX standards were scanned on a MicroTek ScanMaker 9800XL in 16-bit grayscale settings without corrections. NIH ImageJ software (version 1.48v; http://rsbweb.nih.gov/ij/) was used to measure optical density (OD). A separate set of slides from each subject was stained with cresyl violet to provide anatomical guides for the COX activity measurements. The cresyl violet-stained sections were used to create masks defining regions of interest on the corresponding COX-reacted slides. Sections were excluded from analysis if they showed damage within a region of interest due to tissue processing. An exponential standard curve was created using OD values from the COX standards on the dot blot (r^2=0.97; Figure 2A).

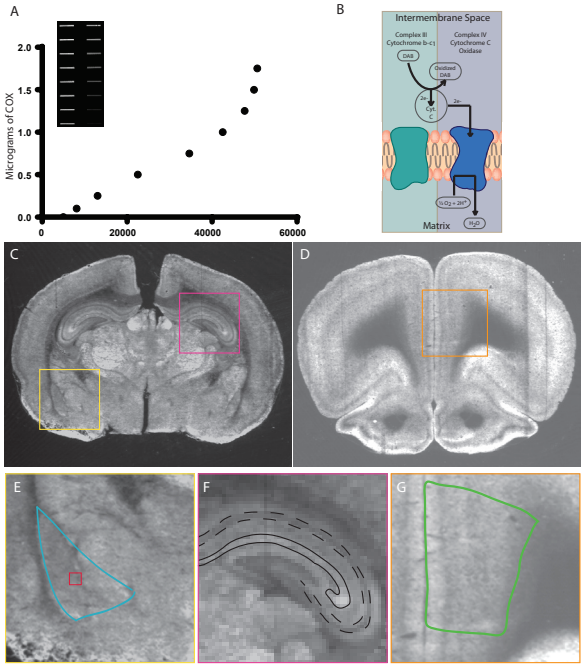

Figure 2. Measurements of COX activity within a brain region are done by comparison to known standards. (A) The optical density of COX activity within the same incubation medium creates an exponential curve (R^2= 0.97). (B) The oxidation of DAB by the cytochrome C that is reduced by the cytochrome c oxidase in the tissue allows visualization of the COX activity. (C) Displays a brain section that has been reacted with the COX assay and contains both amygdala and hippocampal regions. (D) Displays a brain section which has been reacted with the COX assay and contains the prefrontal cortex region (E) The amygdala (AMY; blue outline), (F) hippocampus, including the cellular (dashed black outline) and molecular (solid black outline), and (G) prefrontal cortex (PFC; green outline) were inverted, outlined and optical density measurements were taken within the brain regions on two separate days and by two individuals to prevent bias.

Using the COX-reacted sections, we measured OD levels in three brain regions known to regulate emotional behavior: the amygdala, the hippocampus, and the prefrontal cortex. These measurements were made in at least four sections spaced 240 µm apart across the rostro-caudal extent of the hippocampus, the amygdala, and the prefrontal cortex. Analysis of the hippocampus evaluated two layers of the cornu ammonis (CA) regions: the pyramidal cell layer and the innermost molecular layer, where the hippocampal neurons synapse.

For each section measured, the Image J rectangle tool was used to create five non-overlapping boxes

(0.002 cm^2) that were randomly placed within a region of interest. Measurements from each subject from each brain region were averaged to yield a single value per animal for each brain region (or brain subregion). These values were then used for statistical comparison. Two independent, blinded experimenters analyzed the tissue sections; their results were compared for consistency across users and averaged together for subsequent analysis.

Statistical Analysis

Data were analyzed using GraphPad Prism Software (Version 6.00 for Windows, GraphPad Software, La Jolla California USA, www.graphpad.com). All data sets were normally distributed. Student t-tests were used to compare HR vs. LR COX activity within each brain region (or subregion) of interest.

Results

We measured COX activity in the brains of seven-day-old HR/LR rat pups to assess possible metabolic differences that could correspond to HR/LR metabolic gene expression observed at this age (Table 1). Our analysis focused on three brain areas known to regulate emotional behavior: the amygdala, the hippocampus, and the prefrontal cortex. Figure 2A shows the standard curve generated by processing a dot blot with known COX standards. OD measurements for those standards created an exponential curve (R^2=0.97). Figure 2C and 2D show representative tissue sections processed for COX activity, highlighting the brain regions that were analyzed, including the prefrontal cortex (Figures 2D and 2G), the amygdala (Figures 2C and 2E), and sublayers of the hippocampus (pyramidal cell layer and inner molecular layer; Figures 2C and 2F, dashed and solid lines, respectively).

In the P7 amygdala, HRs displayed higher COX activity compared to LRs (p=0.0028, t=3.824, df=11; Figure 3A). In the P7 prefrontal cortex, HR and LR pups showed equivalent levels of COX activity (p=0.5714, t=0.5820, df=12; Figure 3B). As illustrated in Figure 2F, COX activity varied within sublayers of the hippocampus. We decided to focus our initial analysis on two sub-layers: the pyramidal cell layer and the molecular layer, where the hippocampal cells synapse. Figure 4 shows COX activity in the hippocampus of P7 HR/LR pups. We found that HRs showed increased COX activity in both the pyramidal cell layer (p=0.0219, t=2.602, df=13; Figure 4A) and molecular layer (p=0.0069, t=3.208, df=13; Figure 4B) compared to LRs. The other layers, apical and basal, show similar trends in COX activity (data not shown). In our analysis, we assessed COX activity separately in the cellular and molecular layers of CA1, CA2, and CA3 subregions. There were no subregion differences; therefore, the data were combined across CA1-3 regions for the presented bar graphs.

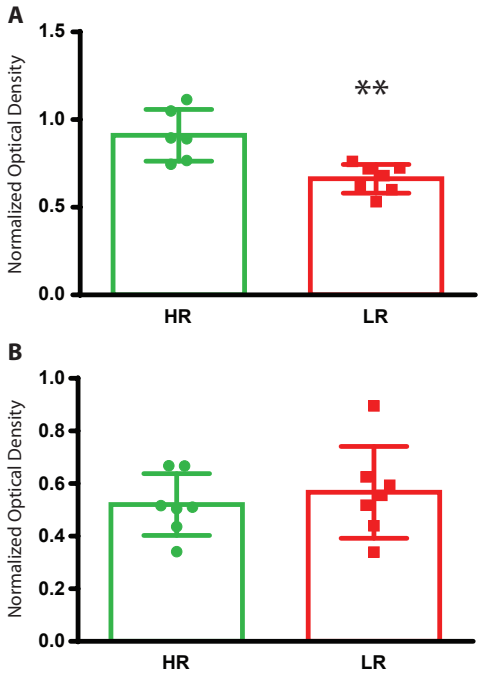

Figure 3. Normalized Optical Density of COX activity measured in specific brain regions: prefrontal cortex (PFC) and amygdala (AMY). (A) Top panel depicts average normalized optical density of COX activity in the amygdala of P7 HR versus LR rats. This symbol (**) indicates a p-value <0.01. (B) Bottom panel depicts normalized optical density of COX activity in prefrontal cortex of P7 HR vs. LR rats.

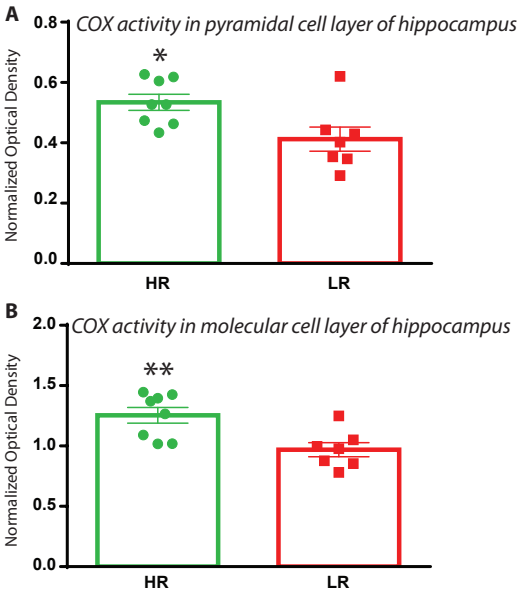

*Figure 4. Cytochrome c oxidase (COX) levels in hippocampus of seven day-old HR vs. LR rats. We evaluated COX activity within two sub-layers of the cornu ammonis (CA) region: the pyramidal cell layer and the innermost molecular layer, where the hippocampal neurons synapse. (A) At postnatal day seven (P7), HR pups showed higher COX activity in the cellular layer of CA compared to LR pups (p=0.0219). (B) HRs also exhibited greater COX activity in the molecular layer of CA compared to LRs (p=0.0069). ** indicates p-value <0.01; * indicates p-value <0.05.*

Discussion

Previous work in our laboratory revealed marked differences in the developing brains of HR/LR rats, including differences in hippocampal structure, gene expression, and cell proliferation,[3] as well as marked differences in gene expression in the amygdala during the first two postnatal weeks (McCoy, C.R., Clinton, S., et al., unpublished data). These differences in gene expression included several genes involved in metabolic activity (Table 1), leading us to hypothesize that HR/LR pups exhibit differences in metabolic activity within key limbic brain areas such as the amygdala and the hippocampus. The current study examined COX activity (an indicator of relative metabolic activity) in the P7 brain of HR and LR pups. We found significantly higher COX activity in the amygdala and hippocampus of HR pups compared to LR pups, with no significant differences in the prefrontal cortex.

Although there have been past studies of COX activity in brain tissue from rodent models of depression and anxiety, these studies mainly focused on adult subjects.[10-12] One such study examined levels of COX activity across brain regions of five distinct rodent models of depression, such as exposure to environmental adversity via chronic variable stress or chronic social defeat. By sampling several rodent depression models, the study aimed to identify brain areas that are universally implicated in stress response and vulnerability to depression-like behavior. Their results indicated that vulnerability to a depression-like phenotype is generally associated with higher COX activity levels in the brain, especially within the reticular thalamus, hippocampal CA3 region, granular and agranular retrosplenial cortices, and pontine nuclei. Vulnerability to depression-like behavior correlated with region-wide increases in COX activity in several brain regions, while exposure to stress tended to decrease oxidative metabolism relative to controls. One notable exception was in the median raphe, in which COX activity was increased in "depression-vulnerable" animals that were exposed to chronic stress. This study also examined connectivity patterns between brain areas, concluding that interregional correlations were more affected (either abolished or reversed) by chronic stress. Interestingly, this correlation was not found to persist for circuits involving the hippocampus.[10]

Brain and behavioral abnormalities related to a depression-like phenotype may be triggered by innate biological differences, environmental factors, or a combination of both. Since these earlier studies involved chronic stress exposure,[10] it is difficult to isolate which differences arise from inborn biological differences and which are a result of environmental stressors. A separate study aimed to address this concern by comparing baseline COX activity in the brains of one-day-old congenitally helpless vs. non-helpless rats.[8] The study examined COX activity within several brain regions and found decreased COX activity in approximately one-third of the regions examined in helpless compared with non-helpless newborn rats. The most striking observation was that brain regions that were most underactive at birth become the most hyperactive in adulthood in helpless vs. non-helpless animals. The authors hypothesized that this reversal may result from an abnormal flip of the hypothalamic-pituitary-adrenal axis (HPA) during development of the rodent depression model, a time point which has not yet been studied.[8] Our study aimed to map oxidative metabolism during development to identify this possible shift. While these previous studies can answer important questions about brain activity at birth or when adult behaviors are observed, we are interested in how these differences are formed during neurodevelopment. By tracking neuronal activity along emotionally relevant circuits during development, we can find when these connections are made and how the circuitry diverges through development. We began such lines of investigation here, but they must be more thoroughly studied and include more developmental time points if a better understanding is to be achieved.

Previous studies of COX activity in brain tissue have linked this metabolic process to synaptic transmission, with more recent studies delineating molecular mechanisms that regulate COX as well as genes essential for glutamatergic synaptic transmission.[7,13] Such studies revealed several transcription factors that mutually regulate all thirteen subunits of the COX enzymatic protein, as well as subunits of *N*-Methyl-D-aspartate (NMDA) and α-Amino-3-hydroxy-5-methyl-4-isoxazolepropionic acid (AMPA) glutamatergic receptors. Nuclear respiratory factors 1 and 2 (NRF-1 and NRF-2) as well as specificity protein 4 (Sp4) each bind to promoters of all COX subunit genes, multiple NMDA receptor subunit genes (*Grin1*, *Grin2a*, and *Grin2b*), and AMPA receptor subunit gene *Gria2*.[14-22] NMDA and AMPA receptors critically regulate synaptic plasticity, synaptogenesis, and formation of neuronal circuitry, processes that are essential for proper neural and ultimately behavioral development.[23-25] Given our observation of diminished COX activity in multiple brain regions of LR vs. HR P7 pups and considering the shared transcription factors (NRF-1, NRF-2, and Sp4) known to regulate both COX activity and glutamatergic synaptic activity, it is tempting to speculate that differences in glutamate neurotransmission may contribute to the divergent HR/LR behavioral phenotypes. Thus, it will be important for future studies to investigate the relative expression of glutamatergic genes *Grin1*, *Grin2a*, *Grin2b*, and *Gria2* in addition to assessing synaptic markers and perhaps electrophysiological properties within the developing HR/LR hippocampus and amygdala.

Future experiments will extend our current findings by evaluating COX activity in additional brain areas of the P7 HR/LR brain. For example, the amygdala is a heterogeneous region composed of multiple functionally-distinct nuclei. A more detailed analysis may reveal nucleus-specific COX changes in the P7 HR vs. LR amygdala. We will also extend our analyses to study HR/LR brains at other developmental

time points, including P14 and P21 and eventually adulthood, to determine whether our observed HR/LR differences (with HRs showing higher COX activity in multiple limbic brain regions relative to LRs) persist across development. Overall, this work aims to understand how distinct patterns of brain development may lead to disparate emotional behavioral phenotypes, and thus to help shed light on neurobiological processes that give rise to emotional disorders in humans.

References

1. Cloninger, C. R., Svrakic, D. M., & Przybeck, T. R. Can personality assessment predict future depression? A twelve-month follow-up of 631 subjects. *J Affect Disord*. 92, 35-44 (2006).

2. Stead, J. D., Clinton, S., Neal, C., et al. Selective breeding for divergence in novelty-seeking traits: Heritability and enrichment in spontaneous anxiety-related behaviors. *Behav Genet*. 36, 697-712 (2006).

3. Clinton, S. M., Stead, J. D., Miller, S., Watson, S. J., & Akil, H. Developmental underpinnings of differences in rodent novelty-seeking and emotional reactivity. *Eur J Neurosci*. 34, 994-1005 (2011).

4. Hirschfeld, R. M. History and evolution of the monoamine hypothesis of depression. *J Clin Psychiatry*. 61, 4-6 (2000).

5. Gardner, A. & Boles, R. G. Beyond the serotonin hypothesis: Mitochondria, inflammation and neurodegeneration in major depression and affective spectrum disorders. *Prog Neuropsychopharmacol Biol Psychiatry*. 35, 730-743 (2011).

6. Adzic, M., Lukic, I., Mitic, M., et al. Brain region- and sex-specific modulation of mitochondrial glucocorticoid receptor phosphorylation in fluoxetine treated stressed rats: effects on energy metabolism. *Psychoneuroendocrinology*. 38, 2914-2924 (2013).

7. Wong-Riley, M. T. Bigenomic regulation of cytochrome c oxidase in neurons and the tight coupling between neuronal activity and energy metabolism. *Adv Exp Med Biol*. 748, 283-304 (2012).

8. Shumake, J., Conejo-Jimenez. N., Gonzalez-Pardo, H., & Gonzalez-Lima, F. Brain differences in newborn rats predisposed to helpless and depressive behavior. *Brain Res*. 1030, 267-276 (2004).

9. Melendez-Ferro, M., Rice, M. W., Roberts, R. C., & Perez-Costas, E. An accurate method for the quantification of cytochrome C oxidase in tissue sections. *Journal of neuroscience methods*. 214, 156-162 (2013).

10. Harro, J., Kanarik, M., Kaart, T., et al. Revealing the cerebral regions and networks mediating vulnerability to depression: Oxidative metabolism mapping of rat brain. *Behav Brain Res*. 267, 83-94 (2014).

11. Harro, J., Kanarik, M., Matrov, D., & Panksepp, J. Mapping patterns of depression-related brain regions with cytochrome oxidase histochemistry: Relevance of animal affective systems to human disorders, with a focus on resilience to adverse events. *Neurosci Biobehav Rev*. 35, 1876-1889 (2011).

12. Sampedro-Piquero, P., Zancada-Menendez, C., Begega, A., Mendez, M., & Arias, J. L. Effects of forced exercise on spatial memory and cytochrome c oxidase activity in aged rats. *Brain research*. 1502, 20-29 (2013).

13. Wong-Riley, M. T. Cytochrome oxidase: An endogenous metabolic marker for neuronal activity. *Trends in neurosciences*. 12, 94-101 (1989).

14. Dhar, S. S., Ongwijitwat, S., & Wong-Riley, M. T. Nuclear respiratory factor 1 regulates all ten nuclear-encoded subunits of cytochrome c oxidase in neurons. *J Biol Chem*. 283, 3120-3129 (2008).

15. Dhar, S. S., Liang, H. L., & Wong-Riley, M. T. Nuclear respiratory factor 1 co-regulates AMPA glutamate receptor subunit 2 and cytochrome c oxidase: Tight coupling of glutamatergic transmission and energy metabolism in neurons. *J Neurochem*. 108, 1595-1606 (2009).

16. Dhar, S. S. & Wong-Riley, M. T. T. Coupling of energy metabolism and synaptic transmission at the transcriptional level: Role of nuclear respiratory factor 1 in regulating both cytochrome c oxidase and NMDA glutamate receptor subunit genes. *Journal of Neuroscience*. 29, 483-492 (2009).

17. Johar, K., Priya, A., Dhar, S., Liu, Q., & Wong-Riley, M. T. Neuron-specific specificity protein 4 bigenomically regulates the transcription of all mitochondria- and nucleus-encoded cytochrome c oxidase subunit genes in neurons. *J Neurochem*. 127, 496-508 (2013).

18. Priya, A., Johar, K., & Wong-Riley, M. T. Specificity protein 4 functionally regulates the transcription of NMDA receptor subunits GluN1, GluN2A, and GluN2B. *Biochimica et biophysica acta*. 1833, 2745-2756 (2013).

19. Priya, A., Johar, K., Nair, B., & Wong-Riley, M. T. Nuclear respiratory factor 2 regulates the transcription of AMPA receptor subunit GluA2 (Gria2). *Biochimica et biophysica acta*. 1843, 3018-3028 (2014).

20. Priya, A., Johar, K., Nair, B., & Wong-Riley, M. T. T. Specificity protein 4 (Sp4) regulates the transcription of AMPA receptor subunit GluA2 (Gria2). *Biochimica et Biophysica Acta - Molecular Cell Research*. 1843, 1196-1206 (2014).

21. Priya, A., Johar, K., & Wong-Riley, M. T. Nuclear respiratory factor 2 regulates the expression of the same NMDA receptor subunit genes as NRF-1: Both factors act by a concurrent and parallel mechanism to couple energy metabolism and synaptic transmission. *Biochim Biophys Acta*. 1833, 48-58 (2013).

22. Ongwijitwat, S. & Wong-Riley, M. T. Is nuclear respiratory factor 2 a master transcriptional coordinator for all ten nuclear-encoded cytochrome c oxidase subunits in neurons? *Gene*. 360, 65-77 (2005).

23. Loftis, J. M. & Janowsky, A. The N-methyl-D-aspartate receptor subunit NR2B: Localization, functional properties, regulation, and clinical implications. *Pharmacology & therapeutics*. 97, 55-85 (2003).

24. Tanaka, H., Grooms, S. Y., Bennett, M. V., & Zukin, R. S. The AMPAR subunit GluR2: Still front and center-stage. *Brain research*. 886, 190-207 (2000).

25. Palmer, C. L., Cotton, L., & Henley, J. M. The molecular pharmacology and cell biology of alpha-amino-3-hydroxy-5-methyl-4-isoxazolepropionic acid receptors. *Pharmacological reviews*. 57, 253-277 (2005).

The Use of Metabolomic Profiling to Diagnose Obesity in Mice

Jessica Maya[1] and J. Daniel Sharer[2]

[1]Department of Biology, University of Alabama at Birmingham, Birmingham, AL, USA
[2]Department of Human Genetics, Emory University School of Medicine, Atlanta, GA, USA

Abstract
The purpose of this experiment was to create personalized metabolomic profiles for types of obesity based on organic acid levels. Three groups of mutant mice (*ob/ob*, *Mc3r* knockout, and *Mc4r* knockout) and a control group known as studs were used to create the profiles. Multiple urine samples were collected and compared between the groups. Initial preparations were made for the testing of organic acids, which were the metabolites used for the profiles, and the samples were processed through a gas chromatograph-mass spectrometer. The resulting levels of 33 organic acids, including two internal standards and control levels, were analyzed. The data were interpreted and the concentrations of acids were graphed. Potentially, after finding the averages of each group, the profiles could be used to correctly diagnose other mice with matching metabolomic profiles depicting a type of obesity. This would represent a less intrusive and more personal type of medical tool that could be used in everyday diagnosis of metabolic diseases.

Keywords: Stud, *ob/ob*, *Mc3r*, *Mc4r*, gas chromatography, mass spectrometry

Introduction
More than 60 % of adults in the United States are classified as overweight or obese. While the most common cause of obesity is a dietary surfeit of calories, there are some types of obesity that are a result of treatable pathologies.[2] Because of this fact, accurate and discerning diagnostics are very important when trying to treat a patient's obesity successfully. This study focuses on the use of metabolomic profiling to diagnose types of obesity in a set of mice. In this method, a blood or urine sample is taken from a patient and tests are performed in order to determine characteristics of the individual's metabolism and thereby to inform a diagnosis.[1] Because it is noninvasive, focused on changes in systems that are affected by many different disease pathways, and quantitative, this method of profiling could become a useful type of diagnostic test for a number of different diseases.

This study's focus was the metabolomic profiling of different groups of obese mice according to their levels of organic acids. The groups representative of obesity were *ob/ob* mice, melanocortin 3 receptor (*Mc3r*) gene knockout mice, and melanocortin 4 receptor (*Mc4r*) gene knockout mice. As a preliminary step, however, summary investigations were made of the current use of metabolomic profiling in medicine and the current state of knowledge regarding the human analogues of the three mouse obesity groups.

Metabolomic Profiles Used in Modern-day Medicine
The uses of metabolomic profiling have been demonstrated in many recent studies. Metabolomics is basically an "approach that attempts to profile all the metabolites in a biological matrix." [2] It is analytical in nature and has been applied mostly to animal studies thus far, with only a few human studies to date. Mass spectrometry is the most widely used tool for this type of analysis, though gas and liquid chromatography are also common. Medical disorders for which profiling is thought to have particular promise include diabetes, obesity, and other associated disorders. In one study, the profiles of leptin-deficient mutant mice were recorded and analyzed.[3] The study was able to relate increased levels of leptin to energy homeostasis, glucose homeostasis, and overall obesity. It concluded that leptin was able to be analyzed using this method and that obesity was associated with its deficiency.

The Role of ob/ob
Leptin is a hormone that is secreted by adipose tissue to signal the neuroendocrine system that body energy stores are low. It is released in proportion to fat mass and regulates appetite as well as the activity of the thyroid, adrenal, pituitary, and other related glands. As a result, leptin deficiency causes over-eating and sluggish physical activity.[4] The discovery of this hormone in the 1990s gave hope to the medical community that a portion of people with obesity could be helped with the manipulation of this hormone. Individuals with an *ob/ob* genotype are homozygous in a certain allele that causes non-functionality of leptin receptors. It is a gene mutation known as the "obesity gene" that is "responsible for a severe syndrome of obesity with insulin resistance."[5] The gene encodes a fat-specified mRNA and a protein, which is regulated in adipose tissue. Thus, leptin can be present in the *ob/ob* individual, but the receptor/binding sites do not work such that leptin signaling is affected. Early diagnosis of a leptin deficiency is important, as this type of condition is treatable in a different way than primary obesity. A supplement of leptin along with controlled diet and exercise can lead to a quicker and more successful treatment of the patient's condition.[14]

The Role of Mc3r

The melanocortin 3 receptor gene has been found to impact the regulation of weight gain and can be a predisposing factor to obesity if mutated. The pathway of melanocortin regulates energy by stopping over-eating, increasing energy expenditure, and reducing the storage of energy.[6] It was found that mice deficient in the *Mc3r* gene had increased body fat and decreased lean mass, which was "not caused by increased food intake but arose from increased feed efficiency."[7] Metabolic rates in these mice were found to be the same as normal rates; hormones released from the thyroid were undisturbed, and the respiratory exchange rate was unchanged as well. The causes of their obesity were therefore their susceptibility to high fat diet-induced obesity and their inactivity. Another study also confirmed the *Mc3r* knockout mutation as an associative gene to obesity. Research also shows that *Mc3r* can be a predisposing gene that contributes to an increased adiposity, or fat cell accumulation, which could indicate pre-obesity in a subject.

The Role of Mc4r

Mutations in the melanocortin 4 receptor gene are the most frequent monogenic causes of severe early onset obesity. In humans the *Mc4r* mutation results in a syndrome of hyperphagic obesity that can be present with either dominant or recessive inheritance patterns. There is also a marked increase in bone mineral density, which affected all subjects in one study.[8] Although research is still being done on the prominence of the mutation of the *Mc4r* gene in severe obesity cases, there are studies that suggest that this gene is more significant than previously thought since it can be influential in both a dominant and recessive state. As of now, genetic testing is the only method for definitive diagnosis of *Mc4r*-linked obesity. It is important to diagnose this type of obesity early because, without aggressive treatment, it is very unlikely to be resolved. The knowledge of this condition allows patients to fully realize the importance of their everyday eating behavior.

This Study's Hypothesis

The working hypothesis of this study is that the type of obesity in a random sample can be correctly diagnosed solely by metabolomic profiling of organic acids.

Materials and Methods

Materials

A high performance liquid chromatograph (HPLC) with a tandem mass spectrometer (Micromass Quattro micro API Technologies) was used to test creatinine levels, along with proprietary software (Masslynx). Quality control samples (high and low) were also provided by the UAB Genetics Lab to make sure the instrument was in working condition and was reading the levels correctly for both the high and low ranges of levels. The animals used were C57BL/6 mice as the stud group of mice, *ob/ob* mice, *Mc3r* knockout mice, and *Mc4r* knockout mice. In order to read the organic acid levels, an organic acid extraction kit was used along with the BGL Library for organic acid level readings and the software linked to the chromatograph.

Animals

The size of each group of mice varied from 3 to 6 useable profiles: 6 studs, 4 *ob/ob*, 5 *Mc3r* knockout, and 3 *Mc4r* knockout.

Creatinine Determination

Urine samples were gathered from the obese mouse lab. These included urine samples from stud mice, *ob/ob* mice, *Mc3r* knockout mice, and *Mc4r* knockout mice. All were placed on ice to be tested in the genetic metabolomics lab. The creatinine levels, measured in micromoles, were determined by gathering 2 µL to 5 µL of the urine sample and running it through an HPLC. The observed levels were used to determine the volume of urine to use in the actual testing of organic acids, i.e., the volume containing 1 µmol of creatinine.

Extraction

These amounts were aliquoted into extraction tubes, and quality controls were added that acted to keep the organic acid levels in a testable range. 0.4 mL of 5 M NaOH and 0.8 mL of hydroxylamine were added. The volume of each sample was raised to 1.5 mL by adding deionized water, and each extraction tube was vortexed. The tubes were capped and heated in a water bath at 70 °C for 30 min. The tubes were then cooled for 10 min at room temperature. Then, 0.8 mL of 5 M HCl was added, and 0.2 mL of 2.5 mM α-ketocaproic acid and 0.2 mL of 1 mM tetracosane were added to each tube as internal standards. The samples were extracted with 6 mL of ethylacetate:ether. The tubes were then placed into the Vortex mixer for 10 min. The extraction tubes were centrifuged for 1 min. The lower aqueous layer of the samples was then removed and discarded. Two mg of sodium sulfate was added to the extract. The tubes were mixed thoroughly and centrifuged for 3 min. The anhydrous extracts were transferred into derivatization tubes and placed on a heating block at 50 °C to 55 °C. Each tube was dried under a stream of nitrogen for 25 min.

Derivatization

Approximately 0.2 mL of the derivatization mixture was added to the dry extract in order to enable chromatographic separation. The tubes were capped tightly, vortexed, and heated in a heating block at 80 °C to 85 °C for 30 min. The tubes were cooled to room temperature and transferred to individually labeled autosampler vials. The vials were taken to the gas chromatographer for testing.

Analyzing the Data

Once the quality controls were checked, the sample data files analyzed using the software packaged with the

chromatograph. The spectrum for the integrated peaks was analyzed. The integration for each individual peak, signifying a level of a particular organic acid in moles, was checked and corrected manually if necessary. The resulting levels of each organic acid present were transferred into graphical analysis software to be better investigated and compared. The 33 organic acids analyzed were as followed: Lactate, glycolic acid, glyoxylic acid, oxalic acid, pyruvic acid, 3-hydroxybutyric acid, 2-hydroxy isovaleric acid, ketoisovaleric acid, acetoacetic acid-diTMS (peak 1), acetoacetic acid (peak 2), acetoacetic acid-diTMS (peak 3) 2-keto-3-methylvaleric acid, ethylmalonic acid, ketoisocaproic acid, succinic acid, 2-ketocaproic acid diTMS, glyceric acid, fumeric acid, glutamic acid, 3-methylglutamic acid, adipic acid, hydroxyproline, 2-hydroxyglutarate, 3-hydroxy-3-Methylglutaryl-CoA, 2-ketoglutaric acid, hydroxyPAC, SUB, aconitic acid, citric acid, sebacic, phydroxylactic acid, phydroxypyruvic acid, and the control compound tetracosane (c-24; internal standard).

Data Collection and Analysis

Once all data were acquired for each type of obese mouse as well as the stud mice, the levels for each acid were averaged within the groups. Metabolomic profiles were made with these means. Standard deviations for the levels of each acid were also computed to facilitate comparison among individuals. These profiles were then used to generate conclusions regarding the type of obesity represented in previously gathered samples of urine. Thus, it was possible to test the reliability and specificity of metabolomic profiling as a diagnostic method.

Results

Organic acid metabolomic profiles were generated to show the normal (95 % population-inclusive) range of the levels of each organic acid for each mouse type. The averages and standard deviations of each organic acid were found. Then, a range was calculated by adding and subtracting two standard deviations from the mean.

Figures 1-4 display the graphs of the ranges of normal organic acid levels in each type of mouse. These are the working profiles for the mice. The lighter bars indicate the upper bound, and the darker bars indicate the lower bound.

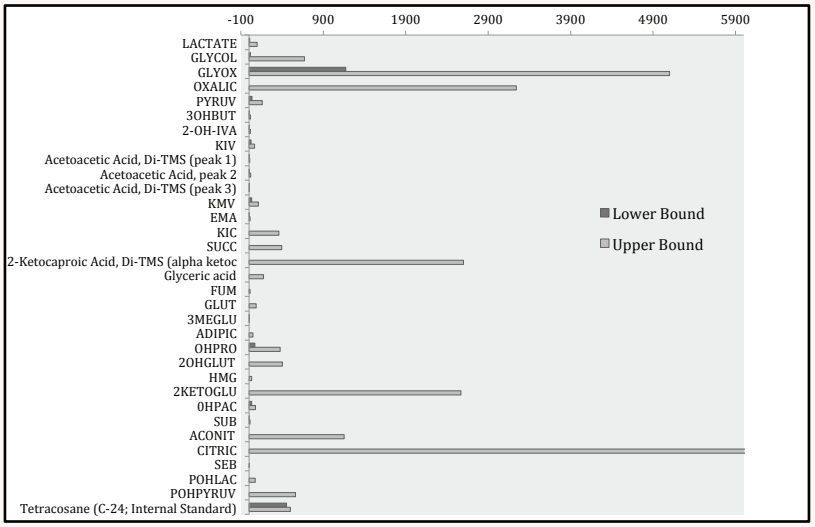

Figure 1. Stud Profile. These are the 33 organic acid levels that make up the profile of the stud group of mice at a 95 % accuracy range.

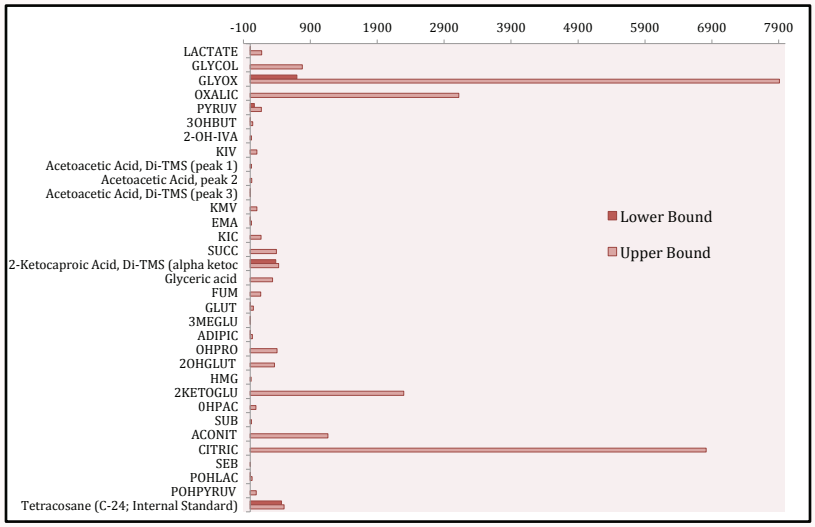

Figure 2. ob/ob Profile. These are the 33 organic acid levels that make up the profile of the ob/ob group, or leptin deficient group, of mice at a 95 % accuracy range.

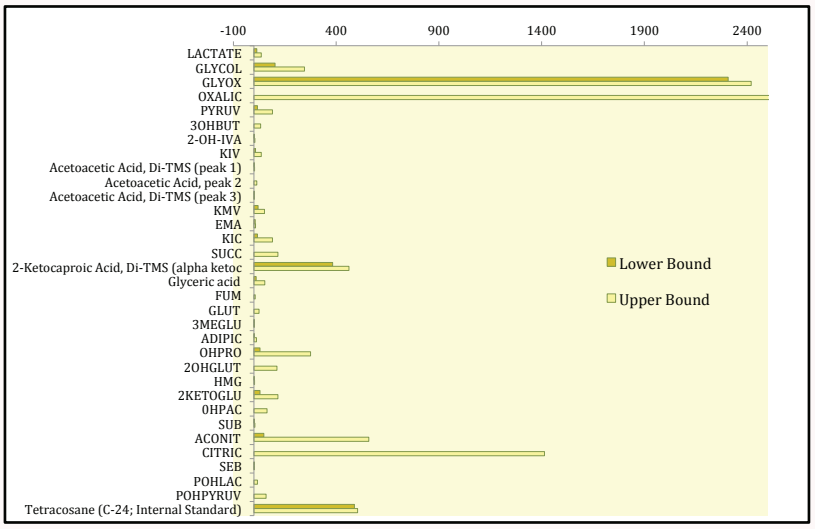

Figure 3. Mc3r *Profile. These are the 33 organic acid levels that make up the profile of the* Mc3r *group of mice at a 95 % accuracy range.*

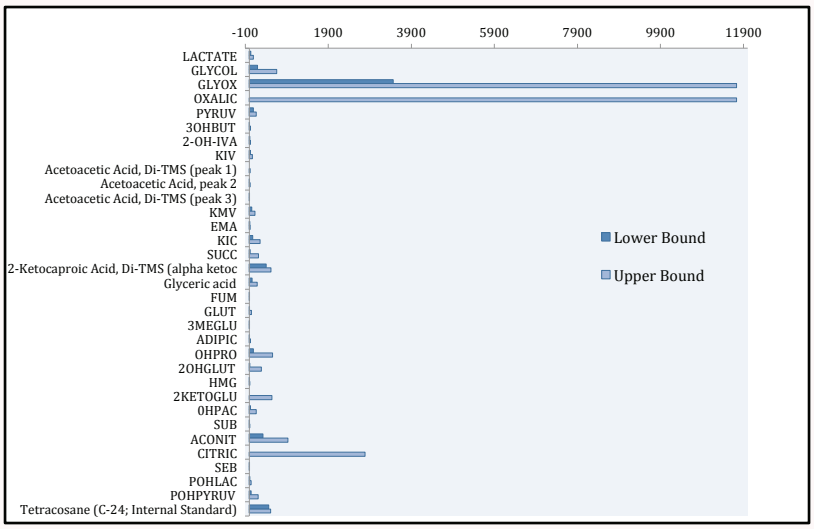

Figure 4. Mc4r *Profile. These are the 33 organic acid levels that make up the profile of the* Mc4r *group of mice at a 95 % accuracy range.*

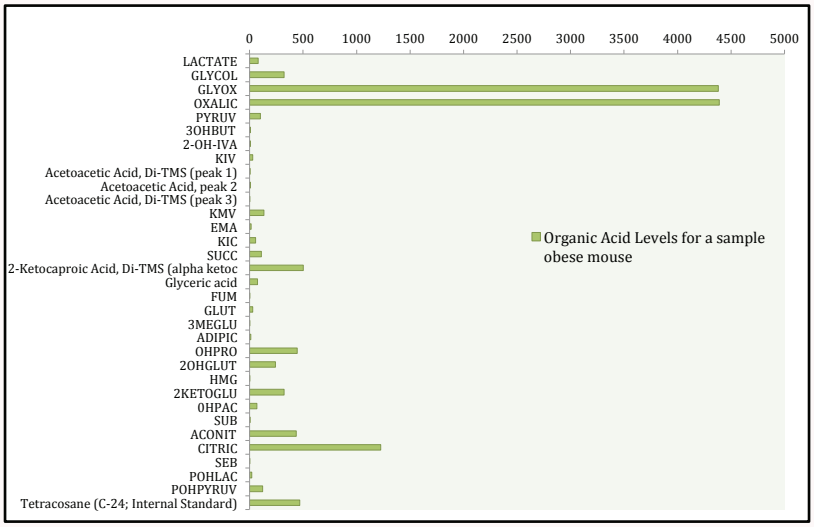

Figure 5. Organic Acid Levels of Unknown Obese Mouse Sample. This figure shows the 33 organic acid levels of an unknown sample of an obese mouse that will be compared to the three profiles created in this project.

Next, a metabolomic profile was generated from a randomly-selected urine sample from one of the three mutant mouse types.

The random sample profile was compared to the three population standard profiles to allow its identification with (i.e., a diagnosis of) one of the three types of obesity under study.

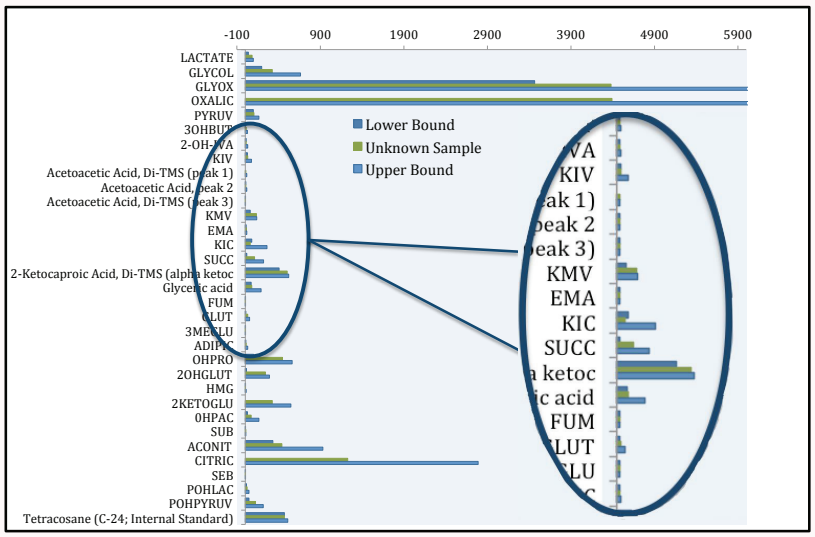

Figure 6. Mc4r *Profile Compared to Unknown Sample. When compared to the unknown sample,* Mc4r *fit the sample nearly perfectly, having only one or two discrepancies that went above or below the 95 % boundaries.*

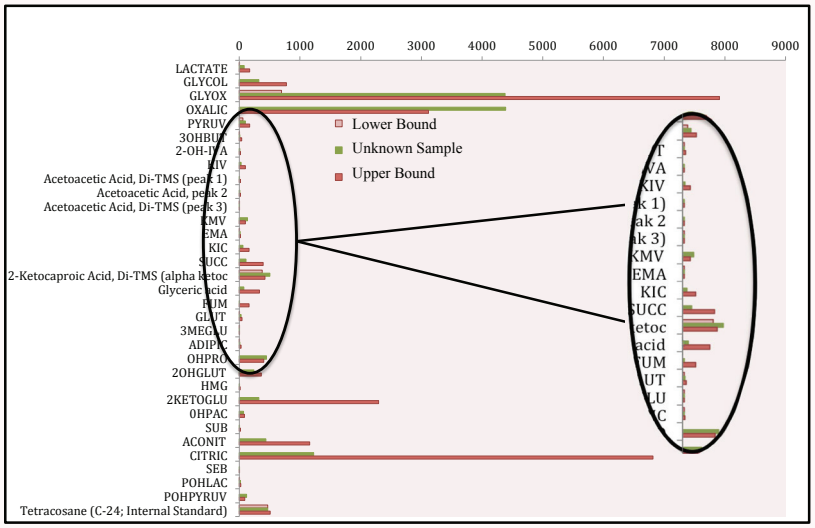

Figure 7. ob/ob *Profile Compared to Unknown Sample. When compared to the* ob/ob *profile, it can be seen that in more than 5 organic acid levels were higher than what the upper bound dictates. These include oxalic, kmv, OHPro, hmg, and POH Pyruvic acid.*

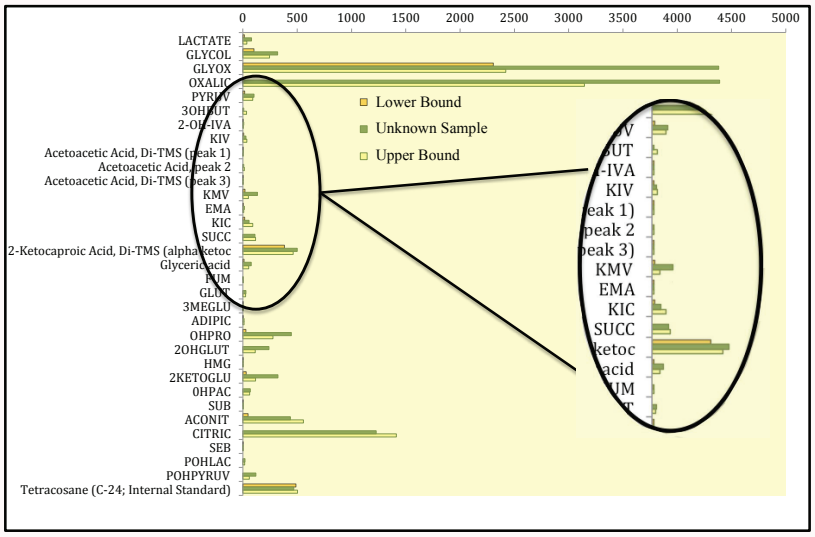

Figure 8. Mc3r *Profile Compared to Unknown Sample. In the* Mc3r *profile, multiple levels were much higher than the profile illustrates, and so this type of obesity can automatically be removed as a possible diagnosis of this sample.*

Comparison of the random sample profile revealed a highly specific and strong pattern of similarity with the standard *Mc4r* profile (Figure 4), which is seen particularly easily, for example, by examining the levels of glyoxylate acid and oxalic acid.

Discussion

Because a strong and specific pattern of similarity was observed between the random sample profile and the standard *Mc4r* profile (i.e., the levels of organic acids in Figure 5 could only fit the profile of the *Mc4r* mouse in Figure 4, and not that of any other mouse type), the hypothesis was

confirmed and reliable, selective diagnosis was possible. Thus, diagnostically useful metabolomic profiles can be created for genetic variants of obesity using organic acids as the only metabolites profiled, such that the type of obesity in a random sample can be correctly diagnosed solely by the profiles produced. The results of this project suggest that metabolomic profiling is a possibility for clinically useful obesity diagnoses given multiple samples and adequate control of potential confounding variables.

One variable other than the obesity gene that could affect the profiles is the time of day at which each urine sample was collected: the mouse variants may have different eating habits, and the levels of certain organic acids could fluctuate as a function of the time elapsed since a meal. The age of the mice is another variable, but since most of these mice samples were collected at a young age before the onset of obesity, this is not a particular problem for this study.

Further study in this area is needed to understand the effects of the diets, collection times, and habitat conditions of the mice. Increasing the sample sizes for each mouse population would give the data more precision. Other diseases could also be studied to see if the same diagnostic method used here could also be used to diagnose other illnesses. Finally, other metabolites such as amino acids could be tested as metabolomic profile analytes to determine whether they allow for more accurate diagnosis.

References

1. Bogdanov, M., Matson, W.R., Wang, L., Matson, T., Saunders-Pullman, R., Bressman, S.S., & Flint Beal, M. Metabolomic profiling to develop blood biomarkers for Parkinson's disease. *Brain: A Journal of Neurology*. 131, 389-396 (2008).

2. Griffin, J.L., & Nicholls, A.W. Metabolomics as a functional genomic tool for understanding lipid dysfunction in diabetes, obesity and related disorders. *Pharmacogenomics*. 7, 1095–1107 (2006).

3. Saadat, N., IglayReger, H.B., Myers, M.G. Jr., Bodary, P., & Gupta, S.V. Differences in metabolomic profiles of db/db and s/s leptin receptor mutant mice. *Physiological Genomics*. 44, 374-381 (2012).

4. Bates S.H., & Myers, M.G. The role of leptin–STAT3 signaling in neuroendocrine function: An integrative perspective. *J Mol Med*. 82 12-20 (2004).

5. Frederich, R.C., Löllmann, B., Hamann, A., Napolitano-Rosen, A., Kahn, B.B., Lowell, B.B., & Flier, J.S. Expression of ob mRNA and its encoded protein in rodents: Impact of nutrition and obesity. *J Clin Invest*. 96, 1658-1663 (1995).=

6. Lee, Y.S., Poh, L.K., Kek, B.L., & Loke, K.Y. The role of Melanocortin 3 receptor gene in childhood obesity. *Diabetes*. 56, 2622-2630 (2007).

7. Lee, Y.S., Poh, L.K., & Loke, K.Y. A novel Melanocortin 3 receptor gene (Mc3r) mutation associated with severe obesity. *The Journal of Clinical Endocrinology & Metabolism*. 87, 1423–1426 (2002).

8. Farooqi, I.S., Yeo, G.S., Keogh, J.M., Aminian, S., Jebb, S.A., Butler, G., Cheetham, T., & O'Rahilly, S. Dominant and recessive inheritance of morbid obesity associated with Melanocortin 4 receptor deficiency. *J Clin Invest*. 106, 271-279 (2000).

9. Calton, M.A., Ersoy, B.A., Zhang, S., Kane, J.P., Malloy, M.J., Pullinger, C.R., Bromberg, Y., Pennacchio, L.A., Dent, R., McPherson, R., Ahituv, N., Vaisse, C. Association of functionally significant Melanocortin-4 but not Melanocortin-3 receptor mutations with severe adult obesity in a large North American case–control study. *Human Molecular Genetics*. 18, 1140-1147 (2009).

10. Vaisse, C., Clement, K., Durand, E., Hercberg, S., Guy-Grand, B., & Froguel, P. Melanocortin-4 receptor mutations are a frequent and heterogeneous cause of morbid obesity. *J Clin Invest*. 106, 253-262 (2000).

11. Margetic, S., Gazzola, C., Pegg, G.G., & Hill, R.A. Leptin: A review of its peripheral actions and interactions. *Int J Obes Relat Metab Disord*. 26, 1407-1433 (2002).

12. Makowski, L., Noland, R.C., Koves, T.R., Xing, W., Illkayeva, O.R., Muehlbauer, M.J., Stevens, R.D., Muoio, D.M. Metabolic profiling of PPARα−/− mice reveals defects in carnitine and amino acid homeostasis that are partially reversed by oral carnitine supplementation. *FASEB J*. 23, 586-604 (2009).

13. Graham, K.S., & Leibel R.L. Yellow mice, red hair, and childhood obesity: the melanocortinergic pathway in energy homeostasis. *J Pediatr*. 139, 177-181 (2001).

14. Farooqi, I.S., Jebb, S.A., Langmack, G., Lawrence, E., Cheetham, C.H., Prentice, A.M., Hughes, I.A., McCamish, M.A., & O'Rahilly, S. Effects of recombinant Leptin therapy in a child with congenital Leptin deficiency. *The New England Journal of Medicine*. 341, 879-883 (1999).

Addendum: Definitions of Terms and Abbreviations

Studs: Term used in the lab for the control mice. These are C57 black 6 mice to be compared to the mutant mice.

Leptin: A protein hormone that regulates energy intake and expenditure.

ob/ob: These mice are leptin deficient, causing their appetites to increase and their metabolisms to decrease. This leads to obesity.

Mc3r (Oregon homozygous): This mouse type has a knockout of the melanocortin 3 receptor (*Mc3r*) gene in the brain. When this gene is inactivated, it causes increased fat mass and reduced lean mass, so the mice are longer but not as seemingly fat as *ob/ob* mice. They are still considered obese.

Mc4r (Southbeach mutation): The mutation of the melanocortin 4 receptor (*Mc4r*) seen in these mice causes a change in the control of appetite and general eating behavior. It causes over-eating and is the common case of human obesity. It is also inheritable obesity.

Gas Chromatography Mass Spectrometer: A machine used to separate and identify different components of a sample, in this case, organic acids. The chromatograph separates the different components of the sample, then the spectrometer ionizes the components in a sample by a direct bombardment of electrons, and software is used to detect and quantify levels of each organic acid in the sample.

Structural Genomics and Its Importance for Gene Function

Michael Falahat and Denise Monti

Department of Biology, University of Alabama at Birmingham, Birmingham, AL, USA

Abstract

This study sought to test whether current bioinformatics programs are sufficient to extract valuable data regarding a gene found in the mycobacteriophage *Holli*. Specifically, we examined whether current bioinformatics tools could be used to predict putative gene functions for unknown genes, in this case *Holli* gp 54 (gene product 54), located on the right arm of the genome map. We used protein prediction websites such as I-TASSER to aid in gene function prediction. We found that gene function could not be predicted based on results collected from current bioinformatics tools. We concluded that current bioinformatics tools do not provide concrete gene function predictions, though they do help us in selecting noteworthy genes that can be studied through wet lab experiments for more accurate data.

Introduction

Bacteriophages are viruses that infect bacteria. Phages are found everywhere and are much smaller than their hosts. The basic structure of a phage consists of a capsid, where its DNA or RNA genome is stored, and a tail.[1] A specific type of bacteriophage, called a mycobacteriophage, is a bacteriophage that targets bacteria in the genus *Mycobacterium*. The mycobacteriophage settles onto the surface of the mycobacterium host and then injects its genomic DNA into the host cell. Next, phages reproduce inside the microbe to multiply and eventually explode out of (i.e., "lyse") the host.[2]

Identifying functions for phage genes can be very useful for phage therapy, in which bacteriophages are used to treat infections caused by pathogenic bacteria, by facilitating more targeted and controlled therapy.[3] Many protein-coding genes found in a mycobacteriophage are unique for that phage. The function of gene 54 in the mycobacteriophage *Holli* is unknown and is currently being studied. Gene 54 is located on the right arm of the genome map and consists of 91 base pairs. In recent years, there has been an exponential increase in the number of genomes sequenced in full, but the sequences of genes and their corresponding protein products alone do not provide insight into gene functions in the cell.[4] Rather, examination of the structures of unknown proteins may help us to predict the specific function of the gene product. To understand the function of proteins, wet lab experiments such as recrystallization of the protein can be performed. However, this method is costly and time consuming.

In this study, we used current bioinformatic tools to identify possible structures for putative gene products of gene 54. A program called "Phamerator" helped us to identify the phams, or related sequences, and the clusters to which the gene belongs. [5] In this program, getting the sequence for the same gene from different phages was possible. Programs like Clustal Omega and T-COFFEE were used to compare the sequences of genes from different phages and gave us valuable information that was used to help predict the function of the gene.

Understanding protein functions can help with understanding cell function. When human cells do not work properly, understanding altered protein functions can help with the development of appropriate strategies to treat various diseases. Phage therapy, in which bacteriophages are used to treat bacterial infections, is an active field of research. Understanding the function of proteins within mycobacteriophages can potentially help with the treatment of human diseases.

Materials and Methods

Genes were termed using DNAMaster, a genome annotation and exploration tool. A gene of interest was selected for function prediction. Phamerator was used to identify the gene's pham and clusters represented in the pham. Clustal Omega (Figure 2) was used to assess the conservation of amino acids amongst genes in the same pham. I-TASSER was used to model possible structures for the gene being studied, and C-scores for these structures were determined. The C-score represents the confidence score for estimating the quality of predicted models. It is calculated based on the significance of threading template alignments and the convergence parameters of the structure assembly simulations.[7] Higher C-scores represent more reliable structures. Z-scores were also determined. A Z-score greater than 1 represented a good alignment, and in general the Z-score represents the difference between the raw and average scores in units of the standard deviation. Proteins with high structural similarities in PDB (Protein Data Bank) were analyzed for a possible protein function based on structural similarities and protein structures stored in PDB. TM-scores, which compares the query protein structure and the structure in PDB based on their given and known residue equivalency, were taken into consideration as well. TM-score is the scale for measuring the structural similarity between two structures. Higher TM-scores represent better structural alignment, a TM-score

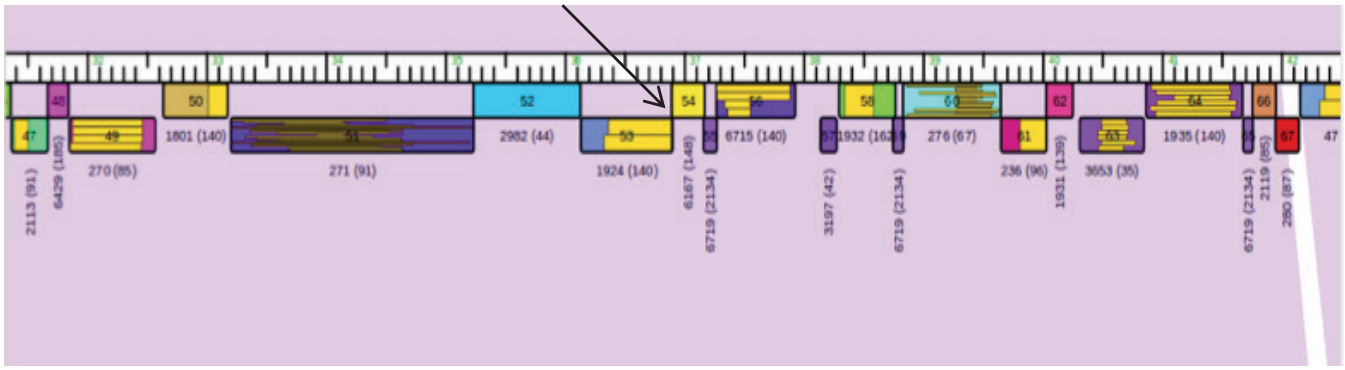

Figure 1. Section of a genome map of mycobacteriophage Holli *showing the gene studied (gene 54) in the right arm of the genome. The number 6167 under gene 54 indicates the pham number, and the number in parentheses indicates the clusters (A4) contained in that pham.*[8]

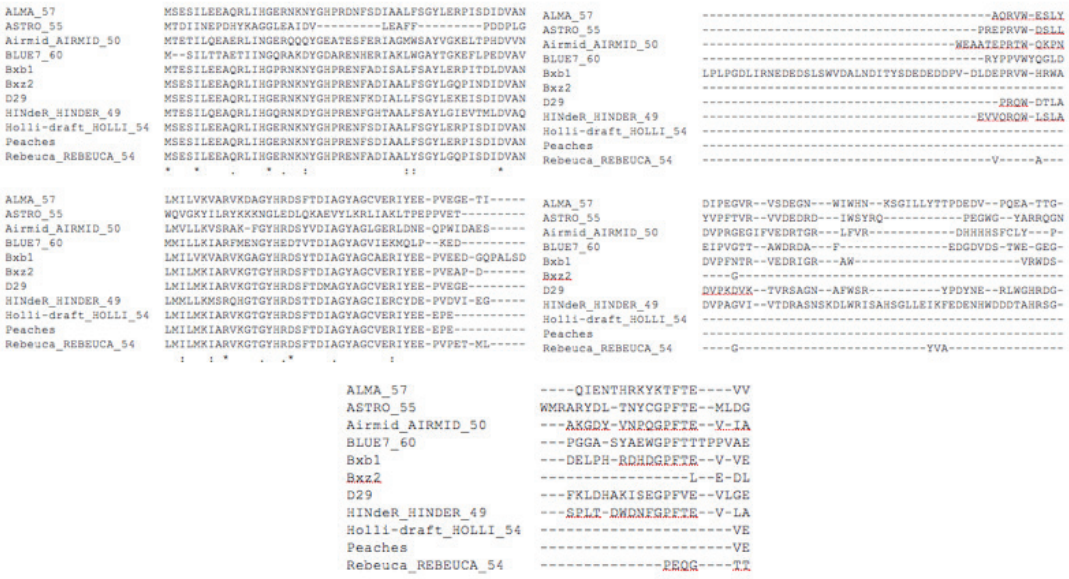

Figure 2. Protein sequence alignment for A1-A10 gene using Clustal Omega

This shows an alignment for gene A1-A10. The star under some of the columns indicate that the nucleotide was a one-to-one match for all the different phages; however, this is a poor alignment since it did not contain many stars. These data were studied and based on this alignment no observation was seen.

greater than 0.5 indicates a model of correct topology, and a TM-score less than 0.17 indicates a random similarity.[7]

Results

Gene 54 is a gene found in mycobacteriophage *Holli*. Part of the genome map for *Holli* is shown in Figure 1. A genome map consists of a left arm and a right arm. This section of the genome map shows the genes that are contained in this section of the right arm of the phage *Holli*. Each box represents a gene, and the width of the box indicates the length of the gene in base pairs. *Holli* gp 54, or gene product 54, is located in the right arm of the genome map. This gene is 91 base pairs long and has 1:1 match with gp 53 of the mycobacteriophage Peaches.[6] *Holli* gp 54 has a pham number of 6167. This pham contains 54 clusters, including A1 through A2, J, and K4.

Based on the data collected from the bioinformatics programs used, gene function could not be assigned to the gene found in *Holli*. The same gene found in clusters A1 through A2 was submitted to Clustal Omega for alignment (Figure 2). The protein sequence for the gene found in *Holli* was submitted to I-TASSER, an online platform for protein structure and function predictions. I-TASSER calculated a C-score representing a confidence score for estimating the quality of predicted models based on the significance

of threading template alignments and the convergence parameters of the structure assembly simulations. The four models with the highest C-scores predicted by I-TASSER are presented in Figure 3. The C-scores, ranging between −5 and −2, were poor. The best C-score was −2.29 (Figure 3).

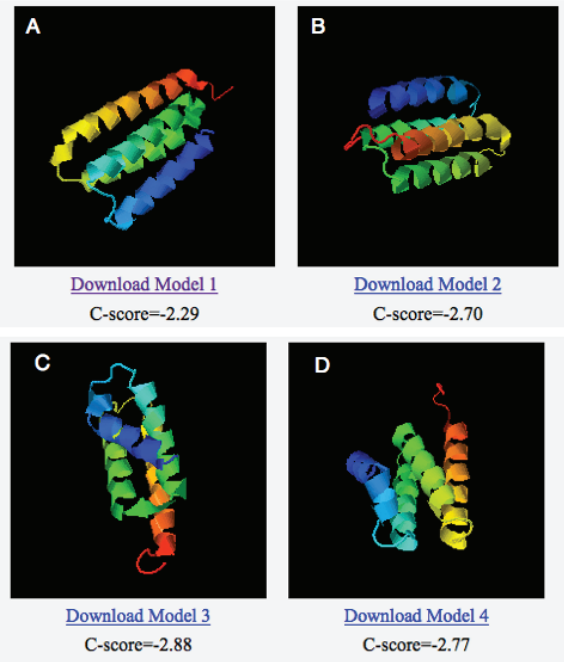

Figure 3. Top four protein models predicted by I-TASSER for gene in phage Holli

I-TASSER generates tens of thousands of conformations, called decoys. Based on the pair-wise structure similarity, I-TASSER reports up to five models that correspond to the five largest structure clusters. The C-score (confidence score) indicates the structures with the largest partition function (or lowest free energy).[4]

I-TASSER also generates many templates; however, I-TASSER uses templates with the highest significance in the threading alignments. This significance is measured by the Z-score, which is the difference between the raw and average scores in units of standard deviation.[7] Each threading template used by I-TASSER contains a normalized Z-score of the threading alignment. In Table 1, the top three threading templates showed poor Z-scores of 0.82, 0.60, and 0.75. These results represent poor normalized Z-scores because they are less than 1. The top threading template, a virulence factor from *Campylobacter jejuni* (1vqrA), has an unknown function; an anthranilate phosphoribosyl-transferase (1o17A) codes for a transferase; and a core-binding domain of bacteriophage lambda integrase (2oxoA) codes for a DNA-binding protein.

Proteins with highly similar structure, as indicated by I-TASSER, were also studied (Table 2). The top three proteins had TM-scores of 0.812, 0.737, and 0.727; however, percentage identities were extremely poor. Percentage identities for the top three proteins were 0.043, 0.043, and 0.00. Prediction could not be made according to this data. Model structures of proteins whose structure is similar to the predicted structure of the gene product of *Holli* gene 54 are shown in Figure 4. Two structures were missing a large portion of the predicted structure of this gene product (Figure 4A and 4B). A third structure (Figure 4C) had no missing portions, but its identity was 0.

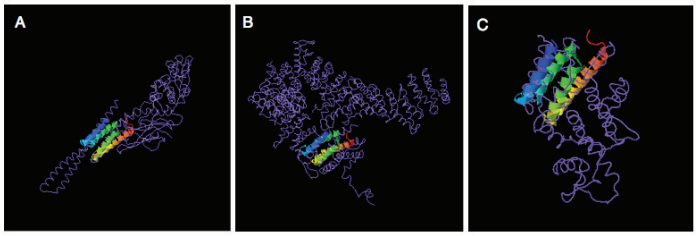

Figure 4. Structures with highly similar structure in PDB to Holli *gene 54*

Structures A, B, and C show the structures for proteins with structures highly similar to that of Holli gene 54 in PDB from Table 2. Structures A and B are missing a large portion of the protein it has been compared to. While structure C contains most of the structure it has been compared to, its identity is 0 according to Table 2.

The same gene from mycobacteriophage Bxb1 was submitted to I-TASSER. Results as shown in Figure 5 had a lower C-score in the top models when compared to the models for the gene in *Holli*. The second model in both Bxb1 and *Holli* codes for a transferase enzyme. This prediction of function could not stand because of a poor Z-score. Figure 6 shows proteins with high structural similarities in PDB for Bxb1. Protein A was predicted to function as a hydrolase inhibitor, and proteins B and C were predicted to function as protein transporters. Compared to the functions observed in *Holli*, the predicted functions were different. In *Holli*, the top three proteins had functions of a transcription protein, a DNA-binding protein, and a signaling protein. Function could not be predicted based on these results.

Table 1. Top 3 Threading Templates for Holli *gene*

Rank	PDB Hit	Iden1	Iden2	Cov.	Norm. Z-score
1	1vqrA	0.12	0.21	0.88	0.82
2	1o17A	0.16	0.18	0.84	0.60
3	2oxoA	0.12	0.24	0.97	0.75

Table 2. Proteins with highly similar structure in PDB (Protein Data Bank) for Holli *gene*

Rank	PDB Hit	TM-score	RMSD[a]	IDEN[a]	Cov.
1	1y1uC	0.812	2.26	0.043	0.989
2	3s4wA	0.737	2.70	0.043	0.967
3	3t5vA	0.727	2.54	0.000	0.967

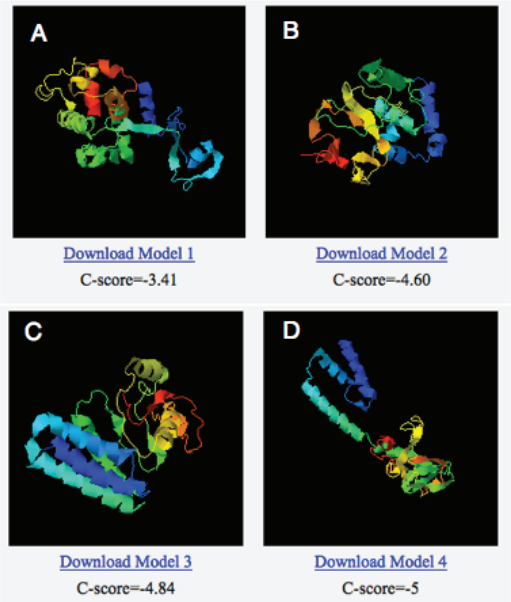

Figure 5. Top four models predicted by I-TASSER for Bxb1 *gene*

For further investigation on predicting the function of the protein encoded by the gene studied in Holli*, the same gene from* Bxb1 *(an A1 subcluster) was also submitted to I-TASSER.* Bxb1 *is one of the members of pham 6167. These top models predicted by I-TASSER had an extremely low C-score. These models look significantly different than the models predicted for the gene in* Holli*. Despite the significant difference in structure, the second model in both* Holli *and* Bxb1 *functions as a transferase; however, this is not enough evidence to support this prediction due to the poor Z-score.*

Discussion

Data gathered from various programs such as I-TASSER indicate that predicting a function for the gene *Holli* using current bioinformatics tools is impossible. Protein structures sent from I-TASSER for the gene in *Holli* did not provide sufficient data to provide predictions of a gene's function. More data were gathered when the gene found in Bxb1 was submitted to I-TASSER. Comparisons among proteins with highly similar structures in PDB could be made according to the data collected from Bxb1; however, inconsistency exists between the data from *Holli* and that from Bxb1. As a result, there were not sufficient results to predict a function.

During the study, we observed that the second best threading template sent from I-TASSER for both *Holli* and Bxb1 coded for a transferase. We came close to predicting that this gene codes for a transferase; however, the Z-score for this threading template in *Holli* is 0.62, which is low. A good Z-score is greater than 1, representing a good alignment. When looking at the second best threading template for Bxb1, the Z-score was 0.58, which is also poor. While it was predicted that the gene coded for a transferase enzyme, there was not strong evidence for this prediction based on the results collected.

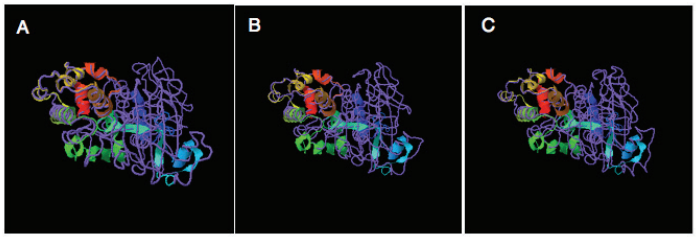

Figure 6. Proteins with highly similar structure in PDB (Bxb1)

In the above figures, protein A represents a hydrolase inhibitor. Proteins B and C represent a protein transporter. These functions are different than the proteins with highly similar structure in PDB for the gene in Holli*. In* Holli*, the top three proteins represents a transcription protein, a DNA-binding protein, and a signaling protein. Due to these dissimilarities, gene function could not be predicted for the gene found in* Holli*.*

Our study indicates that wet lab experiments must be performed to provide accurate function predictions of a gene, despite the fact that this process is costly and time consuming. Our study did show that bioinformatics tools can provide weak predictions to help narrow down or speculatively identify the functions of proteins in a cell. Wet lab experiments can then be guided and performed based on the bioinformatics predictions. Although the gene being studied in *Holli* did not provide adequate information to predict protein function, knowing this type of information helped us determine which genes in *Holli* are worth investigating using wet lab experiments.

References

1. Cresawn, S.G. et al. Comparative genomics of Cluster O mycobacteriophages. *PLOS ONE*. 10, e0118725 (2015).
2. Travis, J. All the world's a phage. *Science News*. 164, 26–28 (2003).
3. Khan Mirzaei, M. & Nilsson, A.S. Isolation of phages for phage therapy: A comparison of spot tests and efficiency of plating analyses for determination of host range and efficacy. *PLOS ONE*. 10, e0118557 (2015).
4. Skolnick, J., Fetrow, J. S., & Kolinski, A. Structural genomics and its importance for gene function analysis. *Nature Biotechnology*. 18, 283–287 (2000).
5. Cresawn, S. G. et al. Phamerator: A bioinformatic tool for comparative bacteriophage genomics. *BMC Bioinformatics*. 12, 395 (2011).
6. Broadway, L. & Engelsen, A. Details for Phage Peaches. *Phagesdb*. (2008). http://phagesdb.org/phages/Peaches/
7. Yang, J., Yan, R., Roy, A., Xu, D., Poisson, J., & Zhang, Y. The I-TASSER suite: Protein structure and function prediction. *Nature Methods*. 12, 7–8 (2015).
8. Lawrence, J. DNA Master. Department of Biological Sciences. *University of Pittsburgh*. (2009).

inquiro staff

Chief Editors

Chapin Cavender

Chapin Cavender is a fourth-year student in the University Honors Program majoring in Physics. He conducts research with Dr. Vladimir Parpura in the Department of Neurobiology investigating the mechanisms of secretory vesicle trafficking in astrocytes. In the fall, he will enter the Biophysics, Structural & Computational Biology graduate program at the University of Rochester to pursue a Ph.D. in Biophysics.

John Decker

John Decker is a Junior in the University Honors Program, pursuing a major in Neuroscience and minors in Chemistry, Biology, and Mathematics. His research is supervised by Dr. Paul Gamlin in the Department of Ophthalmology and broadly relates to the neural control of eye movements. His interests include the outdoors, sports, arts and music, and many other topics, and he plans to pursue a Ph.D. after completing his undergraduate studies.

Assistant Editor

Maggie Collier

Maggie Collier is a sophomore Biomedical Engineering student and a member of the Science and Technology Honors Program. Under the mentorship of Dr. Ho-Wook Jun, Maggie researches the use of peptide amphiphiles in a common brain aneurysm treatment known as embolization. Once she earns her degree, Maggie hopes to pursue an M.D./Ph.D., establish a career in research, and continue to incorporate her love for writing into her scientific interests.

Editorial Board

Hriday Bhambhvani

Hriday Bhambhvani is currently a sophomore pursuing a double major in neuroscience and applied mathematics with a minor in chemistry. Since the latter half of his senior year of high school, he has worked in the lab of Dr. James Meador-Woodruff in the University of Alabama School of Medicine's Department of Psychiatry and Behavioral Neurobiology. There, Hriday investigates the pathophysiology of schizophrenia and is particularly interested in aberrant synaptic plasticity and cytoskeletal dynamics. Aside from his research, Hriday has a vested interest in local education reform and enjoys playing soccer, teaching, and reading.

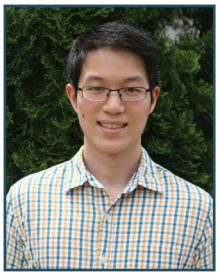

Alexander Chang

Alexander is a sophomore pursuing a B.S. in Molecular Biology and a minor in chemistry. He is a member of the University Honors Program and a Research Ambassador. Currently, he is conducting plant research at the genetic level with Dr. Mukhtar in the UAB Department of Biology. During his free time, he enjoys playing cello, discovering music, and cooking food.

Bliss Chang

Bliss Chang is a Senior majoring in Biochemistry and Biology. He researches under the mentorship of Dr. Elizabeth Sztul and Dr. Jamil Saad. His undergraduate research has focused on the structure function relationships of various proteins. He will be researching the structural basis for treating Alzheimer's Disease at the Max Planck Institute for Biophysical Chemistry in Germany on a Fulbright Scholarship.

Daniel Gilliam

Daniel is a junior in the Science and Technology Honors Program and the Early Medical School Acceptance Program double majoring in Neuroscience and Chemistry. He works in Dr. David Sweatt's lab on the epigenetic processes underlying learning and memory. Daniel plans to pursue a Ph.D. in either Neurobiology or Biochemistry. In his spare time he enjoys reading, hiking, and playing piano and cello.

Tamara Imam

Tamara Imam is a sophomore University Honors Program student majoring in neuroscience and minoring in chemistry and political science. She was born and raised in Madison, Alabama and graduated from Bob Jones High School. In addition to working for *Inquiro*, she is a staff writer for the *Kscope* and serves on USGA as a Senator for the College of Arts and Sciences. Upon graduation, she hopes to attend law school.

Emily Jennings

Emily Jennings is a sophomore in the Honors College majoring in Neuroscience with expected minors in Biology, Chemistry, Physics, and Psychology. She conducts research with Dr. Thomas van Groen in the Department of Cell, Developmental, and Integrative Biology concerning cerebrovascular amyloid angiopathy and its relationship with the cognitive impairment associated with Alzheimer's Disease. After completing her undergraduate degree, Emily plans to pursue a medical degree. In her spare time, she enjoys playing the violin and spending time outdoors.

Roxanne Lockhart

Roxanne Lockhart is a senior in the University Honors Program. She is a Molecular Biology major and has researched with Dr. Farah Lubin in the Department of Neurobiology as a 2013 Beckman Scholar. Her current project, under the direction of Dr. Candace Floyd, focuses on post-translational protein modifications in a post-traumatic brain injury model. She has been part of the *Inquiro* Editorial Board since 2012 and was a member of the Undergraduate Research Association. She is currently the President of Phi Sigma Biological Sciences Honor Society at UAB, and will graduate with Honors in Biology and as a member of the Biology Scholars Program. After graduation, Roxanne plans to continue research before joining a Medical Scientist Training Program.

Susmita Murthy

Susmita Murthy is a junior double-majoring in History and Biology. She plans on attending medical school after the completion of her undergraduate degree. She has done research in the lab of Dr. Michael Miller in the Department of Cell Biology studying the effects of Amyotrophic Lateral Sclerosis in C. Elegans.

Aashka Patel

Aashka Patel is a sophomore pursuing a major in Neuroscience and a minor in Chemistry. She is part of the Early Medical School Acceptance Program and the University Honors Program. She currently studies frontotemporal dementia in Dr. Erik Roberson's lab in the Department of Neurobiology. She also serves as a UAB Ambassador and is a member of the UAB Ethics Bowl Team. In her free time, Aashka enjoys spending time with her family.

Ranjani Ponnazhagan

Ranjani Ponnazhagan is a junior Neuroscience major in the University Honors Program and Early Medical School Acceptance Program. A recipient of the Parkinson's Disease Foundation Student Fellowship, she conducts research in Dr. David Standaert's lab focusing on the role of inflammation in PD. She enjoys hiking and attending concerts and plans to attend UAB's medial school.

Ambika Srivastava

Ambika Srivastava is pursuing a Masters of Public Health in Epidemiology as well as a Masters of Engineering in Design and Commercialization at UAB. She recently graduated as a Biomedical Engineering major with a concentration in Tissue Engineering/ Biomaterials. She performed research in Dr. Mary McDougall's lab at UAB's School of Dentistry Oral Health Research Institute identifying differential gene expressions in malignant mesenchymoma versus normal cells. During her free time, Ambika likes to dance to Bollywood songs and watch Bollywood movies.

Amy Stewart

Amy Stewart is a junior Neuroscience major in the University Honors Program. She is researching the antidepressant effects of ketamine in Dr. Lori McMahon's lab and plans to get a Ph.D. and pursue a career in research. In her free time, she enjoys reading and playing the flute.

Marina Triplett

Marina Triplett is a sophomore in the Science and Technology Honors and Chemistry Scholars programs. She is pursuing a degree in Chemistry with minors in Biology and Spanish. She conducts research in the Department of Pharmacology and Toxicology in the lab of Dr. Mary-Ann Bjornsti, where she is studying the effects of camptothecin and human topoisomerase I mutations on DNA supercoiling and yeast cell viability. After completing her undergraduate degree, she plans to earn a Ph.D. in Biochemistry or Genetics and pursue a career in scientific research. In her spare time, she enjoys watching classic films and listening to classic rock music.

Neha Udayakumar

Neha Udayakumar is a sophomore in the Science and Technology Honors and BioScholars programs. Her research in the Department of Biology investigates the effect of dietary compounds on the epigenetic regulation of breast cancer. Aside from academics, she is a freelance graphic designer and has an interest in medical illustration. She plans to pursue a career as a physician in the future.

inquiro

acknowledgements

Without the help and support of UAB faculty and staff, the vision of Inquiro could not have been made a reality. Many thanks to the following individuals:

2014 Faculty Reviewers:
Dr. Stephen Barnes
Dr. Jessy Deshane
Dr. Todd Green
Dr. Joseph Harrison
Dr. Karen Jaunarajs
Dr. Karolina Mukhtar
Dr. Kazu Nakazawa
Dr. James Patterson

Dr. Mike Sloane and the University Honors Program
Dr. Diane Tucker and the Science and Technology Honors Program
Ryan McAnulty, UAB Printing Services (production and printing)

A special thanks to Dr. Suzanne Austin, Senior Vice Provost, and Dr. Tomader Ali, Coordinator for Undergraduate Research.

The production and publication of this journal was made possible through the funding supplied by the Office for Student and Faculty Success of the University of Alabama at Birmingham.

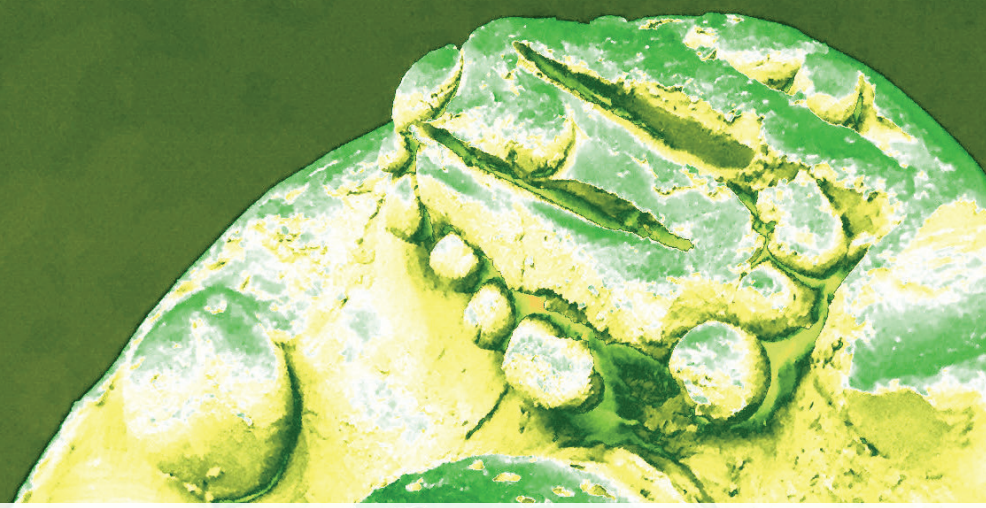

2015-2016 *Inquiro* Submission Guidelines

Any UAB undergraduate student participating in scientific research and/or any undergraduate student participating in research at UAB is invited to submit a manuscript to be considered for publication in the 2015-2016 issue of *Inquiro*. Papers will be subject to anonymous review by faculty and students.

The deadline for submission is October 9, 2015; however, students participating in summer research at UAB or at another institution are encouraged to submit by September 1, 2015.

The journal accepts submissions in the following categories:

Short reports: A short report should give a concise overview of an original research project. Its content is comparable to that of science posters. The suggested length is 1000 – 2000 words.

Long papers: A long paper should give a substantial description of an original research project. It should include detailed discussions of the methods utilized and the results obtained. The suggested length is 2500 – 4000 words.

Research narratives: A research narrative describes an author's personal experiences in research using an editorial or narrative style. The suggested length is 600 – 800 words.

Initial submissions should follow these guidelines:

1. All submissions should be submitted as Microsoft Word documents, double spaced and formatted in 12 pt Times New Roman font. Pages should be numbered with the name of the primary author appearing in a header on every page.
2. Research papers should be written in third person. Research narratives should be written in first person.
3. Research papers should include a title, the full name(s) and affiliation(s) of the author(s), and the following sections: Abstract, Introduction, Materials and Methods, Results, Discussion, Conclusion, and References. Please consult the Manuscript Guidelines for Authors on our website for more specific instructions on each section.
4. Figures, tables and graphs should be submitted in their original formats in the highest resolution possible. They may be submitted as separate files or embedded in the text of the document in the locations in which the author would like them to appear in a published version. If submitted separately, please indicate in the manuscript where the figures should appear.

Research papers can be submitted through the Submit page on our website. Before submitting, please ensure that your mentor has read and approved of your manuscript. Your mentor will automatically receive an email requesting his or her approval of your submission.

Research narratives can be submitted through email. Include the article title as well as your name, university, major, and class standing in the body of the email.

Please send any questions or comments to inquiro@uab.edu. Students who wish to join the *Inquiro* staff may also contact the editors at this address.

For more information or to view previous publications, visit our website at uab.edu/inquiro.

inquiro

Volume 8 • 2014

THE UNIVERSITY OF ALABAMA AT BIRMINGHAM